Journal of Northwest Atlantic Fishery Science

Volume 51

2020

Northwest Atlantic Fisheries Organization
Halifax, Nova Scotia, Canada

ISSN-0250-6408

CITATION

Manuscripts for the *Journal of Northwest Atlantic Fishery Science*, since Volume 35, are published electronically and are freely available at http://journal.nafo.int. This hardcopy bound volume is a compilation of the web-based articles. Citations should refer to the electronic publication following the format shown on the first page of each article and include the doi. Note that the cited year of publication is the year of the upload to the web and not the print year of this hardcopy compilation.

Journal
of
Northwest Atlantic
Fishery Science

Volume 51
2020

Printed and Distributed in December 2020
Northwest Atlantic Fisheries Organization

401-1601 Lower Water Street, Halifax, Nova Scotia, B3J 3P6 Canada
Tel.: (+1 902) 468–5590 • Fax: (+1 902) 468–5538
Email: journal@nafo.int • Website: http://journal.nafo.int • www.nafo.int

ISSN: 0250-4408

Journal of Northwest Atlantic Fishery Science

Scientific publications by ICNAF and NAFO have been in existence since ICNAF began in 1949 with the ICNAF Special Publication series dealing with proceedings of scientific symposia. The ICNAF Research Bulletin was started in 1964 to provide a means of publishing results of scientific research relevant to ICNAF. The *ICNAF Research Bulletin* was terminated in September 1979 after the issue of Number 14. The first volume of the NAFO Journal of Northwest Atlantic Fishery Science was published in December 1980, after NAFO came into force replacing ICNAF in 1979.

The Northwest Atlantic fisheries have a rich history, and a great deal of research has been sponsored and encouraged by NAFO and its predecessor ICNAF. NAFO has been a leader amongst international organizations in the application of science to fishery management and in the regulation of fisheries in areas beyond national jurisdiction. In accordance with its mandate to disseminate information on fisheries research to the scientific community, the Scientific Council of NAFO publishes the Journal of Northwest Atlantic Fishery Science, which contains peer-reviewed primary papers, and NAFO Scientific Council Studies, which contains unrefereed papers of topical interest and importance to the Scientific Council. Lists of these and other NAFO publications are given on the back of this issue.

Editorial Policy

The Journal provides an international forum for the primary publication of original research papers, with emphasis on environmental, biological, economic and social science aspects of fisheries and their interactions with marine habitats and ecosystems. While the Journal is intended to be regional in scope, papers of general applicability, and methodological and review papers, irrespective of region, are considered. Space is available for notes and letters to the editor to facilitate scientific discussion of published papers. Both practical and theoretical papers are eligible. All papers are peer-reviewed to determine their suitability for primary publication. Associate Editors arrange for the peer-reviews and ensure that the papers accepted for publication meet the high standards required for the Journal. Manuscripts approved for publication are accepted with the understanding that they are not copyrighted, published or submitted elsewhere except in abstract form. There are no page charges.

Editorial Board

The Scientific Council of NAFO publishes the *Journal of Northwest Atlantic Fisheries Science*, containing peer-reviewed primary literature detailing original research of relevance to fisheries science and management in the Northwest Atlantic Ocean. Articles are published electronically under a Creative Commons (Canada) 2.5 license, and are freely available at https://journal.nafo.int. NAFO Scientific Council has resolved to produce annual or bi-annual bound print volumes and these represent a compilation of the web based articles published throughout the year. Additionally, the journal supports the use of digital object identifiers (doi) for electronic media and encourages others to support this initiative. The journal is also indexed in the Aquatic Sciences and Fisheries Abstracts (ASFA) database.

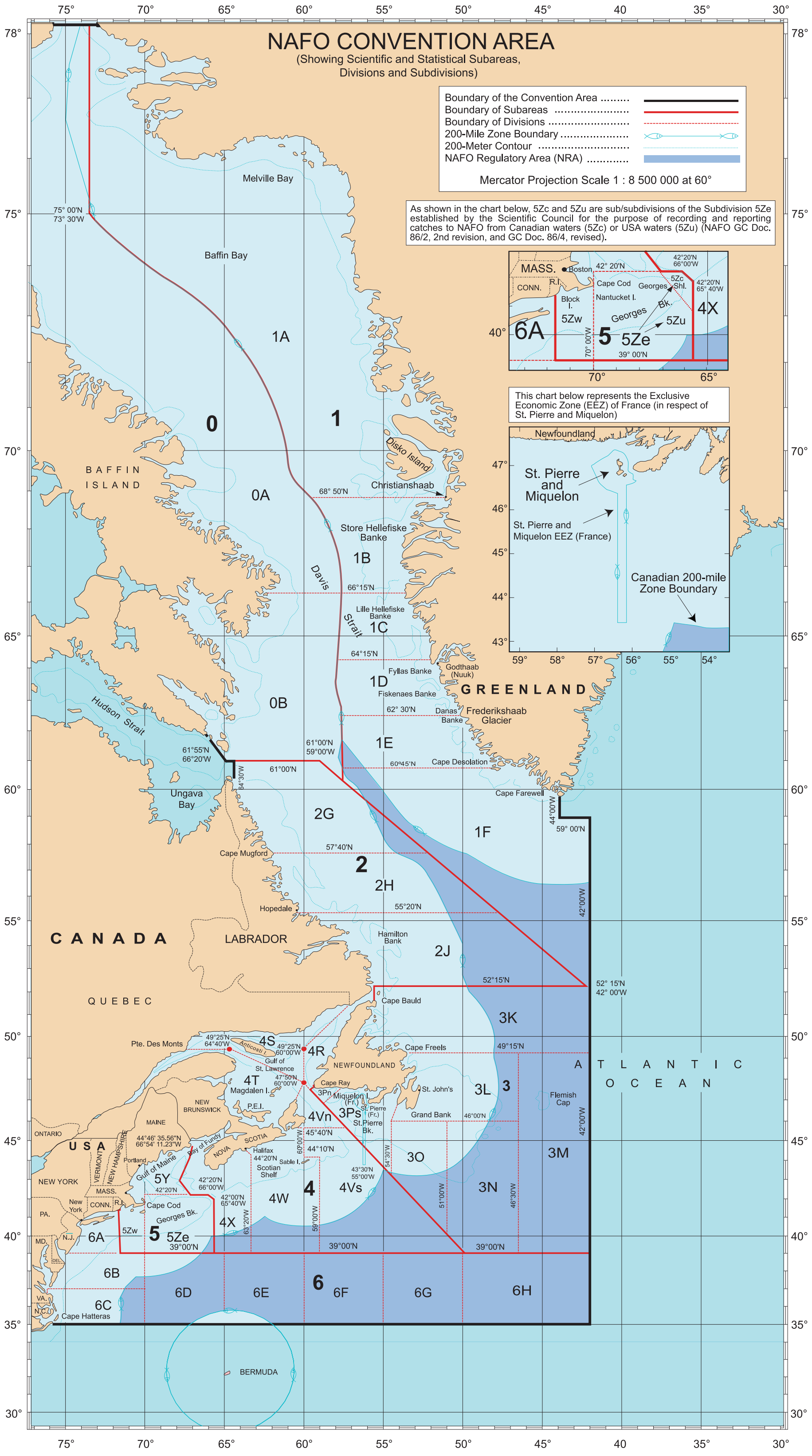

As shown in the chart below, 5Zc and 5Zu are sub/subdivisions of the Subdivision 5Ze established by the Scientific Council for the purpose of recording and reporting catches to NAFO from Canadian waters (5Zc) or USA waters (5Zu) (NAFO GC Doc. 86/2, 2nd revision, and GC Doc. 86/4, revised).

This chart below represents the Exclusive Economic Zone (EEZ) of France (in respect of St. Pierre and Miquelon)

June 2015

Contents

J. Northw. Atl. Fish. Sci., Vol. 51: 1–13 Publication (Upload) date: 11 Jun 2020

A brief examination of underwater video and hook-and-line gears for sampling black sea bass (*Centropristis striata*) simultaneously at 2 Mid-Atlantic sites off the Maryland coast

Daniel W. Cullen (contact author)*[1] and Bradley G. Stevens[2]
[1]Department of Natural Sciences, University of Maryland Eastern Shore, Henry O. Tanner Airway Sciences Building, Building 915, 30806 University Boulevard South, Princess Anne, Maryland 21853, USA; Phone: 410-651-6520; *Email: bwtegu@gmail.com
*Email address for contact author

[2]Department of Natural Sciences, Living Marine Resources Cooperative Science Center, University of Maryland Eastern Shore, Henry O. Tanner Airway Sciences Building, Building 915, 30806 University Boulevard South, Princess Anne, Maryland 21853, USA; Phone: 410-651-6066; Email: bgstevens@umes.edu

Cullen, D.W., and Stevens, B.G. 2020. A brief examination of underwater video and hook-and-line gears for sampling black sea bass (*Centropristis striata*) simultaneously at 2 Mid-Atlantic sites off the Maryland coast. *J. Northw. Atl. Fish. Sci.*, 51**:** 1–13. https://doi.org/10.2960/J.v51.m725

Abstract

This study briefly examined the simultaneous use of 2 gear types, single underwater video and hook-and-line, for sampling black sea bass (*Centropristis striata*) in Mid-Atlantic waters off the Maryland (USA) coast. Fish were sampled from 4 July to 3 August 2012 at two locations with varying bottom habitats ranging from sand and mud to natural hard bottom. First, the relationship between estimates of abundance of black sea bass sampled with the two gear types was examined using least-squares regression analysis. Second, abundance estimates were compared using linear mixed-effects models to determine whether abundance differed between the two sampling locations. In general, positive linear relationships were found between abundance estimates produced by underwater video and hook-and-line sampling methods. Abundance estimates of fish sampled with both gears was also found to be greater for the location with more complex bottom habitat. The results suggest that, if utilized together, both gear types have the potential to provide useful information about the abundance of black sea bass in Mid-Atlantic coastal waters.

Key words: black sea bass, hook-and-line, Mid-Atlantic, simultaneous sampling, underwater video

Introduction

Fishery-dependent data such as catch per unit of effort (CPUE) are commonly used in stock assessments given that they are assumed to be proportional to population abundance. Studies investigating the relationship between CPUE and abundance have demonstrated that the assumption of proportionality between the two does not hold true for all species or for fish caught in variable habitats and at different times (Richards and Schnute, 1986; Harley *et al.*, 2001). The need for more accurate estimates of abundance has led to the development of fishery-independent surveys for many species (Pennington and Strømme, 1998; Rotherham *et al.*, 2007). Surveys may adopt a variety of sampling methods to obtain abundance estimates though no methods are without bias (Willis *et al.*, 2000; Wells *et al.*, 2008). Differences in biases and selectivity among different sampling gears have lead to studies comparing the use of multiple gears including underwater video and hook-and-line for assessing fish abundance (*e.g.* Willis and Babcock, 2000; Willis *et al.*, 2000; Parker *et al.*, 2016).

The black sea bass (*Centropristis striata*) is a commercially and recreationally important fish species in the Northwest Atlantic Ocean (Moser and Shepherd, 2009). North of Cape Hatteras, NC, *C. striata* in Mid-Atlantic waters are migratory with individuals inhabiting inshore hard bottom (*i.e.* hard structurally complex habitat; Steimle and Zetlin, 2000) and reef habitats from spring to autumn and deeper offshore shelf waters during the winter

(Drohan *et al.*, 2007). Black sea bass are harvested inshore with hook-and-line and fish traps and offshore with bottom trawls (Shepherd and Terceiro, 1994). Fishery independent data used to estimate abundance for the species come from seasonal bottom trawl surveys performed by the National Marine Fisheries Service (NEFSC, 2017). However, the hard bottom habitats occupied by *C. striata* during its inshore residency make sampling with bottom trawl gears ineffective (Musick and Mercer, 1977). Stock assessments for the species have suggested that sampling fish on hard bottom (NEFSC, 2017) habitats with alternative gears (*e.g.* fish traps, hook-and-line, underwater video gears) may provide useful data for population assessment and management.

In this study, we used single remote unbaited underwater video and hook-and-line gears for sampling black sea bass simultaneously on structurally complex habitats ranging from sand and mud to natural hard bottom composed of rocky outcroppings, gravel, and boulders (Steimle and Zetlin, 2000). We hypothesized that if the two methods follow changes in abundance in the same manner, then the relationship between the two will be proportional and that both methods should produce correlated estimates of abundance when employed at the same time and location. Specific objectives were to: 1) examine the relationship between counts of black sea bass sampled simultaneously with underwater video and hook-and-line gears at sites with different types of bottom habitat, and 2) determine whether sampling with underwater video and hook-and-line gears would produce differences in counts of black sea bass at sites with different types of bottom habitat and presumed fish densities.

Materials and methods

Sample sites

Sampling took place on eight days from 4 July to 3 August 2012 at 2 sites located off the Maryland coast (Fig. 1). To compare underwater video and hook-and-line gears for sampling black sea bass, 2 sites (separated by 20.3 km) were chosen based on their types of bottom habitat. Site 1 (37°59′14″N, 74°54′30″W) was characterized by a sandy bottom with mud, shell, gravel, and aggregations of small to large cobbles and was classified as an unstructured site. In contrast, site 2 (38°09′09″N, 74°47′41″W) was classified as highly structured since it consisted of a mixture of sand, mud, cobbles, large rocks, and low relief hard bottom habitat [*i.e.* rocky outcroppings and boulders or other structures partly covered with sea whips (*Leptogorgia* spp.) and stony corals]. The choice of sites (*i.e.* site 1 = unstructured; site 2 = structured) allowed for a simultaneous comparison of the two gears for sampling black sea bass on variable habitats with presumed differences in fish densities. Sites were visited separately on alternate days for a total of four times each during the study period. Sampling took place during daylight hours from 0900 to 1600 Eastern Daylight Savings Time at depths ranging from 29 m to 31 m at both sites. Bottom water temperatures varied from 12.8°C to 14.4°C and 11.7°C to 14.6°C at site 1 and site 2, respectively.

Video sampling and video processing

Underwater videos were collected using a rectangular (91 cm length × 61 cm width × 91 cm height) video system constructed of galvanized and zinc plated slotted steel angle along the top, 5.1 cm wide slotted square corner posts, and 3.8 cm wide slotted square side and center bars (Fig. 2A). The main camera consisted of a Canon FS-30 camcorder with a wide angle lens in an Equinox HD-6 underwater housing mounted in the center (58 cm from the bottom of the frame). The camera housing was tilted in a slightly downward facing position that provided the camera with standardized view of the bottom habitat (see Fig. 2B and 2C for examples) and fish when present. A strip of slotted steel flat was wrapped around the housing to help secure it in place. Three backup GoPro HD Hero 1 cameras (720-pixel resolution, 170° angle of view) in underwater housings were faced outward at slight angles (to match the position and direction of the central mounted main camera) from the right and left sides and the back of the frame.

Eight 40 min unbaited video system deployments (*i.e.* the system was deployed without a bait source) were made at a site on each sampling date. Deployments of the system were conducted by first locating a soft sediment area on the bottom using a fish finder (FCV-582L; Furuno Electric Co. Ltd., Nishinomiya City, Japan); soft sediment areas were identified prior to deployments to ensure that the video system did not land on rocks or other bottom structures when present. The system was then lowered to the bottom slowly with a polypropylene rope that was affixed to a surface buoy. After 40 min, the system was lifted to the vessel with a hydraulic pot-hauler. The vessel was moved ~20 m from the first deployment location and deployed for the next sample; camera batteries were changed after four deployments of the system. Because water current may influence counts of fish on videos (Bacheler *et al.*, 2016), near-bottom current velocity (m s^{-1}) was measured during deployments with a SeaHorse Tilt Current Meter (SeaHorse TCM; *OkeanoLog*, North Falmouth, MA; Sheremet, 2010) mounted to a nearby deployed fish trap. Further, since overhead cloud cover could potentially reduce natural lighting on the bottom and affect the ability to observe and count fish on videos, cloud cover (%) at

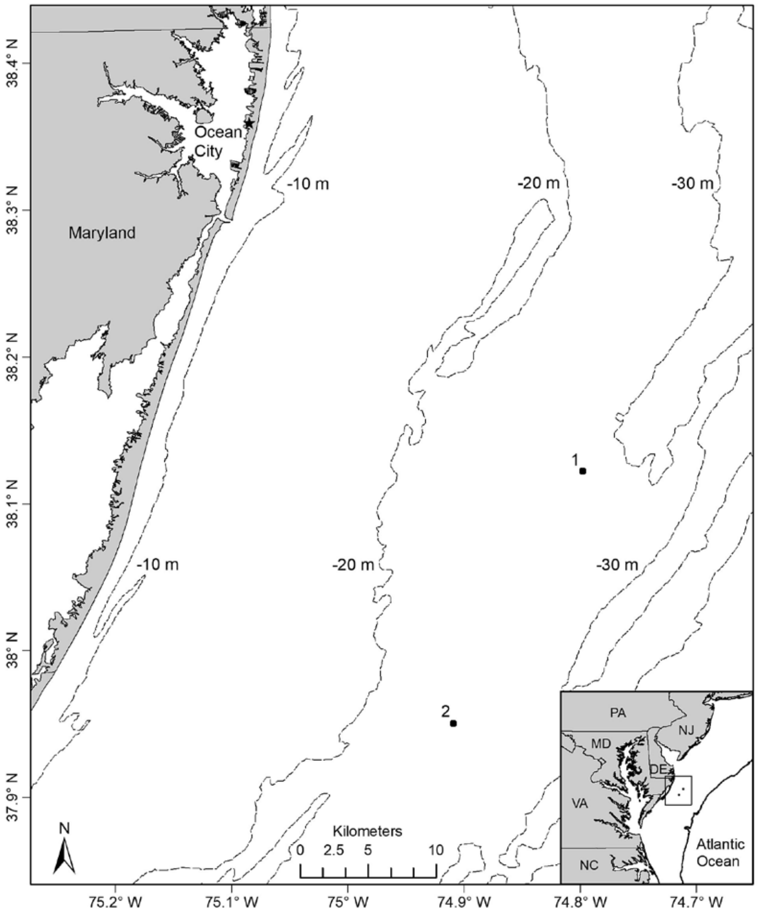

Fig. 1. Map showing the location of the 2 sites (numbered black symbols; 1 = site 1 and 2 = site 2) where black sea bass were sampled with underwater video and hook-and-line gears, respectively, from 4 July to 3 August 2012 in the Mid-Atlantic. The inset depicts the location of the 2 sites along the Atlantic coast of the United States.

each site was recorded during each deployment. Cloud cover (%) was determined on a given sampling day by visually estimating the percentage of sky covered by clouds directly above the vessel. Estimates ranged from 0% to 100% with 0% indicating no cloud cover and 100% indicating absolute cloud cover while values falling within the range represented partly to mostly cloudy conditions.

In the laboratory, videos were processed using a standard video editing software (Adobe Premiere Pro CS5, vers. 5.0; Adobe Systems Incorporated, San Jose, CA). Generally, videos from the main camera were selected for processing however on one occasion (18 July) fogging of the underwater housing made them unsuitable for viewing. In this case, videos from one of the backup cameras were randomly selected for processing. We chose a 30 min video interval for counting because the highest observations of fish occurred within the first 15 min of video (Cullen and Stevens, 2017). Counts for black sea bass were made using the MeanCount counting method (Schobernd *et al.*, 2014). MeanCount is the mean across counts of fish observed in a sample of frames from the video (Schobernd *et al.*, 2014); here, 60 single frames were sampled systematically, one every 30 s for 30 min of video. We selected MeanCount over other video counting metrics commonly reported in the literature including MaxN (*i.e.* the maximum count of individuals of a focal species observed at a single time point on the video; Campbell *et al.*, 2015) because Schobernd *et al.* (2014) found it to both have similar variation to MaxN and scale linearly with true abundance. However, during processing, MaxN values were noted at a single time point on each video to serve as a reference for the peak number of fish observed on videos. The video system was allowed to settle on the bottom for the first ~60 s or more of video before counting was initiated.

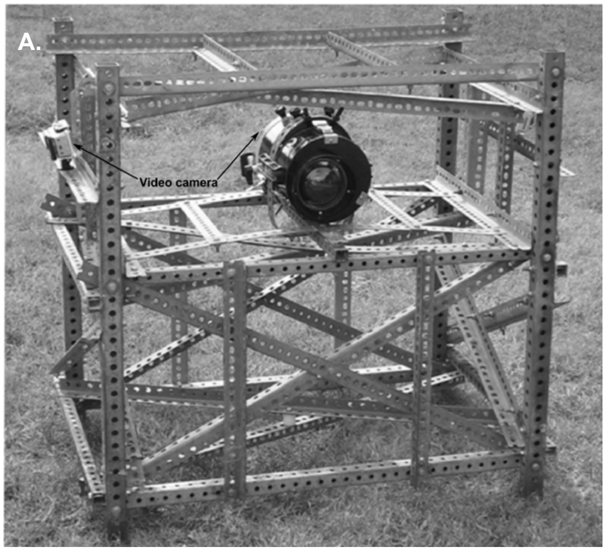

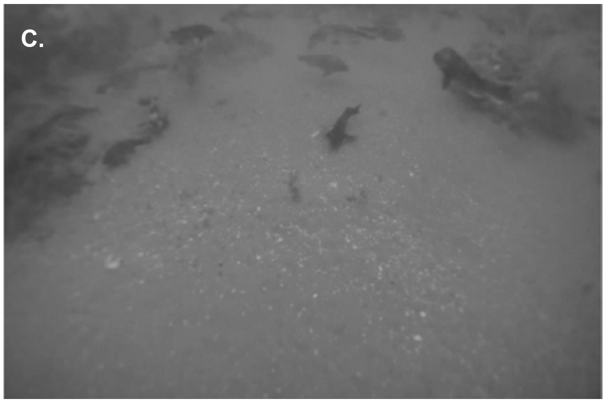

Fig. 2. (**A**) Unbaited video system outfitted with a central Canon FS-30 camcorder and 3 GoPro Hero 1 HD cameras used to sample black sea bass from 4 July to 3 August 2012 at 2 sites in the Mid-Atlantic. Two (*i.e.* right facing, backward facing) of the GoPro Hero 1 HD cameras are not visible. (**B**) Still video image showing an example of sand habitat with two visible black sea bass observed at site 1 (**C**) and hard bottom habitat with rocks, outcroppings, sea whip corals, and visible black sea bass observed at site 2.

Hook-and-line sampling

Hook-and-line sampling was conducted concurrently with video sampling using 6 ft (1.8 m) PENN Mariner one piece fiberglass fishing rods and PENN 209 Level Wind reels (Penn, Philadelphia, PA) equipped with 30 lb (13.6 kg) monofilament line. While drifting over a site, three fishers were assigned a fishing position (1, 2, or 3) on the starboard side of the boat (Harms *et al.*, 2010). Each fisher simultaneously dropped a 3 hook (size = 3/0 Mustad octopus hooks; O. Mustad & Son A.S., Gjovik, Norway) sampling rig assembled with barrel swivels, a 0.23 kg lead sinker, and bait (northern shortfin squid, *Illex illecebrosus*; whole squid were sliced into 5–8 cm strips). Four hook rig drops were made by each fisher for a maximum bottom time of 3 min per hook rig drop though lines could be retrieved prior if a bite was felt or to avoid losing hooked fish. On few occasions, the maximum soak time was exceeded due to bottom snags, line tangles, or gear issues. Fishing occurred adjacent to the deployment sites of the video system. Because hook rig drops on top of or over the system could have resulted in hook snags, we made four drifts adjacent to the deployment site. While fishing, a stopwatch was used to record the timing of four different events including when the sinker hit the bottom, when the first bite was felt, when retrieval of the hook rig commenced, and when the rig reached the surface (Harms *et al.*, 2010). Upon retrieval, each hook rig was inspected and information pertaining to fish catches, bait (bait remaining, no bait), and hook loss resulting from bottom snags was recorded. All fish caught were identified to species prior to release.

Data analysis

A total of 64 (n = 32) video system deployments and 768 (n = 384 per site) hook rig drops were made during the study period. Estimates of CPUE (hereafter referred to as hook-and-line CPUE) for black sea bass sampled with hook-and-line gear were calculated as the number of fish caught per 3 min drop of a 3 hook rig. Values were averaged across the three fishers to obtain a single hook-and-line CPUE value corresponding to each video system deployment (n = 32 for each site; n = 8 per day).

First, the precision of untransformed estimates of MeanCount (hereafter referred to as video CPUE) and hook-and-line CPUE were compared using the relative standard error [(RSE = Standard error/mean) * 100; equation obtained from Newman *et al.*, 1997)]. Second, relationships between untransformed video CPUE and hook-and-line CPUE and cloud cover (%) and current velocity (m s^{-1}) were examined with Spearman's rank correlation tests (Sokal and Rohlf, 1995). Third, we used least squares regression analysis to examine whether the relationship between video CPUE and hook-and-line CPUE estimates was linear or non-linear (Bacheler *et al.*, 2013a). Prior to any analyses, data were checked for normality and variance homogeneity and log-transformed by taking the base 10 logarithm of the variable (video CPUE; hook-and-line CPUE) + 1 (*i.e.*, $\log_{10}[X + 1]$); we added 1 to video CPUE and hook-and-line CPUE estimates because the data contained some values of 0 for both variables. Log-transformations of the data were used to meet the normality and variance homogeneity assumptions of the least squares regression and other parametric statistics when used (Sokal and Rohlf, 1995; Cullen and Stevens, 2017). The relationship between $\log_{10}$-transformed estimates of video CPUE and hook-and-line CPUE were examined using data for each site individually (n = 32) and pooled (n = 64) (Kulbicki, 1988; von Szalay *et al.*, 2007). Further, the relationship between $\log_{10}$-transformed estimates of video CPUE and hook-and-line CPUE averaged by site and date ($n = 8$) was also examined. First, we assessed whether the relationship between $\log_{10}$-transformed estimates of video CPUE and hook-and-line CPUE was nonlinear with the quadratic model $\log_{10}(\text{hook-and-line CPUE} + 1) = a + b * \log_{10}(\text{video CPUE} + 1) + c * \log_{10}(\text{video CPUE}+ 1)^2$ where a is the y intercept and b, and c are constants. Here, if the c parameter was found to be significantly different (P <0.05) from 0, we concluded that there was evidence of a non-linear relationship between $\log_{10}$-transformed estimates of video CPUE and hook-and-line CPUE (Bacheler *et al.*, 2013b). If the c parameter was found to not differ significantly from 0, a linear model with the form $\log_{10}(\text{hook-and-line CPUE} + 1) = a + b * \log_{10}(\text{video CPUE} + 1)$ was fitted to the data. The assumptions of normality, variance homogeneity, and autocorrelation were checked for model validation. All models were fitted using the stats package (R Core Team, 2018) in RStudio, vers. 1.1.442 (RStudio Team, 2018).

Lastly, linear mixed-effects models were used to test for differences in estimates of video CPUE between sampling sites and estimates of hook-and-line CPUE between sampling sites (Cullen and Stevens, 2017). Models included $\log_{10}$-transformed video CPUE (*i.e.* $\log_{10}[\text{video CPUE} + 1]$) or $\log_{10}$-transformed hook-and-line CPUE (*i.e.* $\log_{10}[\text{hook-and-line CPUE} + 1]$) as the response variable, site as a fixed effect, and sampling date as a random effect because multiple non-independent video system deployments and hook rig drops were conducted on each sampling date. Linear mixed-effects models were fitted with restricted maximum likelihood using the 'nlme' (Pinheiro *et al.*, 2018) package in RStudio (RStudio Team, 2018). Analysis of variance was used to extract the F values and Wald test P values for the fixed effect (*i.e.* sampling site) (Cullen and Stevens, 2017).

Results

In total, black sea bass were observed on videos obtained from 60 (93.8%) of the 64 video system deployments (site 1 = 30, site 2 = 30) while at least 1 black sea bass was caught during 359 (46.7%) of the 768 [site 1 = 85 (22.1%), site 2 = 274 (71.4%)] hook rig drops. The frequency of videos collected during video system deployments with 0 observations of black sea bass, corresponding to hook rig drops with 1 or more black sea bass caught, was 0 for both site 1 and site 2, respectively. Conversely, the frequency of hook rig drops with 0 black sea bass caught, corresponding to videos with 1 or more black sea bass observations, was 3 for site 1 and 24 for site 2.

The total number of black sea bass caught with hook-and-line gear at site 1 and site 2 was 124 and 421, respectively. Other species caught with hook-and-line gear included bluefish (*Pomatomus saltatrix*; n = 18) and summer flounder (*Paralichthys dentatus*; n = 2).

Estimates of video CPUE and hook-and-line CPUE were variable by site and date but were generally greater for site 2 (Fig. 3A, 3B). Values of MaxN, noted for each video deployment, also varied by site and date and ranged from 0 to 14 fish (mean ± standard error = 2.906 ± 0.486) for site 1 and 0 to 16 fish (mean ± standard error = 4.906 ± 0.618) for site 2 (Fig 3A, 3B); MaxN data were not considered further for analyses. Comparably, untransformed video CPUE estimates had greater variances and lower precision than those of untransformed hook-and-line CPUE (Table 1). Cloud cover (%) values ranged from 0 to 90% (mean ± SD = 17.375 ± 21.511%) for site 1 and 0 to 75% for site 2 (mean ± SD = 25.156 ± 27.104%), while current velocity (m s^{-1}) ranged from 0.050 to 0.300 m s^{-1} (mean ± SD = 0.319 ± 0.096 m s^{-1}) and 0.049 to 0.178 m s^{-1} (mean ± SD = 0.087 ± 0.032 m s^{-1}) for site 1 and 2, respectively. The Spearman's rank correlation analyses produced a significant correlation between video CPUE estimates and cloud cover ($\boldsymbol{\rho} = -0.268$; $P < 0.05$) but not current velocity ($\boldsymbol{\rho} = -0.062$, $P > 0.05$) while hook-and-line CPUE was not significantly correlated with cloud cover ($\boldsymbol{\rho} = -0.091$, $P > 0.05$) or current velocity ($\boldsymbol{\rho} = -0.227$, $P > 0.05$).

Evidence of a non-linear relationship, indicated by a significant P value for the c parameter, between video CPUE

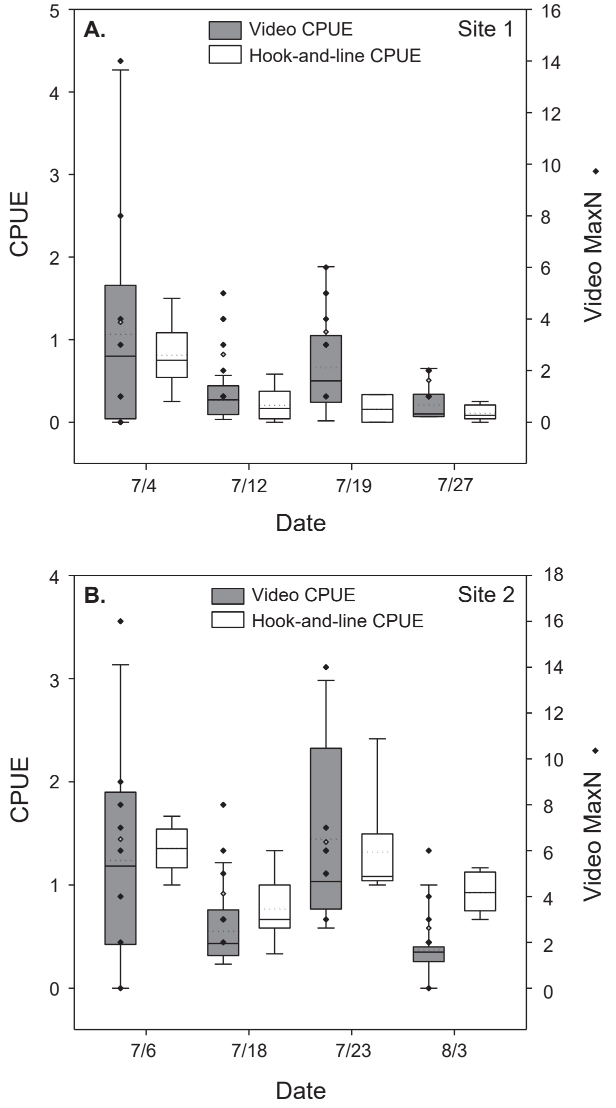

Fig. 3. Box plots comparing video CPUE (*i.e.* MeanCount; the mean across counts in a sample of frames from a video) and hook-and-line catch per unit of effort (hook-and-line CPUE; catch per angler per drop of a 3 hook rig) estimates for black sea bass sampled with underwater video and hook-and-line gears, respectively, from 4 July to 3 August 2012 at 2 sites (**A**, site 1; **B**, site 2) in the Mid-Atlantic. Video CPUE and hook-and-line CPUE estimates were calculated for eight video system deployments per day. The upper and lower box limits are 25th and 75th percentiles, error bars are 10th and 90th percentiles, and solid and dashed lines represent medians and means, respectively. Estimates of MaxN (*i.e.* the maximum count of individuals of a focal species observed at a single time point on the video; black diamonds) and average MaxN (gray diamonds) corresponding to each video deployment (overlayed on the Video CPUE boxes) are given for each date. Note scales of y-axes differ.

and hook-and-line CPUE estimates was found only for site 1 data (quadratic model; parameter estimate ± standard error, $a = 1.279 \pm 0.478$, $b = -0.767 \pm 0.299$, $c = 0.159 \pm 0.030$; $P < 0.05$, $R^2 = 0.199$) (Fig. 4). Positive linear relationships were found for the site 2 data (linear model; slope ± standard error = 0.149 ± 0.056, $P = 0.093$, $R^2 = 0.091$), pooled data (site 1 + site 2; linear model; slope ± standard error = 0.223 ± 0.099, $P = 0.028$, $R^2 = 0.075$), and data averaged by site and date (linear model; slope ± standard error = 0.867 ± 0.308, $P = 0.031$, $R^2 = 0.569$) (Fig. 4).

The linear mixed-effects models indicated that only estimates of $\log_{10}$-transformed hook-and-line CPUE were significantly different between sites (Table 2; Fig. 5). The variance for the residuals and standard error of the random effects around the population intercept were small for both models. The intraclass correlation coefficients (ICC = [Intercept SE] / [Intercept SE + Residual variance]; Zurr *et al.*, 2009) denoted the presence of low to intermediate correlations between video CPUE and hook-and-line CPUE values from the same sampling days (Table 2).

Discussion

This study is the first to use underwater video and hook-and-line gears for sampling *C. striata* simultaneously in Mid-Atlantic coastal waters. In general, our results indicated that abundance estimates for black sea bass sampled with underwater video and hook-and-line gears differed between sampling sites with different types of bottom habitat. We chose two sampling locations, one unstructured site with sand, shell, gravel, and cobbles and another structured site with a mixture of habitat types ranging from sand to boulders and rocky outcroppings colonized with emergent epifauna, and presumed that higher black sea bass densities would be associated with greater habitat complexity. Both underwater video and hook-and-line gears produced higher video CPUE and hook-and-line CPUE estimates at site 2 with more complex bottom habitat. This result is not unexpected as higher richness and diversity of reef fish have been reported for habitats with greater complexity (*e.g.* Schobernd and Sedberry, 2009; Bacheler *et al.*, 2013a). In the Mid-Atlantic, higher abundances of fish including black sea bass have been reported to correlate with greater coverage by the sea whip *L. virgulata* on artificial reefs (Schweitzer and Stevens, 2019). However, little information on the types and intricacies of natural black sea bass habitats has been documented. Even so, Fabrizio *et al.* (2013) examined seasonal habitat associations of black sea bass in a temperate site off the coast of New Jersey and found that fish preferred relatively shallow areas with

Table 1. Mean, standard error (SE), variance (Var), and relative standard error (RSE) for untransformed estimates of video CPUE (*i.e.* MeanCount; the mean across counts in sample of frames from a video) and untransformed estimates of hook-and-line catch per unit of effort (hook-and-line CPUE; catch per angler per drop of a 3 hook rig) for black sea bass (*Centropristis striata*) sampled by underwater video and hook-and-line gears, respectively, from 4 July to 3 August 2012 at 2 sites in the Mid-Atlantic.

Gear type	Sampling site	Mean	SE	Var	RSE
Video CPUE	Site 1	0.554	0.153	0.747	27.580
	Site 2	0.904	0.148	0.698	16.329
	Pooled (site 1 + site 2)	0.729	0.152	0.742	20.885
Hook-and-line CPUE	Site 1	0.323	0.067	0.142	20.688
	Site 2	1.094	0.072	0.166	6.587
	Pooled (site 1 + site 2)	0.708	0.097	0.303	13.735

coarse materials including gravel, rocks, and outcroppings over deeper (>27.5 m) areas and those with finer sediments. Additionally, black sea bass numbers increased as bottom complexity increased. Our results and those of Fabrizo *et al.* (2013) suggest that more intricate habitats in the Mid-Atlantic may support larger numbers of black sea bass. Accordingly, further inshore studies examining the use of underwater video or hook-and-line gears for sampling black sea bass in the Mid-Atlantic should be focused in areas with greater habitat complexity.

In most cases, positive linear relationships between video CPUE and hook-and-line CPUE estimates were found, however, values of video CPUE were more variable and less precise than those for hook-and-line CPUE for both sites and the pooled site data. This result could be due to our sampling approach. First, because sampling with hook-and-line gear required the use of bait, simultaneous sampling with underwater video gear may have attracted fish to or away from the video system during any given deployment (Bacheler *et al.*, 2017). This could have resulted in more variability in video CPUE values among subsequent samples. Second, although both methods were conducted simultaneously, the use of underwater video gear involved deploying the video system at a fixed location while sampling with hook-and-line gear included hook rig drops while drifting over a site. Before each video system deployment, the captain positioned the vessel over bottom habitat however it was not possible to control where the video system landed. Based on our videos, when the frame landed far from structure fewer black sea bass were observed than when it landed closer (Cullen and Stevens, 2017). The opposite occurred when fishing since we encountered fish as we drifted over the site. Though catch was not certain, the probability may have increased or decreased as we passed over different structures. Faster drifts over a site may have also limited the time that baits were on the bottom and available to fish. Additionally, the duration of sampling differed for the two gears as video system deployments were at least 30 min while the total time for 4 hook-and-line gear samples was ~12 min. Hook rig drops were also constrained to three fish per angler while video counts were not restricted. We based our hook-and-line fishing trials on methods described in a study by Harms *et al.* (2010) in which five hook rig drops were made while drifting over various sampling locations. In our case, anchoring the vessel adjacent to the deployment location of the video system instead of drifting and fishing continuously for the same time interval as video system deployments may have produced estimates of hook-and-line CPUE that were more analogous to video CPUE values. Anchoring, however, may result in declining catches as fish are removed from the immediate area. Based on this, we recommend that hook-and-line sampling be conducted either while drifting or anchoring and the resulting hook-and-line CPUE estimates be compared to video CPUE values collected over the same time interval. In the case of anchoring the vessel, the underwater video system should be deployed for 30-min or more prior to sampling with hook-and-line gear to reduce the likelihood of removing fish from the area and out of the view of the cameras.

There were some limitations to our sampling approach that may have influenced our results. First, the simultaneous use of the two gears for sampling black sea bass likely impaired the sampling independence of each gear. For example, the bait used during hook-and-line sampling could

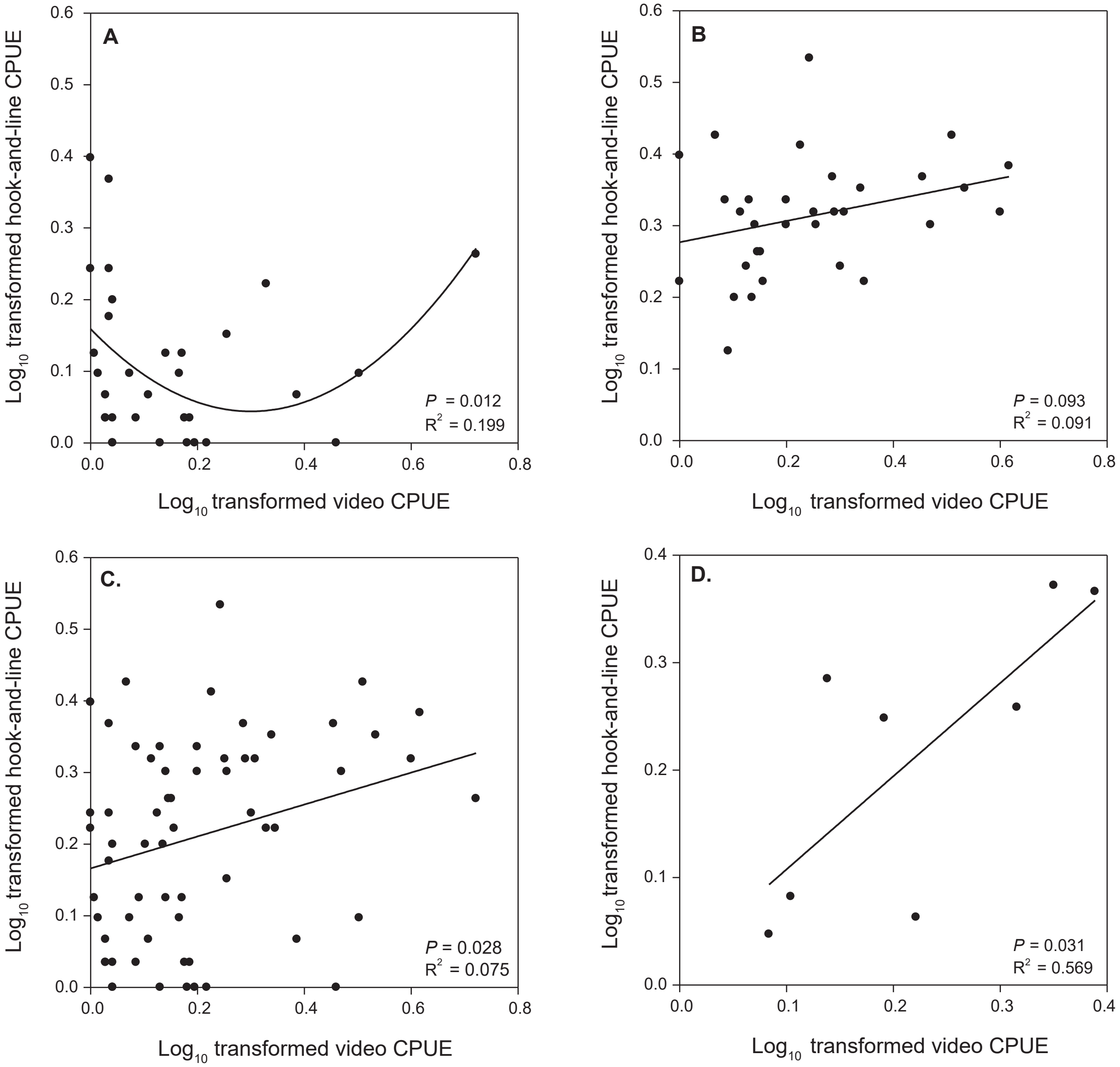

Fig. 4. Relationship between estimates of $\log_{10}$-transformed video CPUE, (*i.e.* MeanCount; the mean across counts in a sample of frames from a video) and $\log_{10}$-tansformed hook-and-line catch per unit of effort (hook-and-line CPUE; catch per angler per drop of a 3 hook rig) for black sea bass sampled with underwater video and hook-and-line gears, respectively, from 4 July to 3 August 2012 at 2 sites in the Mid-Atlantic. (**A**) Estimates for site 1 ($n = 32$), (**B**) Estimates for site 2 ($n = 32$), (**C**) Estimates pooled for site 1 and site 2 ($n = 64$), (**D**) Mean estimates calculated by pooling data by site and date ($n = 8$). The solid line is the predicted line from least squares regression analysis for the relationship between estimates of video CPUE and hook-and-line CPUE and R^2 is the coefficient of determination. *P*-values indicate the significance of the *c* parameter (**A**) and slope parameters (**B; C; D**) for the least squares regression models.

have easily attracted fish away from the video system during deployments (Bacheler *et al.*, 2017). Conversely, fish may have been attracted away from the bait to the video system during deployments if individuals viewed the structure of the video system as an additional or new source of habitat (Cullen and Stevens, 2017). Second, we observed several factors that affected the ability of both gears to sample black sea bass. The daily variation observed (Fig. 3A, 3B) for both video CPUE and hook-and-line CPUE, could partly be related to environmental factors. Current velocity, which may affect fish swimming behavior around the camera frame (Gerstner, 1998) as well

Table 2. Results of linear mixed-effects models used to compare estimates of video CPUE (*i.e.* MeanCount; the mean across counts in sample of frames from a video) and hook-and-line catch per unit of effort (hook-and-line CPUE; catch per angler per drop of a 3 hook rig) for black sea bass (*Centropristis striata*) sampled by underwater video and hook-and-line gears, respectively, from 4 July to 3 August 2012 at 2 sites in the Mid-Atlantic. The standard deviation (SD) for the random effect (Date) represents the variance for each sampling date around the common intercept. Video CPUE and hook-and-line CPUE data were $\log_{10}$-transformed (by taking a logarithm of the variable + 1; *i.e.*, $\log_{10}$[video CPUE + 1], $\log_{10}$[hook-and-line CPUE + 1]) before analysis to help meet the assumptions of the models. The interclass correlation coefficient (ICC) represents the correlation of observations from the same sampling date.

Gear type	Variable effect type	Parameter	df	*F* value	*P* value
Video CPUE	Fixed effects	Intercept	1, 56	36.811	<0.001
		Site	1, 6	2.062	0.201
	Random effects	Date	SD	0.005	
		Residuals	Variance	0.024	
			ICC	0.191	
Hook-and-line CPUE	Fixed effects	Intercept	1, 56	55.600	<0.001
		Site	1, 6	13.326	0.011
	Random effects	Date	SD	0.006	
		Residuals	Variance	0.005	
			ICC	0.552	

as the exposure time of bait on the bottom while fishing (Harms *et al.*, 2010), was negatively correlated with video CPUE and hook-and-line CPUE though neither correlation was significant. However, the success of hook-and-line sampling was occasionally (~15% of hook rig drops) affected by water current velocity and surface winds as we drifted over a given sampling site. Faster water currents and stronger winds caused the vessel to drift at higher rates which reduced the bottom exposure time of the bait thereby resulting in lower catches during some hook rig drops. Conversely, video CPUE estimates were influenced more by cloud cover as indicated by the weak significant negative correlation between video CPUE and cloud cover. At the depths we sampled (29 to 31 m), cloud cover can decrease the amount of natural light that reaches the bottom (Cullen and Stevens, 2017). For deployments with cloud cover greater than 50% ($n = 3$), visibility and the range of observable area around the camera frame was slightly reduced by ~2 m. However, it did not affect our ability to correctly identify and count black sea bass or to identify the types of bottom habitat appearing in the camera field-of-view. The variable pattern in counts between successive sampling days may also be related to tides and/or lunar cycle as these factors have been found to have an influence on the catch rates and behavior of a variety of species (*e.g.* Arendt *et al.*, 2001; Poisson *et al.*, 2010). A preliminary examination of video CPUE and hook-and-line CPUE plotted against tidal data for the sampling period revealed no discernible relationships. Further, additional mechanisms, including the behavioural response of fish to vessel noise as well as changes in diel fish activity patterns may influence the performance of both gears (Willis *et al.*, 2006; De Robertis and Handegard, 2013). Moreover, size selectivity of hooks and density dependent competition for baited hooks may also have an effect on estimates of hook-and-line CPUE (Ralston, 1990; Millar and Willis, 1999; Kuriyama *et al.*, 2019). Overall, failure to find strong correlations between counts and environmental factors (*i.e.* cloud cover, current velocity) may be due to the short duration of our study and small sample sizes. For that reason, further sampling is needed over a longer time period to truly evaluate the influence of environmental variables including lunar cycle on black sea bass CPUE estimates obtained from both underwater video and hook-and-line sampling.

In this study, we used a video counting method that estimated the average number of fish (*i.e.* MeanCount) observed in a series of video frames over a 30 min period of video (*i.e.* 60 single frames were sampled systematically, one every 30 s for 30 min of video). In recent years, the MeanCount metric has been used as an estimate of reef fish abundance in several studies conducted in the Mid- and Southeast Atlantic continental shelf regions of

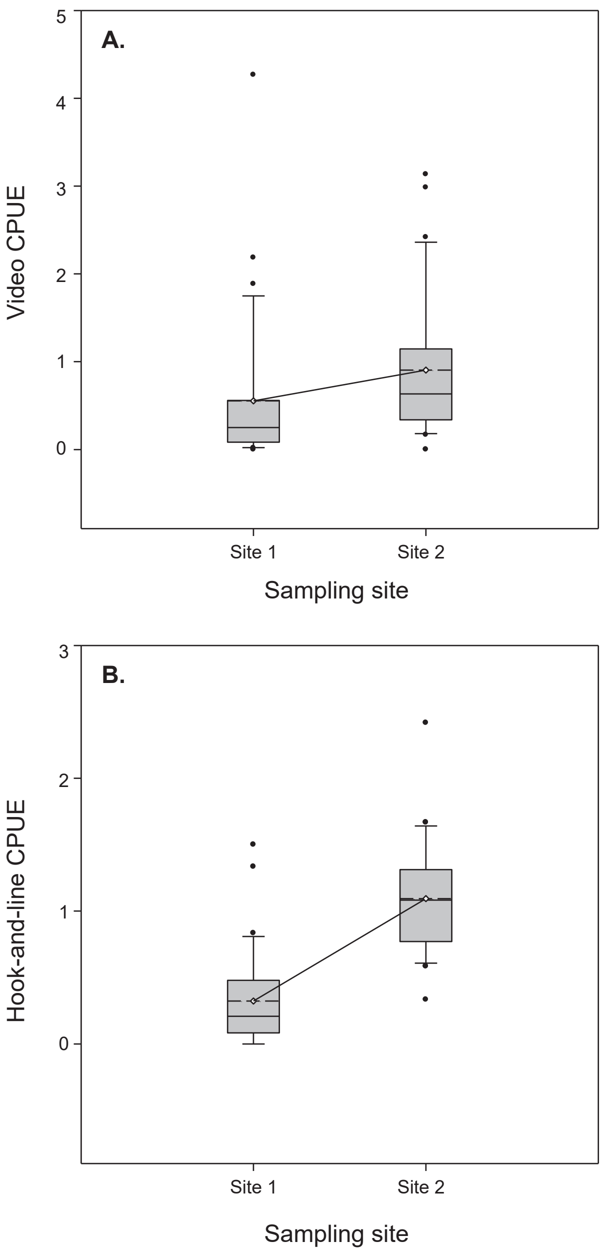

Fig. 5. Box plots of untransformed estimates of (**A**) video CPUE (*i.e.* MeanCount; the mean across counts in a sample of frames from a video) and untransformed estimates of (**B**) hook-and-line catch per unit of effort (hook-and-line CPUE; catch per angler per drop of a 3 hook rig) for black sea bass sampled by underwater video and hook-and-line gears from 4 July to 3 August 2012 at 2 sites in the Mid-Atlantic. The upper and lower box limits are 25th and 75th percentiles, the error bars are 10th and 90th percentiles, the solid and dashed lines represent medians and means, respectively, and the black circles represent outliers. The white diamonds depict the position of the means for (**A**) MeanCount and (**B**) catch per unit of effort for site 1 and site 2, respectively.

the United States (*e.g.* Bacheler *et al.*, 2013a; Bacheler and Shertzer, 2015; Bacheler *et al.*, 2016; Bacheler *et al.*, 2017; Cullen and Stevens, 2017). While the use of MaxN (*i.e.* highest count of individuals of a species observed at a single point during a video segment) is more commonly documented in the literature, we chose MeanCount because it was reported by Schobernd *et al.* (2014) to have similar variation to MaxN and scale linearly with changes in true abundance. In addition, Schobernd *et al.* (2104) found that MaxN had an asymptotic relationship with true abundance and its use may result in abundance estimates that are biased downward for fish populations with increasing abundance or upward for fish populations with decreasing abundance. Oppositely, a comparison of the two metrics by Campbell *et al.* (2015) found that MeanCount had lower precision than MaxN and underestimated the proportion of positive abundance estimates for eight species of reef fish in the Gulf of Mexico. However, Campbell *et al.* (2015) did find evidence of a linear relationship between MeanCount and true abundance and a non-linear relationship between MaxN and true abundance using individual based models that simulated fish spatial movements. To address the non-linearity, the authors concluded that the relationship between MaxN and abundance may become linear if the area viewed by the cameras is expanded to cover a wider spatial area around the video system. Additionally, Campbell *et al.* (2015) suggested that, if multiple cameras are attached to the system, synced, and their videos viewed at the same time, a linear relationship between MaxN and true abundance could be obtained. In our study, we selected videos from a single camera for counting fish in order to estimate MeanCount values. Though we did make a note of MaxN for each video, the values were not included in the data analyses because we did not count fish from the entire area surrounding the video system. Therefore, we concluded that MeanCount was the better metric to use for our data since MaxN may not have shared a linear relationship with black sea bass abundance at each sampling site. However, we do believe the accuracy and precision of the two metrics for counting and estimating the abundance of black sea bass on inshore habitats should be evaluated in the Mid-Atlantic at various locations with different population densities (Stobart *et al.*, 2015). Future studies employing underwater video sampling methods for the species should utilize multiple synchronized cameras that view a wider region around the video system so that both metrics could be estimated correctly for comparison. Their values could also be compared further with other CPUE indices obtained from hook-and-line and/or fish trap sampling (Harvey *et al.*, 2012).

In conclusion, our results indicated that both gear types were capable of sampling the same depths and were able to detect differences in abundance estimates over a small temporal and spatial scale though each had its own advantages and limitations with regard to sampling black sea bass. For example, our single unbaited video system was simple and relatively inexpensive to build, easy to deploy and haul from depth, needed little maintenance or attention while sampling, and provided a way to obtain direct video observations of fish behavior and bottom habitats. However, processing videos and recording fish observations in the laboratory was time consuming and required large amounts data storage space. In contrast, sampling with hook-and-line gear was easy to implement with low-cost equipment and produced less variable abundance estimates but required fresh bait and multiple individuals to sample and record catch information. Hook-and-line sampling also afforded the option of collecting fish size information and biological samples but occasionally caused mortality due to deep hooking and/or barotrauma (Bugley and Shepherd, 1991). Considering the strengths of each gear type, it is recommended that both be used in combination when sampling black sea bass on a range of inshore habitats. Similarly, the sampling limitations of each gear, including the effects of cloud cover and current velocity, provide further evidence that their combined use for sampling black sea bass is warranted. Underwater video could overcome the effects of decreased bottom exposure time of bait due to increased current velocity or wind speed during hook-and-line sampling. In contrast, hook-and-line sampling could provide estimates of CPUE when cloud cover or water turbidly limits bottom lighting and visibility during video system deployments. However, despite the benefits of combined sampling, additional studies are needed to evaluate the sampling efficiencies of both gear types over greater temporal and spatial scales to determine if either could be employed as a survey tool for assessing black sea bass abundance in Mid-Atlantic waters. With larger sample sizes, future studies could evaluate the power of each gear's ability to detect changes (*e.g.* minimum % change, effect size % increase or decrease) in CPUE estimates over space and time as well as between locations with different bottom habitats (Willis *et al.*, 2003; Bennett *et al.*, 2009; Harvey *et al.*, 2012).

Acknowledgements

The authors thank the boat captains who helped with sampling. Thanks to the students who assisted with data collection and anonymous reviewers whose comments improved the manuscript. Financial support for this work was provided by the NOAA Educational Partnership Program with Minority-Serving Institutions (EPP/MSI; FY 2016 Award #NA16SEC4810007) through the NOAA Living Marine Resources Cooperative Science Center at the University of Maryland Eastern Shore.

References

Arendt, M. D., Lucy, J. A., and Evans, D. A. 2001. Diel seasonal activity patterns of adult tautog, *Tautoga onitis*, in lower Chesapeake Bay, inferred from ultrasonic telemetry. *Environmental Biology of Fishes,* **62**: 379–391. https://doi.org/10.1023/A:1012266214143.

Bacheler, N. M., Geraldi, N. R., Burton, M. L., Muñoz, R. C., and Kellison, G. T. 2017. Comparing relative abundance, lengths, and habitat of temperate reef fishes using simultaneous underwater visual census, video, and trap sampling. *Marine Ecology Progress Series,* **574**: 141–155. https://doi.org/10.3354/meps12172.

Bacheler, N. M., Schobernd, C. M., Schobernd, Z. H., Mitchell, W. A., Berrane, D. J., Kellison, G. T., and Reichert, M. J. M. 2013a. Comparison of trap and underwater video gears for indexing reef fish presence and abundance in the southeast United States. *Fisheries Research,* **143**: 81–88. https://doi.org/10.1016/j.fishres.2013.01.013.

Bacheler, N. M., Schobernd, Z. H., Berrane, D. J., Schobernd, C. M., Mitchell, W. A., and Geraldi, N. R. 2013b. When a trap is not a trap: converging entry and exit rates and their effect on trap saturation of black sea bass (*Centropristis striata*). *ICES Journal of Marine Science,* **70**: 873–882. https://doi.org/10.1093/icesjms/fst062.

Bacheler, N. M., Schobernd, Z. H., Berrane, D. J., Schobernd, C. M., Mitchell, W. A., Teer, B. Z., Gregalis, K. C., and Glasgow, D. M. 2016. Spatial Distribution of reef fish species along the southeast US Atlantic coast inferred from underwater video survey data. *PLoS ONE,* **11**: e0162653. https://doi.org/10.1371/journal.pone.0162653.

Bacheler, N. M., and Shertzer, K. W. 2015. Estimating relative abundance and species richness from video surveys of reef fishes. *Fishery Bulletin,* **113**: 15–26. doi:10.7755/FB.113.1.2.

Bennett, R. H., Götz, A., Sauser, W. H. H., Cowley, P. D., and Palmer, R. M. 2009. Optimization of underwater visual census and controlled angling methods for monitoring subtidal temperate reef fish communities. *African Journal of Marine Science,* **31**: 277–287. https://doi.org/10.2989/AJMS.2009.31.3.1.989.

Bugley, K., and Shepherd, G. 1991. Effect of catch-and-release angling on the survival of black sea bass. *North American Journal of Fisheries Management,* **11**: 468–471. https://doi.org/10.1577/1548-8675(1991)011<0468:MBEOCA>2.3.CO;2.

Campbell, M. D., Pollack, A. G., Gledhill, C. T., Switzer, T. S., and DeVries, D. A. 2015. Comparison of relative abundance indices calculated from two methods of generating video count data. *Fisheries Research,* **170**: 125–133. https://doi.org/10.1016/j.fishres.2015.05.011.

Cullen, D. W., and Stevens, B. G. 2017. Use of an underwater video system to record observations of black sea bass (*Centropristis striata*) in waters off the coast of Maryland.

Fishery Bulletin, **115**: 408–418. doi:10.7755/FB.115.3.10.

De Robertis, A., and Handegard, N. O. 2013. Fish avoidance of research vessels and the efficacy of noise-reduced vessels: a review. *ICES Journal of Marine Science,* **70**: 34–45. https://doi.org/10.1093/icesjms/fss155.

Drohan, A. F., Manderson, J. P., and Packer, D. B. 2007. Essential fish habitat source document: black sea bass, *Centropristis striata*, life history and habitat characteristics, 2nd ed. *NOAA Tech. Memo.,* NMFS-NE-200, 68 p.

Fabrizio, M. C., Manderson, J. P., and Pessutti, J. P. 2013. Habitat associations and dispersal of black sea bass from a mid-Atlantic Bight reef. *Marine Ecology Progress Series,* **482**: 241–253. https://doi.org/10.3354/meps10302.

Harms, J. H., Wallace, J. R., and Stewart, I. J. 2010. Analysis of fishery-independent hook and line-based data for use in the stock assessment of bocaccio rockfish (*Sebastes paucispinis*). *Fisheries Research,* **106**: 298–309. https://doi.org/10.1016/j.fishres.2010.08.010.

Harley, S. J., Myers, R. A., and Dunn, A. 2001. Is catch-per-unit-effort proportional to abundance? *Can. J. Fish. Aquat. Sci.,* **58**: 1760–1772. https://doi.org/10.1139/f01-112.

Harvey, E. S., Newman, S. J., McLean, D. L., Cappo, M., Meeuwig, J. J., and Skepper, C. L. 2012. Comparison of the relative efficiencies of stereo-BRUVs and traps for sampling tropical continental shelf demersal fishes. *Fisheries Research,* **125**:108–120. https://doi.org/10.1016/j.fishres.2012.01.026.

Gerstner, C. L. 1998. Use of substratum ripples for flow refuging by Atlantic cod, *Gadus morhua*. *Environmental Biology of Fishes,* **51**: 455-460. https://doi.org/10.1023/A:1007449630601.

Kulbicki, M. 1988. Correlation between catch data from bottom longlines and fish censures in the SW lagoon of New Caledonia. *Proceedings of the 6th International Coral Reef Symposium,* **2**: 305–312.

Kuriyama, P. T., Branch, T. A., Hicks, A. C., Harms, J. H., and Hamel, O. S. 2019. Investigating three sources of bias in hook-and-line surveys: survey design, gear saturation, and multispecies interactions. *Can. J. Fish. Aquat. Sci.,* **76**: 192–207. https://doi.org/10.1139/cjfas-2017-0286.

Newman, S. P., Rasmussen, P. W. and Andrews, L. M. 1997. Comparison of a stratified, instantaneous count creel survey with a complete mandatory creel census on Escanaba Lake, Wisconsin. *North American Journal of Fisheries Management,* **17**: 321–330. https://doi.org/10.1577/1548-8675(1997)017<0321:COASIC>2.3.CO;2.

Millar, R. B., and Willis, T. J. 1999. Estimating the relative density of snapper in and around a marine reserve using a log-linear mixed-effects model. *Australian & New Zealand Journal of Statistics,* **41**: 383–394. https://doi.org/10.1111/1467-842X.00092.

Moser, J., and Shepherd, G. R. 2009. Seasonal distribution and movement of black sea bass (*Centropristis striata*) in the northwest Atlantic as determined from a mark-recapture experiment. *J. Northw. Atl. Fish. Sci.,* **40**: 17–28. https://doi.org/10.2960/J.v40.m638.

Musick, J. A., and Mercer, L. P. 1977. Seasonal distribution of black sea bass, *Centropristis striata*, in the Mid-Atlantic Bight with comments on the ecology and fisheries of the species. *Fishery Bulletin,* **40**: 479–488. https://doi:10.1577/1548-8659(1977)106<12:SDOBSB>2.0.CO;2.

NEFSC (Northeast Fisheries Science Center). 2017. 62nd northeast regional stock assessment workshop (62nd SAW) assessment report. *NEFSC Ref. Doc.,* 17-03, 822 p. https://www.nefsc.noaa.gov/publications/crd/.

Parker, D., Winker, H., Bernard, A. T. F., Heyns-Veale, E. R., Langlois, T. J., Harvey, E. S., and Götz, A. 2016. Insights from baited video sampling of temperate reef fishes: how biased are angling surveys? *Fisheries Research,* **179**: 191-201. https://doi.org/10.1016/j.fishres.2016.02.025.

Pennington, M., and T. Stromme. 1998. Surveys as a research tool for managing dynamic stocks. *Fisheries Research,* **37**: 97–106. https://doi.org/10.1016/S0165-7836(98)00129-5.

Pinheiro, J., Bates, D., DebRoy, S., Sarkar, D., and R Core Team. 2018. nlme: linear and nonlinear mixed effects models. R package vers. 3.1–137. http://CRAN.R-project.org/package=nlme.

Poisson, F., Gaertner, J-C., Taquet, M., Durbec, J-P., and Bigelow, K. 2010. Effects of lunar cycle and fishing operations on longline-caught pelagic fish: fishing performance, capture time, and survival of fish. *Fishery Bulletin,* **108**: 268–281.

R Core Team. 2018. R: a language and environment for statistical computing. R Foundation for Statistical Computing, Vienna, Austria. http://www.r-project.org.

Ralston, S. 1990. Size selection of snappers (*Lutjanidae*) by hook and line gear. *Can. J. Fish. Aquat. Sci.,* **47**: 696–700. https://doi.org/10.1139/f90-078.

Richards, L. J., and Schnute, J. T. 1986. An experimental and statistical approach to the question: is CPUE an index of abundance. *Can. J. Fish. Aquat. Sci.,* **43**: 1214–1227. https://doi.org/10.1139/f86-151.

RStudio Team. 2018. RStudio: Integrated development for R. RStudio, Inc., Boston, MA. http://www.rstudio.com/.

Rotherham, D., Underwood, A. J., Chapman, M. G., and Gray, C. A. 2007. A strategy for developing scientific sampling tools for fishery-independent surveys of estuarine fish in New South Wales, Australia. *ICES Journal of Marine Science,* **64**: 1512–1516. https://doi.org/10.1093/icesjms/fsm096.

Schweitzer, C. C., and Stevens, B. G. 2019. The relationship between fish abundance and benthic community structure on artificial reefs in the Mid-Atlantic Bight, and the importance of sea whip corals *Leptogorgia virgulata*. *PeerJ,* **7**: e7277. http://doi.org/10.7717/peerj.7277.

Schobernd, C. M., and Sedberry, G. R. 2009. Shelf-edge and upper-slope reef fish assemblages in the south Atlantic bight: habitat characteristics, spatial variation, and reproductive behavior. *Bulletin of Marine Science,* **84**: 67–92.

Schobernd, Z. H., Bacheler, N. M., and Conn, P. B. 2014. Examining the utility of alternative video monitoring metrics for indexing reef fish abundance. *Can. J. Fish. Aquat. Sci.,* **71**: 464–471. https://doi.org/10.1139/cjfas-2013-0086.

Shepherd, G. R., and Terceiro, M. 1994. The summer flounder, scup, and black sea bass fishery of the Middle Atlantic Bight and southern New England waters. *NOAA Tech. Rep.*, NMFS 122, 13 p.

Sheremet, V. A. 2010. SeaHorse Tilt Current Meter: inexpensive near-bottom current measurements based on drag principle with coastal applications. Eos, Transactions, American Geophysical Union 91, *Ocean Science Meeting Supplement*, Abstract PO25C-13.

Sokal, R. R., and Rohlf, F. J. 1995. Biometry: The Principles and Practice of Statistics in Biological Research, 3rd ed., W.H. Freeman and Company, New York, 887 pp.

Steimle, F. W., and Zetlin, C. 2000. Reef habitats in the Middle Atlantic Bight: abundance, distribution, associated biological communities, and fishery resource use. *Marine Fisheries Review,* **62**: 24–42.

Stobart, B., Díaz, D., Álvarez, F., Alonso, C., Mallol, S., and Goñi, R. 2015. Performance of baited underwater video: does it underestimate abundance at high population densities? *PLoS ONE,* **10**: e0127559. https://doi.org/10.1371/journal.pone.0127559.

von Szalay, P. G., Somerton, D. A., and Kotwicki, S. 2007. Correlating trawl and acoustic data in the eastern Bering Sea: a first step toward improving biomass estimates of walleye pollock (*Theragra chalcogramma*) and Pacific cod (*Gadus macrocephalus*)? *Fisheries Research,* **86**: 77–83. https://doi.org/10.1016/j.fishres.2007.05.005.

Wells, R. J. D., Boswell, K. M., Cowan Jr., J. H. and Patterson III, W. F. 2008. Size selectivity of sampling gears targeting red snapper in the northern Gulf of Mexico. *Fisheries Research,* **89**: 294–299. https://doi.org/10.1016/j.fishres.2007.10.010.

Willis, T. J., and Babcock., R. C., 2000. A baited underwater video system for the determination of relative density of carnivorous reef fish. *Marine and Freshwater Research,* **51**: 755–763. https://doi.org/10.1071/MF00010.

Willis, T. J., Millar, R. B., and Babcock, R. C. 2000. Detection of spatial variability in relative density of fishes: comparison of visual census, angling, and baited underwater video. *Marine Ecology Progress Series,* **198**: 249–260. https://doi.org/10.3354./meps198249.

2003. Protection of exploited fish in temperate regions: high density and biomass of snapper *Pagrus auratus* (Sparidae) in northern New Zealand marine reserves. *Journal of Applied Ecology,* **40**: 214–227. https://doi.org/10.1046/j.1365-2664.2003.00775.x.

Willis, T. J., Badalamenti, F., and Milazzo, M. 2006. Diel variability in counts of reef fishes and its implications for monitoring. *Journal of Experimental Marine Biology and Ecology,* **331**: 108–120. https://doi.org/10.1016/j.jembe.2005.10.003.

Zurr, A., Ieno, E. N., Walker, N., Saveliev, A. A., and Smith, G. M. 2009. Mixed effects models and extensions in ecology with R, Springer-Verlag, New York, 574 pp.

J. Northw. Atl. Fish. Sci., Vol. 51: 15–31 Publication (Upload) date: 26 Jun 2020

Spatiotemporal variability in Atlantic sea scallop (*Placopecten magellanicus*) growth in the Northern Gulf of Maine

Cameron T. Hodgdon[1,3], Michael Torre[1,2], and Yong Chen[1]

[1]University of Maine, School of Marine Sciences, Orono, ME 04469, USA
[2]University of Washington, School of Aquatic and Fishery Sciences, Seattle, WA 98195, USA
[3]Corresponding Author's Present Institution and Address: University of Maine, School of Marine Sciences, 5741 Libby Hall Room 221, Orono, ME 04469, USA

Cameron T. Hodgdon's Email (Corresponding Author): cameron.hodgdon@maine.edu
Michael Torre's Email: michael.torre@maine.edu
Yong Chen's Email: ychen@maine.edu

Hodgdon, C.T., Torre, M., and Chen, Y. 2020. Spatiotemporal variability in Atlantic sea scallop (*Placopecten magellanicus*) growth in the Northern Gulf of Maine. *J. Northw. Atl. Fish. Sci.*, **51:** 15–31. https://doi.org/10.2960/J.v51.m729

Abstract

Simulation-based assessment tools coupled with large-scale and consistent monitoring efforts contribute to the overall success of the Atlantic sea scallop (*Placopecten magellanicus*; ASC) fishery on the North American east coast. However, data from the Northern Gulf of Maine (NGOM) are usually excluded from the assessment because limited monitoring effort and an overall lack of information regarding the growth of ASCs in this region have led to large uncertainty of fine-scale dynamics. The objectives of this study are to determine if ASC growth varies spatially and/or temporally across the NGOM and if the variation in growth can be explained in part by variability in bottom temperature and bottom salinity. To achieve these objectives, ASC shells have been continually collected through a partnership between the University of Maine and Maine Department of Marine Resources since 2006. Individualistic ASC length-at-age curves are developed to evaluate small and large scale spatio-temporal variabilities. In comparison to ASC growth on Georges Bank and in Southern New England, it appears that ASCs in the NGOM are growing at a similar rate yet have the potential to grow to a larger size. No clear spatio-temporal trends in ASC growth are identified in the NGOM. However, our analysis reveals that bottom temperature and bottom salinity may be influencing inter-annual variabilities and contribute to growth rate differences seen between locations and years. This may imply changes in ASC growth in the future with increasing warming in the Gulf of Maine.

Keywords: Atlantic sea scallop, Environmental drivers, Gulf of Maine, Von Bertalanffy growth parameters

Introduction

The Atlantic sea scallop (*Placopecten magellanicus*; ASC) is a historically important commercial bivalve on the North American east coast. In the United States, ASCs are harvested from Cape Hatteras, North Carolina to Cobscook Bay, Maine (Hart and Chute, 2004). ASC biomass (in metric tons of meat) has more than doubled in the last decade over their range (NEFSC 2018) and ASCs are not overfished and overfishing is not occurring (NEFSC, 2018). This is due largely to extant and detailed approaches used to manage this fishery on a large-scale level. Techniques have been developed that allow for population-wide simulations under different fishing scenarios to determine catch limits per area for consecutive years (Rheuban *et al.,* 2018; NEFSC, 2018). However, areas like the Northern Gulf of Maine (NGOM) are usually excluded from these predictive models because of lack of information regarding the growth of ASCs in these regions. More southern areas such as Georges Bank (GBK) and the Mid-Atlantic Bight (MAB) are high-production fishing grounds for this species and so the bulk of knowledge concerning ASC growth rates has been from samples collected from these areas (Hart and Chute, 2009a; Hart and Chute, 2009b; Mann and Rudders, 2019).

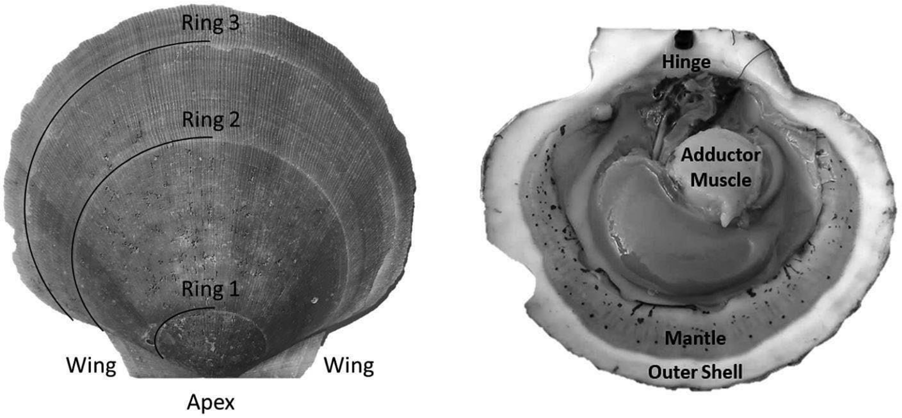

Fig. 1. An ASC top shell (left) and bottom shell (right) with important features labelled. Growth rings are outlined for this three year old specimen.

A scallop is a bivalve mollusk, having two hardened calcium carbonate structures connected by a hinge and a large adductor muscle (Fig. 1). Unlike exoskeletal animals that shed their outer layers during a molt, scallops must expand their shell as they grow (Marin and Luquet, 2004). Because of this, they must constantly be laying down new material. This new material (in the form of the aforementioned calcium carbonate) is set in place on the outer edges of shells, resulting in ring formation much like trees (Hart and Chute, 2009a; Hart and Chute, 2009b). This growth allows for simple calculation of length-at-age curves (a.k.a. growth curves). The rings are formed due to seasonal changes in growth rates; with shell formation being faster in the warmer months and slower in the colder months (Côté *et al.,* 1993; Harris and Stokesbury, 2006; Hart and Chute, 2009a; Hart and Chute, 2009b), forming a single ring per year of growth. This is due to the direct effect that environmental variables (such as temperature and salinity) have on the metabolism of the animals (Côté *et al.,* 1993). Many studies have demonstrated linkages between the rate of ASC growth and environmental conditions such as temperature, salinity, and depth (MacDonald and Thompson, 1985a; MacDonald and Thompson, 1985b; Thouzeau *et al.,* 1991; Harris and Stokesbury, 2006; Hart and Chute, 2009a; Chute *et al.,* 2012), yet few studies have looked at the spatiotemporal variation of these effects at finer spatial scales than large marine ecosystems (LMEs) such as GBK and the MAB.

Climate change is causing the NGOM ecosystem to warm at an accelerated rate compared with a majority of the world's oceans; with an average-per-year increasing temperature of 0.026˚C (Pershing *et al.,* 2015). Bottom temperature and bottom salinity fluctuate around yearly means as seasons change, but these yearly means for both variables are rising in the face of climate change (Pershing *et al.,* 2015; Saba *et al.,* 2016). This means that ASC growth has the potential to change as well. If it can be understood how these environmental variables affect ASC growth in the NGOM, it can be inferred if and how their growth will change into the future.

Understanding spatiotemporal variation in growth is important for the management of any marine resource, especially those in an environment experiencing rapid environmental changes (Maunder and Piner, 2015). Mann and Rudders (2019) stated the importance of understanding age/length structures to inform the current assessment model for ASCs in GBK and the MAB, referring to using this information to enhance the current understanding of ASC recruitment and mortality. Assuming incorrect growth structures can lead to large effects on stock assessment outcomes and incorrect management advice (Maunder and Piner, 2015). Little is known about the NGOM LME as it pertains to ASC growth, accentuating the increased likelihood of wrongly assumed growth parameters. Most information about NGOM ASC growth comes from a singular study by Truesdell (2014), wherein growth is analyzed across different spatial zones in the NGOM. In short, Truesdell (2014) concluded that NGOM scallops grow to larger sizes, yet grow slower than scallops in GBK and the MAB. This study, however, only addresses spatial differences in growth and spatial effects of environmental variables.

The objectives of this study were to 1) Determine if ASC growth varies spatially and/or temporally across the four management zones in the NGOM (Fig. 2) and 2) Determine if variation in ASC growth in these areas and across years can be explained in part by bottom temperature and bottom salinity. To achieve these objectives, von Bertalanfy growth parameters for multiple locations and age

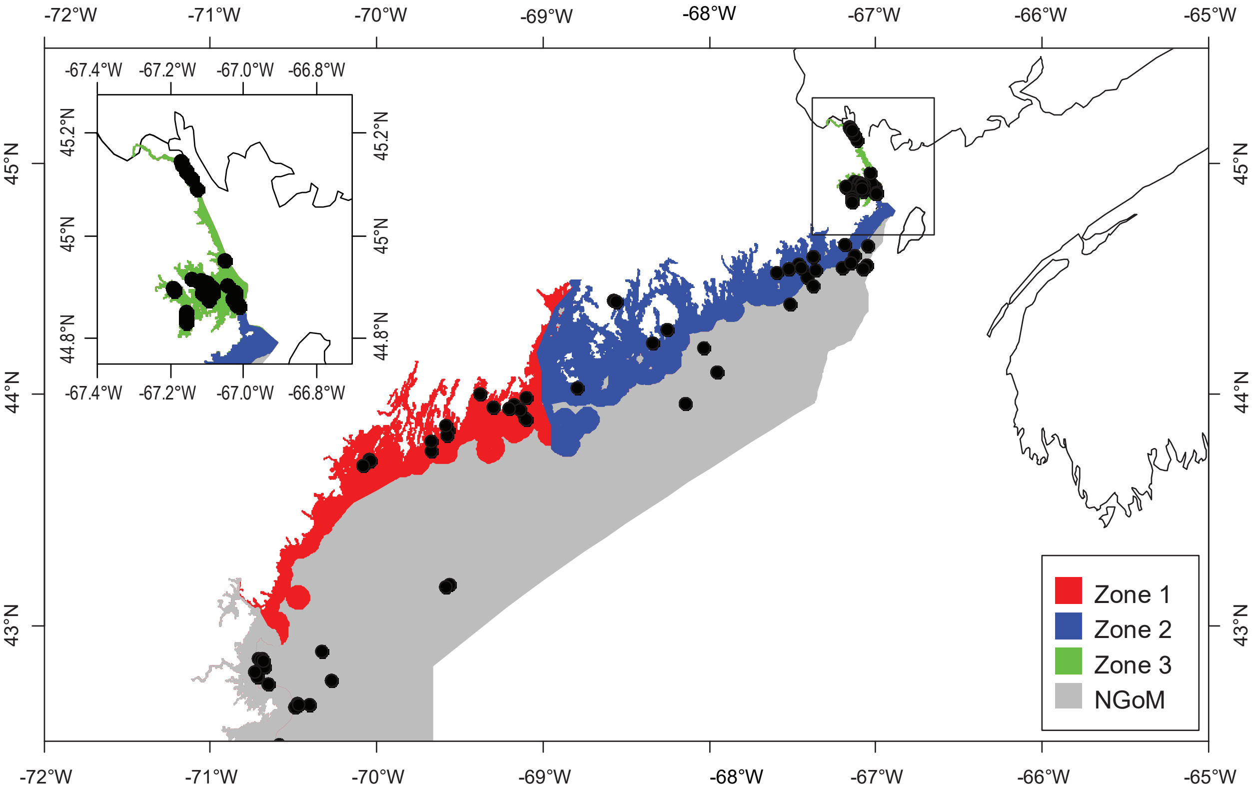

Fig. 2. The Northern Gulf of Maine (management zone 4; grey) with management zones 1–3 colored red, blue, and green, respectively. Black dots represent locations where scallops were collected over the entire survey.

classes are determined using methods from Hart and Chute (2009a) and growth increment data is used in multiple regression analyses to determine relative influence of environmental factors bottom temperature and bottom salinity as well as spatial (latitude and longitude) and time-varying (year of growth) factors. This same process to determine spatiotemporal variation and influence of environmental factors can be applied to many bivalve species whose historical size-at-age is determinable from their shells or for fish species who have reliable otolith size to fish length relationships.

Methods

Study Area

The NGOM management area (Fig. 2) is the most northern extent of the United States' ASC stock. This area is managed on smaller scales: namely inshore (<3 nautical miles (nm) from shore) and offshore (>3nm from shore). The inshore NGOM is split into three distinct management sections: Zone 1 (commonly referred to as the Western Gulf of Maine), Zone 2 (commonly referred to as the Eastern Gulf of Maine), and Zone 3 (Cobscook Bay; Fig. 2), with each zone having slightly different management techniques, but the same management entity: the Maine Department of Marine Resources (MDMR). The offshore NGOM (referred to here as management zone 4) is treated as a single large unit and is managed jointly at both state and federal levels (by MDMR and the New England Fishery Management Council).

The NGOM is characterized as having fluctuating yearly temperatures and salinities, influenced by a combination of the warm and salty North-bound Gulf Stream and the colder, less salty South-bound Labrador Current (Durbin *et al.,* 2003; Wanamaker *et al.,* 2008). Additionally, year to year variations are also present in these variables due to changing ratios of incoming water masses due to climate change (Mills *et al.,* 2013; Pershing *et al.,* 2015), resulting in higher observed temperatures and salinities.

Ageing and Growth Modelling

A partnership between the University of Maine and the MDMR has been responsible for collecting ASC shells from the study area since 2006 which are subsequently stored at the University of Maine until they are aged.

Part of these shells were utilized for Truesdell's (2014) analyses, but the sample size has been greatly improved in recent years with additional samples being collected from broader areas in the NGOM.

Aging of shells followed methods from Hart and Chute (2009a). Each shell is measured from the apex (center of the hinge; Fig. 1) to each consecutive ring, producing a number of data points for each scallop as there are visible rings. The number of rings, though, is not always indicative of absolute age, however. The first two years of growth of an ASC are not as predictable or uniform as from two years onward. Because of this, the one-year growth ring or the two-year growth ring may be the first visible ring. Agers are taught how to infer which year the first visible ring corresponds to based on typical shell size-at-age, as well as which rings are actual growth rings, and which are false rings caused by stress (additionally, each new person introduced to the project partakes in a trial period to make sure their ageing technique does not produce measurements statistically dissimilar from previous agers). The differences between these data points is what is known as incremental growth. Fabens (1965) has modified the von Bertallanfy growth function to model this particular type of growth data. The function is as follows:

$$\mathrm{L}_{t+1} = \exp\left(-\mathrm{K}\right) \times \mathrm{L}_{t} + \mathrm{L}_{\infty} \times \left(1 - \exp\left(-\mathrm{K}\right)\right) \tag{1}$$

where L_t is the length at time t, L_{t+1} is the length at time t+1, L_∞ is the theoretical asymptotic maximum size at which length approaches, and K is the Brody growth coefficient.

Following Hart and Chute (2009a), L_∞ and K were found for each individual ASC via the Ford-Walford method, in which L_∞ and K are found from a linear fit of all L_t and L_{t+1} pairs for each individual with at least 3 growth rings (the same cutoff used by Hart and Chute, 2009a). Once L_∞ and K values were found for each individual, population values for each Zone (1, 2, and 3) as well as for offshore waters were established. Additionally, the entire NGOM population was also split into year classes with sufficient sample sizes (1998–2010). These results could not be obtained from a regression of all data points in each group due to the possibility of large bias (Hart and Chute, 2009a). Nor could they be obtained simply from taking an average of all individual values for L_∞ and K for the same reason. Thus, following the methods outlined by Hart and Chute (2009a),

$$m_i = \exp\left(-K_i\right) \tag{2}$$

$$b_i = L_{\infty,i} \times \left(1 - m_i\right) \tag{3}$$

representing the slope and intercept of each individual's L_{t+1} vs L_t plot respectively, were obtained (with K_i and $L_{\infty,i}$ representing the K and L_∞ of individual i). Additionally, $m = \mathrm{mean}(m_i)$ and $b = \mathrm{mean}(b_i)$, representing the population slope and population intercept respectively, were calculated. Letting α_i and β_i represent the deviations of each m_i from m and each b_i from b, respectively, the equations for approximating population L_∞ and K values are as follows (Hart and Chute, 2009a):

$$\mathrm{L}_{\infty} \cong \frac{b}{1-m} + \frac{1}{(1-m)^2} \times \left(\frac{b \times \mathrm{Var}\left(\alpha_i\right)}{1-m} + \mathrm{Cov}\left(\alpha_i, \beta_i\right)\right) \tag{4}$$

$$\mathrm{K} \cong -\ln(m) + \frac{\mathrm{Var}\left(\alpha_i\right)}{2 \times m^2} \tag{5}$$

with $\mathrm{Var}(\alpha_i)$ and $\mathrm{Cov}(\alpha_i,\beta_i)$, being the variance of α_i and covariance of α_i and β_i, respectively. Additionally, the standard errors (σ) of L_∞ and K were approximated as (Hart and Chute, 2009a):

$$\sigma_{\mathrm{L}_\infty} \cong L_\infty^2 \times \left(\frac{\sigma_b^2}{b^2} + \frac{\sigma_m^2}{(1-m)^2} + \frac{2 \times \sigma_b \times \sigma_m \times \rho}{b \times (1-m)}\right) \tag{6}$$

$$\sigma_k \cong \frac{\sigma_m}{m} \tag{7}$$

with $\sigma_{L\infty}$, σ_K, σ_b, and σ_m representing the standard errors of L_∞, K, b, and m respectively. All calculations were completed using R software (version 3.4.1). All R scripts used in modelling and analyses can be made available upon request.

Modelling Environmental Effects

L_∞ and K cannot be associated with a particular year, only a location (they are constant throughout an individual scallop's life). Thus, these values cannot be matched to any time-dependent environmental covariates. Because of these limitations, a different response variable had to be chosen for regression testing. The variable chosen was the change in length from one ring to the next: the growth over the course of a time-step in millimeters: Δmm. Because ASCs are sedentary after their spat stage (before 1 year old), each Δmm can be associated with a location (latitude and longitude), a time (year of growth), and by extension, abiotic variables associated with those locations and averaged over that year. The variables used in this study were bottom temperature (Figs. 3 and 4) and bottom salinity (Fig. 5). Additionally, because Δmm varies widely between age classes, separate regression tests were conducted for each, allowing for any age-specific environmental interactions to be explored.

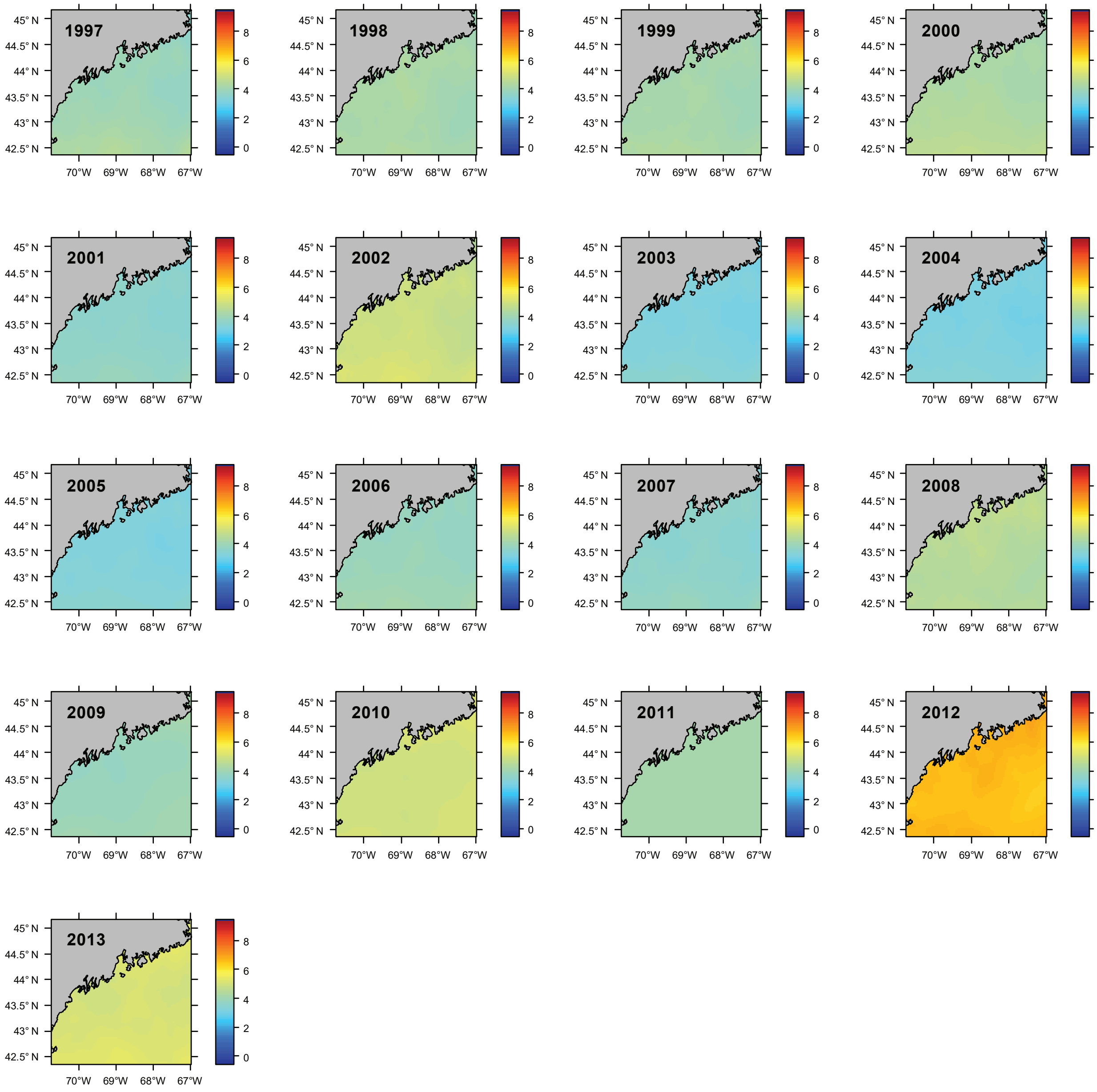

Fig. 3. Average yearly bottom temperature over the study region 1997-2013. Temperature values are in degrees Celsius.

Bottom temperature and bottom salinity data were obtained from University of Massachusetts (UMass) Dartmouth School for Marine Science and Technology (SMAST)'s Finite Volume Community Ocean Model (FVCOM). This geophysical model has been shown to have reliable performance in predicting bottom water parameters at fixed locations called stations, especially for well-stratified areas like the NGOM (Li *et al.,* 2017). For each ASC, an average bottom temperature and salinity was obtained for each year of its growth. If the location of the tow was within ½ kilometer (km) of a FVCOM station, then the closest station was used to determine the abiotic conditions at the tow location. If no FVCOM station existed within ½ km radius, then the average of all FVCOM stations within a 1 km by 1 km grid centered on the tow location was used as a proxy.

Correlation coefficient calculation and variance inflation factor (VIF) tests were used to determine which combinations of predictor variables could be used together to have reliable regression output. Correlation coefficient values outside the range of (-0.5, 0.5) for a correlation coefficient meant those variables could not be used in the same test due to high collinearity. VIF values greater than

10 represent high multi-collinearity and do not allow for those variables to be used together in the same regression (O'brien 2007). These methods were used in tandem: correlation coefficients for all combinations of two factors were calculated and then VIF tests were conducted on all factor combinations used in regressions. This was done as to assume high robustness in factor selection for regression testing.

Three different types of regression testing were conducted on each combination of factors that passed the two-step process above: linear regression (LR), boosted regression trees (BRT), and generalized additive models (GAMs). Model selection was based on root mean squared error (RMSE) and Akaike information criterion (AIC). Additionally, in an effort to further explore patterns in temporal trends, an additional six regression tests were run for each age class with year of growth as the only predictor variable only for ASCs from Cobscook Bay. The intent of these six models was to see if temporal trends could be more readily determinable if spatial differences were ignored.

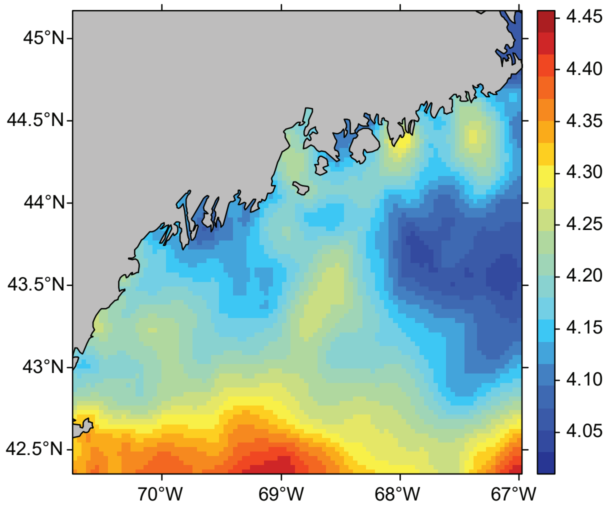

Fig. 4. Average bottom temperature over the study region averaged across years 1997–2013. Temperature values are in degrees Celsius.

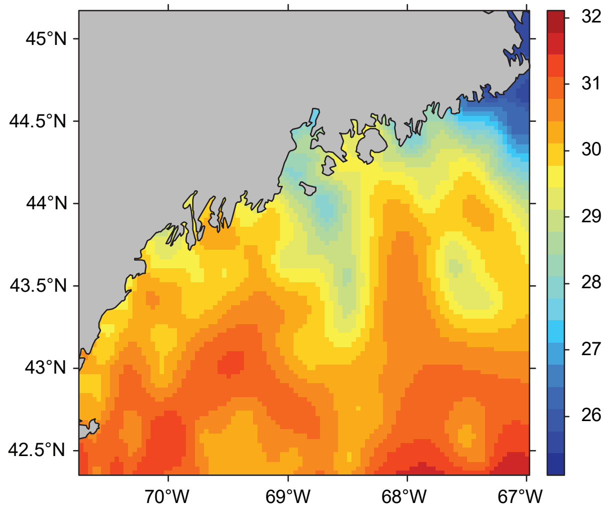

Fig. 5. Average bottom salinity over the study region averaged across years 1997–2013. Salinity values are in parts per thousand.

Results

Spatial Differences in Growth Parameters L_∞ and K

Final L_∞ and K spatial values with associated standard errors are presented in Tables 1 and 2. L_∞ was statistically different in the NGOM compared to Georges Bank (GB) and the Mid-Atlantic Bight (MAB) (One-way Anova test: $F(2, 9030) = 654.54$, $p < 0.01$, Tukey's post hoc: all $p < 0.01$), with an apparent increasing trend in L_∞ with increasing latitude (Table 1). K was statistically different in the NGOM compared to GB and the MAB (One-way Anova test: $F(2, 9030) = 227.50$, $p < 0.01$, Tukey's post hoc: all $p < 0.01$), but no trend was apparent (Table 1). Data for GB scallops and MAB scallops were obtained from Truesdell (2014) and Hart and Chute (2009a).

Table 1. Mean L_∞ and K values with associated standard errors (SE) and sample sizes (*n*) for the Northern Gulf of Maine (NGOM), Georges Bank (GBK), and the Mid-Atlantic Bight (MAB).

	L_∞(mm)		K(1/yr)		
Area	**Mean**	**SE**	**Mean**	**SE**	***n***
NGOM	154.05	0.58	0.45659	0.00384	2 647
GBK	143.9	0.23	0.427	0.00172	4 092
MAB	133.3	0.28	0.508	0.00271	2 294

Table 2. Mean L_∞ and K values with associated standard errors (SE) and sample sizes (*n*) for each of four management zones in the Northern Gulf of Maine.

	L_∞(mm)		K(1/yr)		
Zone	**Mean**	**SE**	**Mean**	**SE**	***n***
1	152.72	1.21	0.44656	0.00877	448
2	173.08	2.01	0.36869	0.00985	298
3	142.97	0.71	0.50646	0.00552	1262
1+2+3	150.3	0.63	0.47154	0.00437	2014
4	166.71	1.36	0.40203	0.00757	639
1+2+3+4	154.05	0.58	0.45659	0.00384	2647

Table 3. Mean L_∞ and K values with associated standard errors (SE) and sample sizes (*n*) for year classes of Atlantic sea scallops from 1998 to 2010.

	L_∞(mm)		K(1/yr)		
Year Class	**Mean**	**SE**	**Mean**	**SE**	***n***
2011	-	-	-	-	2
2010	135.73	2.47	0.61338	0.03821	50
2009	132.73	2.01	0.59659	0.03372	36
2008	149.09	3.68	0.345	0.02594	19
2007	179.43	9.00	0.35026	0.04863	14
2006	155.47	1.75	0.47155	0.0144	111
2005	157.76	2.27	0.38128	0.01262	128
2004	169.36	3.48	0.30349	0.01446	80
2003	155.37	2.54	0.34145	0.01804	59
2002	154.02	3.41	0.27901	0.01909	22
2001	150.17	3.84	0.37391	0.04103	11
2000	140.10	2.23	0.49285	0.02046	79
1999	153.38	3.95	0.36228	0.0204	34
1998	166.09	5.83	0.35855	0.04746	17
1997	-	-	-	-	3
All	154.05	0.58	0.45659	0.00384	2 647

Within the NGOM, L_∞ was statistically different in all 4 management zones (One-way ANOVA test: $F(3, 2643) = 146.02$, $p < 0.01$, Tukey's post hoc: all $p < 0.01$), with highest values in Zone 2 and lowest in Zone 3 (Table 2). K was statistically different across all three inshore zones, but Zone 4 was only statistically different from zones 1 and 3 (One-way ANOVA test: $F(3, 2643) = 67.89$, $p < 0.01$, Tukey's post hoc: $p < 0.01$ for zone parings 1and2, 1and3, 1andoffshore, 2and3, and 3andoffshore, $p > 0.05$ for zone pairing 2andoffshore), with highest values in Zone 3 and lowest values in Zone 2 (Table 2). ASCs in Zone 1 appear to have the potential to grow to larger sizes than those in Zone 2, yet at a slower rate (Table 2). Cobscook Bay scallops (Zone 3) grow very rapidly, but do not reach the large sizes they do in the rest of the NGOM. Additionally, offshore (Zone 4) ASCs tend to grow at similar rates to scallops in Zone 1.

Table 4. Tukey's Post Hoc test results for One-way ANOVA test of L_∞ in year classes 1998 through 2010 ($F(12, 647) = 742.18$, $p < 0.01$). p values are presented right of black boxes and a "*" left of black boxes denotes statistical significance with $\alpha = 0.05$.

	2010	**2009**	**2008**	**2007**	**2006**	**2005**	**2004**	**2003**	**2002**	**2001**	**2000**	**1999**	**1998**
2010	■	<0.01	<0.01	<0.01	<0.01	<0.01	<0.01	<0.01	<0.01	<0.01	<0.01	<0.01	<0.01
2009	*	■	<0.01	<0.01	<0.01	<0.01	<0.01	<0.01	<0.01	<0.01	<0.01	<0.01	<0.01
2008	*	*	■	<0.01	<0.01	<0.01	<0.01	<0.01	<0.01	1.00	<0.01	<0.01	<0.01
2007	*	*	*	■	<0.01	<0.01	<0.01	<0.01	<0.01	<0.01	<0.01	<0.01	<0.01
2006	*	*	*	*	■	<0.01	<0.01	1.00	0.69	<0.01	<0.01	0.03	<0.01
2005	*	*	*	*	*	■	<0.01	<0.01	<0.01	<0.01	<0.01	<0.01	<0.01
2004	*	*	*	*	*	*	■	<0.01	<0.01	<0.01	<0.01	<0.01	<0.01
2003	*	*	*	*		*	*	■	0.85	<0.01	<0.01	0.11	<0.01
2002	*	*	*	*		*	*		■	0.03	<0.01	1.00	<0.01
2001	*	*		*	*	*	*	*	*	■	<0.01	0.11	<0.01
2000	*	*	*	*	*	*	*	*	*	*	■	<0.01	<0.01
1999	*	*	*	*	*	*	*				*	■	<0.01
1998	*	*	*	*	*	*	*	*	*	*	*	*	■

Table 5. Tukey's Post Hoc test results for One-way ANOVA test of K in year classes 1998 through 2010 ($F(12, 647) = 978.41$, $p < 0.01$). p values are presented right of black boxes and a "*" left of black boxes denotes statistical significance with $\alpha = 0.05$.

	2010	**2009**	**2008**	**2007**	**2006**	**2005**	**2004**	**2003**	**2002**	**2001**	**2000**	**1999**	**1998**
2010	■	0.05	<0.01	<0.01	<0.01	<0.01	<0.01	<0.01	<0.01	<0.01	<0.01	<0.01	<0.01
2009	*	■	<0.01	<0.01	<0.01	<0.01	<0.01	<0.01	<0.01	<0.01	<0.01	<0.01	<0.01
2008	*	*	■	1.00	<0.01	<0.01	<0.01	1.00	<0.01	0.05	<0.01	0.29	0.86
2007	*	*		■	<0.01	<0.01	<0.01	0.99	<0.01	0.34	<0.01	0.91	1.00
2006	*	*	*	*	■	<0.01	<0.01	<0.01	<0.01	<0.01	<0.01	<0.01	<0.01
2005	*	*	*	*	*	■	<0.01	<0.01	<0.01	1.00	<0.01	<0.01	0.01
2004	*	*	*	*	*	*	■	<0.01	<0.01	<0.01	<0.01	<0.01	<0.01
2003	*	*			*	*	*	■	<0.01	<0.01	<0.01	<0.01	0.25
2002	*	*	*	*	*	*	*	*	■	<0.01	<0.01	<0.01	<0.01
2001	*	*	*		*		*	*	*	■	<0.01	0.96	0.88
2000	*	*	*	*	*	*	*	*	*	*	■	<0.01	<0.01
1999	*	*			*	*	*	*	*		*	■	1.00
1998	*	*			*	*	*		*		*		■

Temporal Differences in Growth Parameters L_∞ and K

Final L_∞ and K temporal values with associated standard errors are presented in Table 3. L_∞ was statistically different in most year classes than others, but with no discernable trend over the time series (One-way ANOVA test: $F(12, 647) = 742.18$, $p < 0.01$, Tukey's post hoc results presented in Table 4). K was statistically different in some year classes than others, but with no discernable trend over the time series (One-way ANOVA test: $F(12, 647) = 978.4075$, $p < 0.01$, Tukey's post hoc results presented in Table 5).

Regression Model Selection

Correlation coefficients and VIF values (Tables 6 and 7, respectively) allowed for 14 unique combinations of predictor variables. LR could not capture the appropriate

Table 6. A correlation matrix of all predictor variables used in this study. Values denote the correlation coefficients of those predictor variable pairings. Any variable pair corresponding to a correlation coefficient outside the range of (-0.5, 0.5) were not used together in this study. Two pairings were outside this range: Latitude with Longitude and Latitude with Salinity. These combinations could not be used in the same regression analysis. Lat = Latitude, Lon = Longitude, Temp = Temperature, Sal = Salinity, Year = Year of Growth, Δmm = change in scallop shell size from one year to the next: shown here only to determine the direction and strength of relationships with each predictor variable in regression testing.

	Year	**Lat**	**Lon**	**Temp**	**Sal**	**Δmm**
Year	-	-0.16	-0.11	-0.24	0.12	-0.19
Lat	-0.16	-	0.95	0.19	-0.53	0.13
Lon	-0.11	0.95	-	0.13	-0.37	0.11
Temp	-0.24	0.19	0.13	-	-0.11	0.19
Sal	0.12	-0.53	-0.37	-0.11	-	-0.03
Δmm	-0.19	0.13	0.11	0.19	-0.03	-

Table 7. Variance inflation factors (VIF) of fourteen different combinations (rows) of abiotic variables used in the generalized additive models. Blank cells represent the absence of that variable in the combination. No VIF test was done on single parameter models or models with location interaction terms.

	Abiotic Factors				
	Year of Growth	**Latitude**	**Longitude**	**Temperature**	**Salinity**
1	1.07	-	-	1.07	1.02
2	-	-	-	1.01	1.01
3	1.06	-	-	1.06	-
4	1.01	-	-	-	1.01
5	1.07	1.05	-	1.09	-
6	1.03	1.03	-	-	-
7	-	1.04	-	1.04	-
8	1.07	-	1.18	1.07	1.17
9	-	-	1.17	1.02	1.17
10	1.07	-	1.02	1.07	-
11	1.02	-	1.17	-	1.17
12	1.01	-	1.01	-	-
13	-	-	1.02	1.02	-
14	-	-	1.16	-	1.16

Table 8. Root-mean-squared-error (RMSE) values of different generalized additive models for combinations of abiotic variables and age class. Lat = Latitude, Lon = Longitude, Temp = Temperature, Sal = Salinity, Year = Year of Growth. Models surrounded with 'I()' are treated as a single interaction term.

	Age Class					
	0-2	**2-3**	**3-4**	**4-5**	**5-6**	**6-7**
Lat	9.30	8.28	5.80	4.89	4.38	3.69
Lon	9.21	8.16	5.75	4.92	4.32	3.52
Year/Temp/Sal	8.71	8.02	5.61	4.70	4.18	3.49
Temp/Sal	9.03	8.13	5.61	4.77	4.21	3.56
Year/Temp	9.10	8.25	5.69	4.94	4.30	3.67
Year/Sal	8.76	8.07	5.66	4.78	4.21	3.58
Year	9.18	8.39	5.77	5.00	4.31	3.80
Temp	9.58	8.46	5.69	5.04	4.42	3.85
Sal	9.23	8.19	5.80	4.88	4.23	3.64
Year/Temp/Lat	8.72	7.98	5.61	4.68	4.22	3.60
Year/Lat	8.77	8.10	5.69	4.76	4.29	3.62
Temp/Lat	9.13	8.14	5.61	4.74	4.35	3.65
Year/Temp/Sal/Lon	8.39	7.86	5.47	4.61	4.08	3.42
Temp/Sal/Lon	8.72	7.88	5.48	4.64	4.17	3.56
Year/Temp/Lon	8.66	7.93	5.57	4.75	4.21	3.47
Year/Sal/Lon	8.44	7.88	5.57	4.67	4.14	3.56
Year/Lon	8.64	7.99	5.69	4.76	4.27	3.49
Temp/Lon	9.06	7.99	5.57	4.76	4.25	3.50
Sal/Lon	8.92	7.98	5.64	4.73	4.18	3.49
I(Year/Lat/Lon)	8.44	7.76	5.53	4.73	4.34	3.40
I(Temp/Lat/Lon)	8.71	7.76	5.57	4.74	4.31	3.37
I(Sal/Lat/Lon)	8.71	7.69	5.55	4.69	4.11	3.40

trends in the data available. Due to very poor fit, this regression type was rejected. BRT and GAM both well outperformed LR, with BRT usually having lower RMSE (Table 9) and AIC values (Table 13) when compared to GAM (Table 8 for RMSE and Table 12 for AIC). However, GAMs allowed for the additional testing of spatial interaction terms more efficiently. Due to a general agreement in trends between BRT and GAM output, results from both types of regression testing are presented. Conclusions are made from both types of models.

Nineteen BRTs were run for each of six ASC age classes (Tables 9, 11, and 13): totaling 114 regression outputs. Twenty-two GAMs were run for each of six age classes (Table 8, 10, and 12): totaling 132 regression outputs. This discrepancy again is the testing of spatial interactions on single variables. An additional six GAMs were used to explore temporal trends in Cobscook Bay (see section 2.3). Neither GAMs nor BRTs are inherently and universally better than the other and model performance and fit depends on the data set (Martínez-Rincón *et al.,* 2012). This accentuates the importance of testing multiple methodologies for modelling different data sets.

Results of Regression Analyses

Deviances explained (DE) and AICs for all 114 BRTs in this study are presented in Tables 11 and 13, respectively. Highest DEs and lowest AICs usually coincided with each other (most being associated with the BRT with predictor variables year of growth, temperature, salinity, and longitude), with the exception of age classes 3–4 and 5–6.

Even so, differences were not substantial. DEs and AICs for all 132 GAMs in this study are presented in Tables 10 and 12, respectively. Highest DEs and lowest AICs usually coincided with each other (most being associated with the GAM with predictor variables year of growth, temperature, salinity, and longitude), with the exception of age classes 2–3 and 6–7. Even so, differences were not substantial.

DEs for BRTs were usually higher than those for GAMs. All DEs for GAMs were seemingly low; no DE surpassing 27%. The same was true for BRTs, with no DE surpassing 37%. Bottom temperature and salinity, therefore, are only capable of explaining at most 37% of the variance in ASC growth in the NGOM. Salinity alone explained more of the deviance in both types of models than temperature alone for all age classes, meaning ASCs in the NGOM appear to be affected more by salinity than by temperature. Concerning only the GAMs, predictor variables that included an interaction with location (both latitude and longitude) highly outperformed their counterparts; the same variable without a location interaction. This means that both temperature and salinity may affect ASC growth non-linearly over space and influences may vary by location. No clear trend was found to exist as a function of age class. The results of the correlation coefficient matrix (Table 6) seem to reveal that Δmm has very weak positive relationships with each of the predictor variables except for year of growth and salinity, which both appear to be very weak negative relationships.

The six regression analyses using data only from Cobscook Bay ASCs revealed results very similar to results pooled from the entire NGOM (Table 14), with the exception of the BRT for age class 3–4, whose DE was considerably high. In general, ignoring any spatial differences, it appears that year of growth alone does not sufficiently describe trends seen in scallop growth over time. This corroborates findings from section 3.2. It is important to note that of these analyses, only the first three age classes provided reliable results (Table 14). This was due to the often low number of older individuals (>4 years) found in Cobscook Bay over the time series.

Table 9. Root-mean-squared-error (RMSE) values of different boosted regression trees for combinations of abiotic variables and age class. Lat = Latitude, Lon = Longitude, Temp = Temperature, Sal = Salinity, Year = Year of Growth.

	Age Class					
	0-2	**2-3**	**3-4**	**4-5**	**5-6**	**6-7**
Lat	9.03	8.21	5.54	4.77	4.31	3.58
Lon	8.85	8.16	5.52	4.88	4.41	3.66
Year/Temp/Sal	8.74	7.96	5.50	4.72	4.30	3.68
Temp/Sal	8.95	7.99	5.52	4.71	4.26	3.69
Year/Temp	9.01	8.17	5.62	4.90	4.41	3.68
Year/Sal	8.85	8.05	5.59	4.75	4.31	3.63
Year	9.22	8.47	5.74	5.01	4.37	3.77
Temp	9.35	8.22	5.64	4.93	4.37	3.86
Sal	9.10	8.09	5.60	4.79	4.29	3.64
Year/Temp/Lat	8.65	8.06	5.45	4.67	4.34	3.63
Year/Lat	8.71	8.12	5.50	4.73	4.39	3.57
Temp/Lat	8.98	8.14	5.50	4.69	4.34	3.62
Year/Temp/Sal/Lon	8.48	7.81	5.38	4.58	4.30	3.62
Temp/Sal/Lon	8.65	7.87	5.40	4.59	4.25	3.57
Year/Temp/Lon	8.52	8.07	5.43	4.70	4.37	3.69
Year/Sal/Lon	8.52	7.84	5.41	4.65	4.23	3.59
Year/Lon	8.58	8.08	5.50	4.77	4.42	3.69
Temp/Lon	8.77	8.04	5.42	4.70	4.37	3.69
Sal/Lon	8.74	7.88	5.46	4.71	4.26	3.65

Table 10. Deviance explained (DE) of different generalized additive models for combinations of abiotic variables and age class. Lat = Latitude, Lon = Longitude, Temp = Temperature, Sal = Salinity, Year = Year of Growth. Models surrounded with 'I()' are treated as a single interaction term. Highest DE for each are class are bolded.

	Age Class					
	0–2	**2–3**	**3–4**	**4–5**	**5–6**	**6–7**
Lat	9.18	7.70	2.90	14.90	4.16	12.23
Lon	10.82	10.38	4.53	13.86	6.62	20.00
Year/Temp/Sal	20.41	13.41	9.25	21.34	12.89	21.38
Temp/Sal	14.29	11.04	9.26	19.07	11.30	18.00
Year/Temp	13.12	8.36	6.72	13.05	7.72	13.01
Year/Sal	19.49	12.49	7.66	18.79	11.47	17.45
Year	11.46	5.26	3.86	10.99	7.11	6.95
Temp	3.62	3.64	6.61	9.59	2.20	4.18
Sal	10.57	9.78	3.05	15.35	10.73	14.58
Year/Temp/Lat	20.20	14.29	9.28	22.17	11.19	16.17
Year/Lat	19.25	11.80	6.79	19.32	8.09	15.38
Temp/Lat	12.43	10.97	9.19	20.10	5.55	14.10
Year/Temp/Sal/Lon	**26.06**	16.91	**13.58**	**24.28**	**16.84**	24.47
Temp/Sal/Lon	20.07	16.37	13.51	23.22	13.23	18.17
Year/Temp/Lon	21.17	15.48	10.58	19.74	11.42	22.05
Year/Sal/Lon	25.26	16.37	10.38	22.50	14.21	18.06
Year/Lon	21.55	14.03	6.70	19.28	8.84	21.22
Temp/Lon	13.78	14.14	10.54	19.46	9.69	20.78
Sal/Lon	16.51	14.42	8.41	20.32	12.89	21.41
I(Year/Lat/Lon)	25.16	19.08	11.89	20.55	5.77	25.26
I(Temp/Lat/Lon)	20.42	19.06	10.40	19.99	7.05	**26.77**
I(Sal/Lat/Lon)	20.30	**20.35**	11.08	21.57	15.64	25.32

Discussion

ASC in the NGOM appear to be growing to a larger size and growing at dissimilar rates when compared to populations in Georges Bank and the Mid-Atlantic Bight (Table 1; Truesdell, 2014; Hart and Chute, 2009a). A trend in growth coefficient L_∞ seems to be occurring up the Atlantic coast, with ASCs of the Mid-Atlantic Bight having the lowest values and ASCs of the NGOM having the largest (Table 1). This is similar to findings from Truesdell (2014), which showed larger L_∞ values for the NGOM region. Within the NGOM, ASC growth seems to vary spatially: varying between management zones (Table 2). This is again similar to findings by Truesdell (2014), but this study presents higher calculations of both L_∞ and K for most regions. This could be due to the addition of new data since 2014 mostly concentrated inshore, where higher coefficients were observed.

This study expanded on work by Truesdell (2014), calculating growth coefficients for each year class. With low sample sizes questioning the reliability of some year classes, it doesn't appear that ASC growth parameters are changing in a predictable way. They do seem to be fluctuating and ANOVA tests revealed those fluctuations result in year classes that are statistically different from one another. Due to the ever-changing location of MDMR tow stations in this project over the time series coupled with the low sample size per year class in this analysis, this fluctuation and by extent the statistical differences may not be what would be observed with larger sample sizes over the same time series. However, when spatial data were ignored in the Cobscook Bay subsample regression tests (which also have the highest density of samples of any region in this study), there was no more considerable influence of year of growth when compared to the original analyses with spatially pooled data over years.

These differences in growth over time do not match the change in the abiotic parameters observed in this study. Given that the regression analyses revealed that these parameters do have influence on ASC growth in the NGOM, it could be that pooling all data spatially does not allow for observation of these influences. Given that many studies have shown strong links between growth and temperature and salinity (Thouzeau *et al.,* 1991; Stewart and Arnold, 1994; Hart and Chute, 2004), these effects may occur at finer spatial scales than what was used in this study. This highlights the need for more samples in the future so that finer spatial resolutions than what was utilized in this study can be explored.

The regression tests revealed that ASCs in the NGOM appear to be influenced by both temperature and salinity when abiotic data are not observed as spatial averages over time. However, these influences are relatively weak considering the deviance explained values associated with the tests. This highlights an important constriction of this study: abiotic data were temporally averaged in order to be associated with an increment of ASC growth. Future studies should look at abiotic ranges, anomalies, normality of distribution, and the like to infer more fine-scale temporal influences of these variables. Knowing this as a limitation, it can be assumed that the influence of temperature and salinity on ASC growth in the NGOM would be at least as strong as what was observed in this study, but has the potential to be stronger if abiotic data in a form other than yearly averages were utilized.

Additionally, when temperature and salinity were supplied with an interaction term of location, the DE rises substantially. This could mean that ASCs in different areas of the Gulf of Maine respond differently to similar abiotic variables. This is most likely because these variables are acting in this study as a proxy for other variables known to heavily influence ASC growth such as phytoplankton density (Macdonald and Thompson, 1985a; Macdonald and Thompson, 1985b; Macdonald *et al.,* 1987). Phyto-

Table 11. Deviance explained (DE) of different boosted regression trees for combinations of abiotic variables and age class. Lat = Latitude, Lon = Longitude, Temp = Temperature, Sal = Salinity, Year = Year of Growth. Highest DE for each are class are bolded.

	Age Class					
	0–2	**2–3**	**3–4**	**4–5**	**5–6**	**6–7**
Lat	23.09	23.80	17.03	24.05	4.44	18.19
Lon	23.50	23.06	17.82	23.68	5.85	22.67
Year/Temp/Sal	31.89	28.64	24.92	30.28	12.37	24.17
Temp/Sal	28.93	27.89	25.10	27.84	12.56	19.55
Year/Temp	23.88	20.56	19.14	24.53	9.99	8.20
Year/Sal	27.83	25.31	21.31	25.94	10.34	19.31
Year	11.80	4.65	3.93	11.28	7.24	10.22
Temp	20.16	19.69	19.50	24.00	3.09	8.90
Sal	23.46	24.09	20.49	24.03	10.17	16.70
Year/Temp/Lat	34.12	28.07	24.75	27.15	12.01	22.80
Year/Lat	30.77	25.10	20.30	27.44	6.67	19.45
Temp/Lat	29.70	28.00	24.55	27.80	7.56	16.33
Year/Temp/Sal/Lon	**36.37**	**32.25**	26.20	**32.42**	15.34	**25.63**
Temp/Sal/Lon	33.68	32.06	**26.22**	31.21	10.88	25.28
Year/Temp/Lon	33.96	28.62	23.02	30.29	11.60	24.79
Year/Sal/Lon	35.29	30.21	24.31	30.99	15.23	21.11
Year/Lon	30.61	24.69	19.98	26.45	9.62	19.72
Temp/Lon	30.22	28.69	23.97	30.21	6.20	23.30
Sal/Lon	31.40	29.53	25.01	31.92	**15.40**	23.25

Table 12. Akaike information criterion (AIC) of different generalized additive models for combinations of abiotic variables and age class. Lat = Latitude, Lon = Longitude, Temp = Temperature, Sal = Salinity, Year = Year of Growth. Models surrounded with 'I()' are treated as a single interaction term. Lowest AIC values for each age class are bolded.

	Age Class					
	0-2	**2-3**	**3-4**	**4-5**	**5-6**	**6-7**
Lat	14076	12748	10106	5234	2130	904
Lon	14040	12695	10079	5248	2130	893
Year/Temp/Sal	13850	12652	10017	5197	2111	891
Temp/Sal	13980	12690	10015	5208	2110	895
Year/Temp	14006	12752	10045	5271	2121	906
Year/Sal	13862	12669	10042	5213	2114	894
Year	14028	12795	10085	5278	2122	905
Temp	14191	12823	10045	5292	2136	913
Sal	14047	12707	10104	5234	2113	896
Year/Temp/Lat	13860	12649	10017	5189	2115	896
Year/Lat	13867	12684	10052	5204	2120	896
Temp/Lat	14024	12700	10017	5196	2128	905
Year/Temp/Sal/Lon	**13730**	12598	**9958**	**5173**	**2108**	**890**
Temp/Sal/Lon	13864	12605	9957	5179	2110	897
Year/Temp/Lon	13817	12624	9994	5204	2115	893
Year/Sal/Lon	13735	12605	10005	5188	2109	895
Year/Lon	13811	12638	10053	5207	2117	892
Temp/Lon	13992	12635	9993	5205	2128	894
Sal/Lon	13932	12629	10031	5197	2111	894
I(Year/Lat/Lon)	13736	12550	9979	5212	2130	895
I(Temp/Lat/Lon)	13858	12551	10006	5213	2128	894
I(Sal/Lat/Lon)	13860	**12521**	9995	5196	2120	896

plankton represent ASC food supply and mollusk growth has been shown to be highly correlated with phytoplankton density (Pilditch and Grant, 1999; Weiss *et al.,* 2007). Phytoplankton density is a function of temperature, salinity, and other factors (Wagner *et al.,* 2001; Friedland *et al.,* 2015). The interaction term of location could be accounting for some of these other location-sensitive variables in the NGOM. This could also hinder the ability to determine direct abiotic-growth relationships if most influence is acting through a different force and these highly complex abiotic-growth relationships acting through proxy would be difficult for regression models to calculate. This accentuates the assumption that abiotic-growth influences were underestimated in this study. However, this study was aware of this connection when selecting the original model parameters. Given that the Gulf of Maine is changing rapidly in the face of climate change (Pershing *et al.,* 2015), it was important to determine any direct relationships that ASC growth had to the abiotics directly affected by this change: temperature and salinity. This is why no model selection process took place based on AIC. This study was not meant to create a model for ASC growth, but to use multiple models to tease apart relationships.

Even though abiotic-growth relationships were relatively weak in this study, they were still present. These relationships have the potential to be affected in the coming years by climate change. Warming rates for the NGOM are suggested between 0.02˚C and 0.07˚C per year (Pershing *et al.,* 2015) for sea-surface temperature, with bottom temperature experiencing this same trend (Pershing *et al.,* 2015; Saba *et al.,* 2016). Average yearly bottom temperature mean for all sample locations in this study area in recent years (2012–2016) averaged around 7.60˚C. These values are below optimal growth temperatures of 10.0˚C to 15.0˚C for ASC (Thouzeau *et al.,* 1991; Hart and Chute, 2004), and well below the maximum temperature threshold of 21.0˚C (Hart and Chute, 2004). Bottom salinity is also expected to rise for the NGOM under climate change (Saba *et al.,* 2016). Average yearly bottom salinity mean for all sample locations in this study area in recent years (2012–2016) averaged around 31.9‰. These values are below optimal growth salinity of full strength seawater: ~35‰ (Stewart and Arnold, 1994; Hart and Chute, 2004). With temperature and salinity in the NGOM both rising, and because of the relationships teased apart in this study, as well as support from previous research on optimal growth conditions (Thouzeau *et al.,* 1991; Stewart and Arnold 1994; Hart and Chute, 2004), there is potential for ASCs to grow faster and/or larger. However, this conclusion is strictly based on direct and uniform relationships. Most studies focused on determining abiotic influence to ASC growth usually linking fluctuations directly to something like metabolic activity (Pilditch and Grant, 1999) and are done so in the lab. If conclusions from these studies state high influence of variables like temperature and salinity to growth, this may not be that accurate in a natural setting where these variables are acting both directly and through proxy. Because these variables are most likely acting both directly on ASC metabolism and indirectly through things such as food availability and can vary spatiotemporally, it can be difficult to infer the magnitude of the change in ASC growth given large changes in temperature and salinity.

Other ASC stock characteristics like abundance are more easily calculable from abiotic data through use of habitat suitability indices (HSIs). Torre *et al.* (2018) suggests that inshore habitats will become more suitable for ASCs in the NGOM as temperature and salinity rise. With suitable habitat predicted to rise and with a potential for increased growth, the NGOM may be able to support a higher intensity fishery in the future.

Table 13. Akaike information criterion (AIC) of different boosted regression trees for combinations of abiotic variables and age class. Lat = Latitude, Lon = Longitude, Temp = Temperature, Sal = Salinity, Year = Year of Growth. Lowest AIC values for each age class are bolded.

	Age Class					
	0-2	**2-3**	**3-4**	**4-5**	**5-6**	**6-7**
Lat	8271	7272	5334	2659	1082	416
Lon	8261	7290	5318	2663	1077	407
Year/Temp/Sal	8041	7158	5179	2588	1054	408
Temp/Sal	8121	7175	5173	2616	1052	415
Year/Temp	8254	7349	5295	2655	1062	437
Year/Sal	8151	7238	5251	2639	1061	416
Year	8535	7676	5566	2794	1071	431
Temp	8343	7367	5285	2659	1087	433
Sal	8262	7265	5266	2659	1059	419
Year/Temp/Lat	7977	7172	5183	2627	1056	410
Year/Lat	8071	7243	5272	2621	1075	415
Temp/Lat	8100	7172	5185	2617	1072	422
Year/Temp/Sal/Lon	**7912**	**7066**	5154	**2563**	1044	406
Temp/Sal/Lon	7990	7070	**5151**	2577	1061	**405**
Year/Temp/Lon	7982	7158	5219	2588	1058	406
Year/Sal/Lon	7943	7118	5192	2580	1042	414
Year/Lon	8075	7253	5278	2633	1064	415
Temp/Lon	8086	7155	5197	2587	1077	407
Sal/Lon	8053	7134	5175	2566	**1040**	407

Table 14. Deviance explained (DE) and Akaike information criterion (AIC) for three generalized additive models (GAM) and three boosted regression trees (BRT) run using only year of growth as a predictor variable per age class for only the Cobscook Bay region. Low counts of Atlantic sea scallops older than 4 years in Cobscook Bay made results from age classes 4–5, 5–6, and 6–7 unreliable and are thus not presented. Lat = Latitude, Lon = Longitude, Temp = Temperature, Sal = Salinity, Year = Year of Growth.

	Age Class					
	0–2	**2–3**	**3–4**	**4–5**	**5–6**	**6–7**
BRT DE	10.83	4.96	14.34	-	-	-
BRT AIC	6504	5823	4431	-	-	-
GAM DE	15.12	5.18	4.77	-	-	-
GAM AIC	10767	10090	8391	-	-	-

There is need for more research concerning ASC life history and climate change to better understand their dynamics in the inshore NGOM. This study has shown the impact of abiotic variables on ASC growth to be weak yet present in this region. As suggested in other studies, biotic variables such as phytoplankton density, are posited to be more influential to ASC growth with abiotic variables influencing ASC growth directly and through this proxy of food availability. Future research should consider biotic variables as well as geospatial variables such as depth in an effort to better understand the NGOM ASC population dynamics.

Acknowledgements

We thank all the research assistants who help read the scallop ages. We additionally thank Dr. D. Hart and T. Chute of NOAA Northeast Fisheries Science Center and Dr. Sam Truesdell of MA Marine Fisheries for training in scallop aging. Lastly, we thank the Maine Department of Marine Resources and NOAA Fisheries for sample and data collection. The financial support of this study was provided by the Maine Department of Marine Resources and NOAA Scallop RSA Program. There is no conflict of interest declared in this article.

References

Chute, T., Wainright, S., and Hart, D. 2012. Timing of shell ring formation and patterns of shell growth in the sea scallop *Placopecten magellanicus* based on stable oxygen isotopes. *Journal of Shellfish Research*, **31**: 649–662. https://doi.org/10.2983/035.031.0308

Côté, J., Himmelman, J., Claereboudt, M., and Bonardelli, J. 1993. Influence of density and depth on growth of juvenile sea scallops (*Placopecten magellanicus)* in suspended culture. *Canadian Journal of Fisheries and Aquatic Sciences,* **50**: 1857–1869. https://doi.org/10.1139/f93-208

Durbin, E., Campbell, R., Casas, M., Ohman, M., Niehoff, B., Runge, J., and Wagner, M. 2003. Interannual variation in phytoplankton blooms and zooplankton productivity and abundance in the Gulf of Maine during winter. *Marine Ecology Progress Series*, **254**: 81–100. https://doi.org/10.3354/meps254081

Fabens, A. 1965. Properties and fitting of the von Bertalanffy growth curve. *Growth*, **29:** 265–289

Friedland, K., Leaf, R., Kane, J., Tommasi, D., Asch, R., Rebuck, N., Ji, R., Large, S., Stock, C., and Saba, V. 2015. Spring bloom dynamics and zooplankton biomass response on the US Northeast Continental Shelf. *Continental Shelf Research*, **102**: 47–61. https://doi.org/10.1016/j.csr.2015.04.005

Harris, B., and Stokesbury, K. 2006. Shell growth of sea scallops (*Placopecten magellanicus*) in the southern and northern Great South Channel, USA. *ICES Journal of Marine Science*, **63**: 811–821. https://doi.org/10.1016/j.icesjms.2006.02.003

Hart, D., and Chute, T. 2004. Sea scallop, *Placopecten magellanicus*, life history and habitat characteristics. *NOAA Technical Memorandum,* NMFS-NE-189. 32 pp.

Hart, D., and Chute, T. 2009a. Estimating von Bertalanffy growth parameters from growth increment data using a linear mixed-effects model, with an application to the sea scallop *Placopecten magellanicus*. *ICES Journal of Marine Science*, **66**: 2165–2175. https://doi.org/10.1093/icesjms/fsp188

Hart, D., and Chute, T. 2009b. Verification of Atlantic sea scallop (*Placopecten magellanicus*) shell growth rings by tracking cohorts in fishery closed areas. *Canadian Journal of Fisheries and Aquatic Sciences*, **66**: 751–758. https://doi.org/10.1139/F09-033

Li, B., Tanaka, K., Chen, Y., Brady, D., and Thomas, A. 2017. Assessing the quality of bottom water temperatures from the Finite-Volume Community Ocean Model (FVCOM) in the Northwest Atlantic Shelf region. *Journal of Marine Systems*, **173**: 21–30. https://doi.org/10.1016/j.jmarsys.2017.04.001

Marin, F., and Luquet, G. 2004. Molluscan Shell Proteins. *Comptes Rendus Palevol*, **3**(6-7): 469–492. https://doi.org/10.1016/j.crpv.2004.07.009

MacDonald, B., and Thompson, R. 1985a. Influence of temperature and food availability on the ecological energetics of the giant scallop *Placopecten magellanicus* I: growth rates of shell and somatic tissue. *Marine Ecology Progress Series,* **25**: 279–294. https://doi.org/10.3354/meps025279

MacDonald, B., and Thompson, R. 1985b. Influence of temperature and food availability on the ecological energetics of the giant scallop *Placopecten magellanicus* II: reproductive output and total production. *Marine Ecology Progress Series,* **25**: 295–303. https://doi.org/10.3354/meps025295

Macdonald, B., Thompson, R., and Bayne, B. 1987. Influence of temperature and food availability on the ecological energetics of the giant scallop *Placopecten magellanicus* IV: reproductive effort, value and cost. *Oecologia*, **72:** 550–556. https://doi.org/10.1007/BF00378981

Mann, R. and Rudders, D. 2019. Age structure and growth rate in the sea scallop *Placopecten magellanicus*. Virginia Institute of Marine Science, College of William and Mary.

Martínez-Rincón, R., Ortega-García, S., and Vaca-Rodríguez, J. 2012. Comparative performance of generalized additive models and boosted regression trees for statistical modeling of incidental catch of wahoo (*Acanthocybium solandri*) in the Mexican tuna purse-seine fishery. *Ecological Modelling*, **233**: 20–25. https://doi.org/10.1016/j.ecolmodel.2012.03.006

Maunder, M. and Piner, K. 2015. Contemporary fisheries stock assessment: many issues still remain. *ICES Journal of Marine Science*, **72**(1): 7–18. https://doi.org/10.1093/icesjms/fsu015

Mills, K., Pershing, A., Brown, C., Chen, Y., Chiang, F., Holland, D., Lehuta, S., Nye, J., Sun, J., Thomas, A., and Wahle, R. 2013. Fisheries Management in a Changing Climate: Lessons from the 2012 Ocean Heat Wave in the Northwest Atlantic. *Oceanography*, **26**(2): 191–195. https://doi.org/10.5670/oceanog.2013.27

Northeast Fisheries Science Center (NEFSC). 2018. 65th Northeast Regional Stock Assessment Workshop (65th SAW) Assessment Summary Report. US Department Commerce, Northeast Fisheries Science Center Reference Document. 18–08; 38 pages. Available from: http://www.nefsc.noaa.gov/publications/

O'brien, R. 2007. A Caution Regarding Rules of Thumb for Variance Inflation Factors. *Quality and Quantity*, **41**(5): 673–690. https://doi.org/10.1007/s11135-006-9018-6

Pershing, A., Alexander, M., Hernandez, C., Kerr, L., Le Bris, A., Mills, K., Nye, J., Record, N., Scannell, H., Scott, J., Sherwood, G., and Thomas, A. 2015. Slow adaptation in the face of rapid warming leads to collapse of the Gulf of Maine cod fishery. *Science*, **350**(6262): 809–812. https://doi.org/10.1126/science.aac9819

Pilditch, C., and Grant, J. 1999. Effect of temperature fluctuations and food supply on the growth and metabolism of juvenile sea scallops (*Placopecten magellanicus*). *Marine Biology*, **134**(2): 235–248. https://doi.org/10.1007/s002270050542

Rheuban, J., Doney, S., Cooley, S., and Hart, D. 2018. Projected impacts of future climate change, ocean acidification, and management on the US Atlantic sea scallop (*Placopecten magellanicus*) fishery. *PLoS ONE*, **13**(9). https://doi.org/10.1371/journal.pone.0203536

Saba, V., Griffies, S., Anderson, W., Winton, M., Alexander, M., Delworth, T., Hare, J., Harrison, M., Rosati, A., Vecchi, G., and Zhang, R. 2016. Enhanced warming of the Northwest Atlantic Ocean under climate change. *Journal of Geophysical Research: Oceans*, **121**: 118–132. https://doi.org/10.1002/2015JC011346

Stewart, P., and Arnold, S. 1994. Environmental requirements of the sea scallop (*Placopecten magellanicus*) in eastern Canada and its response to human impacts. *Canadian Technical Report of Fisheries and Aquatic Sciences,* 2005:1–36.

Thouzeau, G., Robert, G., and Smith, S. 1991. Spatial variability in distribution and growth of juvenile and adult sea scallops *Placopecten magellanicus* (Gmelin) on eastern Georges Bank (Northwest Atlantic). *Marine Ecology Progress Series*, **74**: 205–218. https://doi.org/10.3354/meps074205

Truesdell, S. 2014. Distribution, Population Dynamics and Stock Assessment for the Atlantic Sea Scallop (*Placopecten magellanicus*) in the Northeast US [PhD Thesis]. University of Maine, Orono, Maine.

Wagner, M., Campbell, R., Boudreau, C., and Durbin, E. 2001. Nucleic acids and growth of *Calinus finmarchicus* in the laboratory under different food and temperature conditions. *Marine Ecology Progress Series*, **221**: 185–197. https://doi.org/10.3354/meps221185

Wanamaker Jr., A., Kreutz, K., Schöne, B., Pettigrew, N., Borns, H., Introne, D., Belknap, D., Maasch, K., and Feindel, S. 2007. Coupled North Atlantic slope water forcing on Gulf of Maine temperatures over the past millennium. *Climate Dynamics*, **31**(2-3): 183–194. https://doi.org/10.1007/s00382-007-0344-8

Weiss, M., Curran, P., Peterson, B., and Gobler, C. 2007. The influence of plankton composition and water quality on hard clam (*Mercenaria mercenaria* L.) populations across Long Island's south shore lagoon estuaries (New York, USA). *Journal of Experimental Marine Biology and Ecology*, **345**: 12–25. https://doi.org/10.1016/j.jembe.2006.12.025

J. Northw. Atl. Fish. Sci., Vol. 51: 33–43 Publication (Upload) date: 08 Jul 2020

Evaluating sampling strategies for collecting size-based fish fecundity data: an example of Gulf of Maine northern shrimp *Pandalus borealis*

Hsiao-Yun Chang and Yong Chen
School of Marine Sciences, University of Maine, Orono, ME 04469, USA
Correspondence: Hsiao-Yun Chang; E-mail: hsiaoyun.chang@maine.edu

Chang, H.-Y., and Chen, Y. 2020. Evaluating sampling strategies for collecting size-based fish fecundity data: an example of Gulf of Maine northern shrimp *Pandalus borealis*. *J. Northw. Atl. Fish. Sci.*, **51:** 33–43. https://doi.org/10.2960/J.v51.m730

Abstract

Fecundity information is critical in determining reproductive potential of a population. Collecting fecundity data, however, can be cost prohibitive or ineffective if a sampling protocol is not well designed. Inappropriate sampling can lead to biased estimates of fecundity, which may result in biased estimate of reproductive potential. Processing egg samples tends to be time-consuming and labour-intensive. For many fish and crustacean species, fecundity is dependent on female sizes. Nevertheless, at extreme size classes, fecundity may decrease or level off due to senescence. In order to account for this maternal effect, female sample of a wide size range need to be collected for developing a complete relationship between fecundity and body sizes. Using the Gulf of Maine northern shrimp, *Pandalus borealis*, as an example, we evaluated two sampling strategies, simple random sampling and size-based stratified random sampling, with a different number of sampling locations and different number of animals sampled per sampling location or length interval. The study shows that both the sampling strategies, simple random sampling and size-based stratified random sampling, can generate representative samples. However, the simulation analysis suggests that when the population size distribution is skewed with a lack of large and/or small individuals, size-based stratified random sampling is preferred due to lower variation in differences of means and medians between samples and the population. This study provides a simulation framework for identifying a cost-effective sampling protocol that can improve the estimate of fecundity, leading to an improved estimate of fish population reproductive potential.

Keywords: effect size, equivalence testing, simple random sampling, stratified random sampling

Introduction

For many crustaceans and fish species, reproductive output of a female individual tends to increase with body size as larger females have higher capacity to accommodate more eggs or offspring (Hannah *et al.*, 1995; Hixon *et al.*, 2014). However, the relationship between reproductive output and female body size is usually not linear. Instead, reproductive output tends to increase approximately exponentially with body size (Hixon *et al.*, 2014; Barneche *et al.*, 2018). At extreme size classes, however, reproductive output of a female may decrease or level off due to senescence (Shelton *et al.*, 2012). In order to account for this maternal effect, a wide range of sizes of females should be collected for developing a comprehensive relationship between reproductive output and female body sizes in order to have a robust estimate of reproductive potential of a population (Marshall *et al.*, 2006).

Sample sizes and locations may also influence the quality of fecundity estimates because of large variability in space and among individuals (Parsons and Tucker, 1986; Hannah *et al.*, 1995). An insufficient number of samples may lead to underestimated or overestimated fecundity for a given size of fish. A large number of samples is usually encouraged for estimating biological traits of a population. However, collecting biological data such as fecundity can be very time-consuming and labour-intensive labouratory processes (Rogers *et al.*, 2019). Excessive samples are not only a waste of resources, but also a source of unnecessary pressure on the population especially when the stock is in an unhealthy status. Therefore, to reach a balance between deriving robust estimates of life history traits and efficient using available resources, an appropriate sampling design is important for collecting biological samples from a population.

Based on availability of resources and samples, two sampling designs are often used to collect biological data like fecundity: simple random sampling (Collins *et al.*, 1998; Pennington and Helle, 2011) and stratified random sampling (Hannah *et al.*, 1995). Simple random sampling is to randomly select samples from a population. Stratified random sampling is to divide the population to more than one group (*e.g.* length-intervals), and to randomly select samples from each group. In general, size-based stratified random sampling is theoretically more appropriate for collecting fecundity data, as it is more likely to include samples from each classification (length intervals), thus able to establish a more complete biological database and fecundity-body size relationship over a full size range. However, it might not be feasible for some species whose gravid individuals are encountered by chance. In addition, it takes extra effort to classify each individual before randomly sampling from each stratum. In this case, simple random sampling is usually used as a default sampling strategy. Nevertheless, whether the samples collected by these two sampling schemes can be representative of the population is rarely discussed.

The Gulf of Maine (GOM) northern shrimp used to support a significant winter fishery for the New England states (ASMFC, 2018), however the shrimp fishery has been on moratorium since 2014 due to presumed recruitment failures which were perceived to be a subsequence of warming water temperature in the GOM in past several years (Richards *et al.*, 2012; ASMFC, 2018). Recruitment is usually related to reproductive potential of a population which can be evaluated with fecundity. However, the relationship between shrimp body sizes and fecundity was estimated in more than thirty years ago using 47 ovigerous females selected for size and wholeness of the egg mass (Haynes and Wigley, 1969). These data were fitted with a parabola for estimating fecundity for females larger than 22-mm (Richards *et al.* 2012, ASMFC 2018): fecundity = $-0.198\ l^2+128.81l-17821$, where l is carapace length (0.1-mm). The body size-fecundity relationship estimated with the parabola was likely biased as small spawners were not included in their study and the estimated parabola equation generated negative values for fecundity when female carapace length was below 20-mm. Therefore, there is a pressing need to develop an updated fecundity database to provide more robust estimates for northern shrimp reproductive potential, which makes northern shrimp an appropriate case study.

The aim is to compare different sampling strategies for estimating fecundity for species such as northern shrimp that have maternal effects on fecundity and the number of ovigerous individuals were unevenly collected in sampling locations. The study can identify a cost-effective sampling design for collecting fecundity data, leading to improved fecundity estimation.

Materials and Methods

This study uses simulation of resampling approach to simulate different sampling strategy scenarios based on collected survey data.

NEFSC fall bottom trawl survey data

The GOM northern shrimp spawning season takes place in late summer and fall, and most females become ovigerous in fall. Therefore, the ovigerous females used for the fecundity study were sampled in the Northeast Fisheries Science Center (NEFSC) fall bottom trawl surveys which were designed for multispecies surveys in the northeast coastal areas. As the surveys are not specifically designed for northern shrimp, in the sampling location with presence of ovigerous females, the number of shrimp varied from one to several hundred among tows. Given the limited resources, it is unrealistic to process all collected shrimp. Thus, there is a need to optimize the number of sampling locations in a year and number of shrimp collected in a sampling location. Moreover, as many other species are collected in the survey, which face similar needs, the methodology developed in this survey are applicable to other species.

The northern shrimp data and tow information were collected by NEFSC fall bottom trawl surveys (Smith, 2002) from 2012 to 2016, including dorsal carapace length (DCL), life stage, date of catch, and longitude and latitude of sampling location. The DCLs of shrimp were measured to the nearest 0.1-mm, from the posterior limit of eye socket to the posterior limit of dorsal carapace (Haynes and Wigley, 1969). Only ovigerous female data were used for simulation as the ultimate goal was to collect fecundity data based on maternal body sizes.

Simulation of resampling study

Data from 2012 to 2016 were resampled separately with two sampling strategies of simple random sampling and size-based stratified random sampling. Sampling locations were randomly resampled without replacement from each year's sampling locations for each scenario. Sampling intensity was determined by the number of shrimp of interest from a sampling location and the percentage of sampling locations in each year.

Simple Random Sampling

The sampling scenarios were considered with the percentage of sampling locations and number of shrimp sampled from each sampling location. Two potential sample sizes (*i.e.*, 10 and 20) were considered for a sampling location in the simulation. For sampling locations with less than the required number of shrimp (*i.e.*, 10 or 20), all shrimp in that location were used. For sampling locations with more than the specified shrimp, 10 or 20 shrimp were randomly sampled without replacement (Fig. 1)

Stratified Random Sampling

For stratified random sampling, minimal and maximal lengths were determined to be the minimum and maximum DCLs of sampled collected in a year with a length interval of 1.5-mm. A given number (1 or 2) of shrimp was sampled from each length interval until no more shrimp were available in that length interval. The sampling scenarios were developed with a different sampling intensity and number of shrimp sampled from each length interval. For sampling locations which had fewer than 10 shrimp collected, all shrimp in that location were used for 1-shrimp scenarios (20 shrimp for 2-shrimp scenarios, Fig. 1)

Equivalence testing

Null hypothesis significance testing framework is commonly used in ecology to examine the differences between the two groups (Martinez-Abrain, 2008; Beninger *et al.*, 2012). However, it is criticized in some ecological studies for the following reasons: (1) a lack of significance ($P>\alpha$) simply means there is no sufficient evidence to reject the null hypothesis, but it does not mean the null hypothesis is true (Brosi and Biber, 2009; Beninger *et al.*, 2012; Lakens, 2017); and (2) the statistical power needed to detect a difference is low. Alternatively, two one-sided equivalence tests within a frequentist framework can be used to ascertain effect quality by specifying meaningful

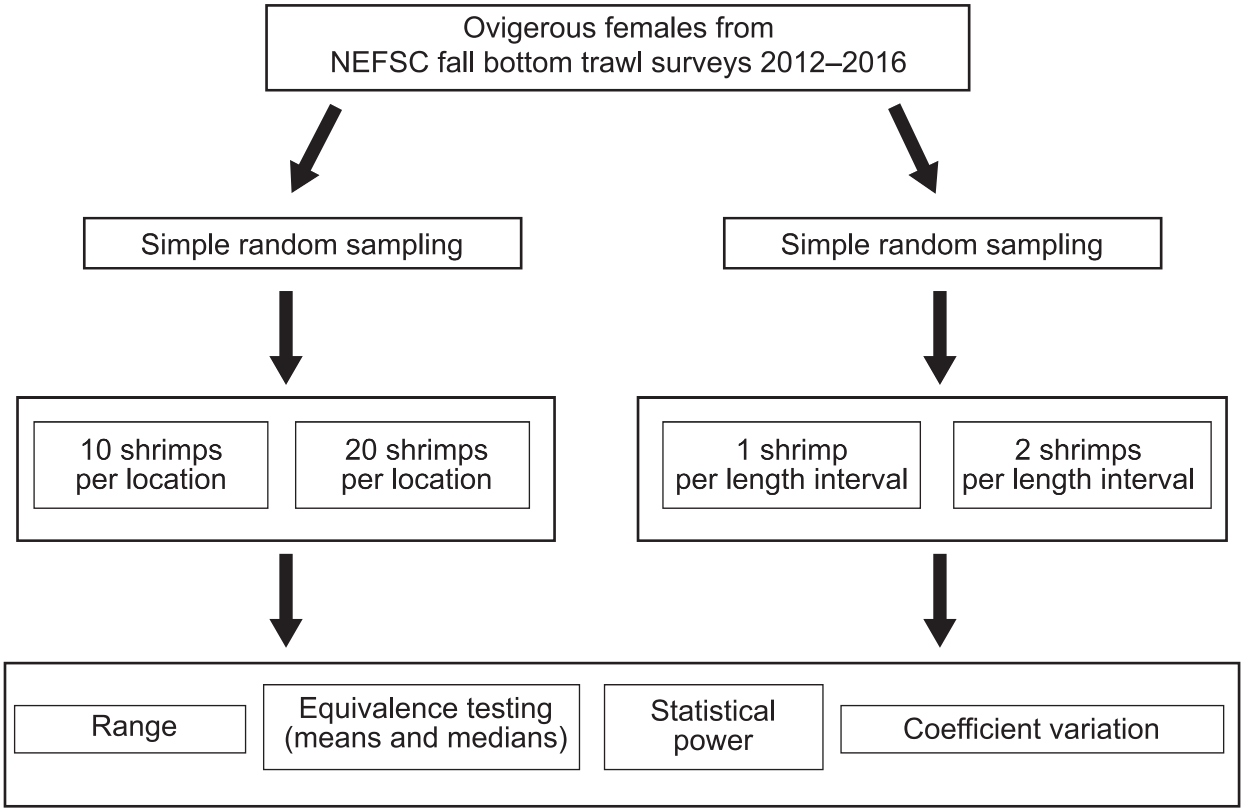

Fig. 1. A flowchart illustrating the procedure of the simulation analysis. Scenarios of 10 and 20 shrimp per sampling location were considered for simple random sampling at different sampling intensity (percentage of sampling locations). Scenarios of 1 and 2 shrimp per 1.5-mm length interval were considered for stratified random sampling at different sampling intensity. Range of simulated dorsal carapace lengths, equivalence testing of means and medians, statistical power, and coefficient of variation were used for examining the simulated samples in each scenario.

effect size based on biological or ecological understanding (Parkhurst, 2001; Lakens, 2017). Moreover, the lower and upper bounds constructed with a priori specified effect size allow the researchers to evaluate significant differences with reduced type II error defined in traditional hypothesis testing (Parkhurst, 2001; Brosi and Biber, 2009). Therefore, instead of using traditional null hypothesis testing, we use two one-sided equivalence testing for the simulated data in each scenario.

Before we performed equivalence testing, a difference of 1.5-mm (Δ) was determined as the minimum effect size that we would like to detect. Effect size was defined as the magnitude of the observed difference (Beninger *et al.*, 2012). Our data suggested that mean DCL of ovigerous females was around 25-mm, which is equivalent to an age of 3.5 years based on age-DCL growth curve (ASMFC, 2018) with age 3 being estimated at 23.5-mm and age 4 at 26.5-mm. We thus determined the effect size interval at 1.5-mm, as shrimp in DCLs smaller or larger than 1.5-mm are likely to be at a different age of years. The lower and upper bounds of equivalence intervals for each sample were constructed as (Nakagawa and Cuthill, 2007; Lakens, 2017):

$$\left(m_s - m_y\right) \pm t_{\alpha,\, df}\, s_{pooled}\sqrt{\frac{1}{n_s}+\frac{1}{n_y}} \qquad (1)$$

$$s_{pooled} = \sqrt{\frac{s_s^{\,2}(n_s-1)+s_y^{\,2}(n_y-1)}{n_s+n_y-2}} \qquad (2)$$

where m_s = mean (or median) DCL of samples from a given scenario in year y; m_y = mean (or median) DCL of all samples collected in year y; $t_{\alpha,\, df}$ = t statistic at a significance level of α at degree of freedom at df; $\alpha = 0.05$, $df = n_s + n_y - 2$; n_s = number of samples of a given scenario; n_y = number of samples collected in year y; s_s = standard deviation of samples from a scenario in year y; and s_y = standard deviation of all the samples collected in year y.

Two one-sided tests were performed to means and medians of samples simulated from each scenario in each year. The null hypothesis is $ei_l \leq \Delta$ and $ei_u \geq \Delta$, and the alternative hypothesis is $-\Delta <$ *equivalence interval* $< \Delta$, where ei_l = lower bound of equivalence interval, ei_u = upper bound of equivalence interval. Both components in the stated null hypothesis must be false to reject the null hypothesis. Thus, if the equivalence interval falls within the equivalence interval, the difference between the means or medians is smaller than the magnitude of effect size we specified.

Statistical power of detecting the specified effect size (Δ = 1.5-mm) was estimated with the number of samples simulated in each scenario at the significance level of 0.05. Statistical power of 0.95 was set as a reference instead of traditional 0.8, as we assume the cost of committing a type II error was the same as that of committing a type I error (Peterman, 1990; Di Stefano, 2003). Coefficient of variation (CV) was also calculated for evaluating the dispersion of samples for each simulation scenario. All analyses were performed in R 3.5.1 (R Core Team, 2018).

Results

Number of sampling locations in each year

The total yearly number of sampling locations and total number of ovigerous females collected in each year from 2012 to 2016 were shown in Table 1. Our data showed that the mean DCL of ovigerous females varied between 24.08 and 25.86 from 2012 to 2016 (Fig. 2). In addition, samples collected in 2014 deviated from normal distribution with a mean at 25.43-mm-DCL and a median of 26.5-mm-DCL, and with an unusual wide standard deviation (SD) of 2.89-mm (SD varied from 1.52 to 1.66 in the other four years).

Equivalence tests

The equivalence tests of means for all the scenarios showed that most equivalence intervals of means fell within the specified effect size interval when at least 20% of the sampling locations were sampled except for 2014 (Fig. 3). Similar results could be found in tests for the difference in medians (Fig. 4). The equivalence interval of medians barely fell within the effect size interval for simulated samples in 2014 even if all stations were sampled.

For means of 20-shrimp scenarios in 2014, the equivalence intervals started to fall within the specified effect size interval when more than 50% of the sampling locations

Table 1. The total yearly number of sampling locations and total number of ovigerous females collected in each year from Northeast Fisheries Science Center (NEFSC) fall bottom trawl surveys 2012–2016.

Year	2012	2013	2014	2015	2016
Total number of sampling locations	16	27	25	37	37
Total number of ovigerous females	13 812	4 732	5 443	2 705	1 605

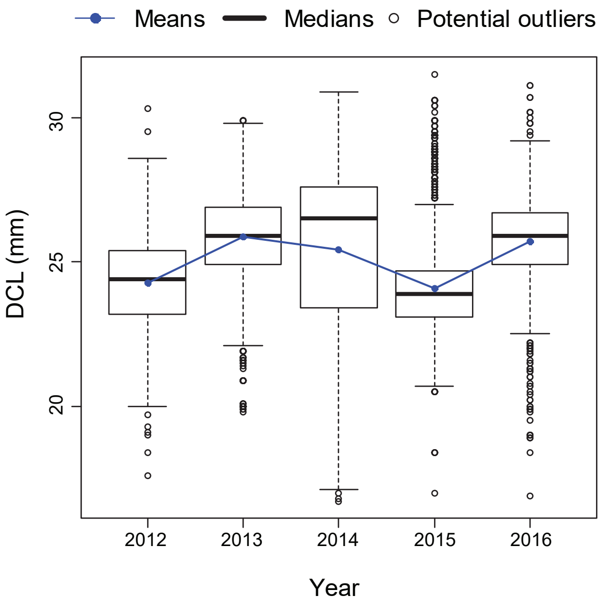

Fig. 2. Boxplots of dorsal carapace length (DCL) of ovigerous female northern shrimp Pandalus borealis, collected from Northeast Fisheries Science Center (NEFSC) fall bottom trawl surveys from 2012 to 2016. The blue symbols are means and the horizontal bars in the boxes are medians. The lower and upper limits of the boxes are the first (Q1) and third (Q3) quartiles (25th and 75 percentiles). The difference between Q1 and Q3 is interquartile range (IQR). Potential outliers are defined as observation points fall outside the range of Q1-1.5*IQR and Q3+1.5*IQR. If potential outliers are presented, the whiskers extend to 1.5 times the IQR from Q1 or Q3. If no outliers are presented, the whiskers extend to the minima and maxima of the distributions.

were sampled. When less than 50% of the locations were sampled in 2014, both sampling strategies failed to reject the null hypothesis. However, the differences in means of simple random sampling had a wider variation than those of stratified random sampling scenarios (Fig. 3).

As for the equivalence tests of medians for 2014 samples, almost all scenarios failed to reject the null hypothesis (Fig. 4). Similar to the equivalence tests of means, when less than 50% of the locations were sampled, the median differences for random sampling method tended to have larger variations than those of stratified random sampling.

Statistical power

The statistical power of detecting the minimal effect size ($\Delta = 1.5$-mm) increased with sampling intensity, when more than 20% of sampling locations were sampled, all scenarios could reach the statistical power of 0.95 except for scenarios of 2014 (Fig. 5). Simulated samples of 2014 could reach the statistical power of 0.95 when at least 30% of the locations were sampled. There was a trade-off between the number of shrimp per location (or length interval) and percentage of sampling locations. Given a sampling strategy, more numbers of shrimp per sampling location (or length interval) could reach the statistical power of 0.95 with a lower percentage of sampling locations. The coefficients of variation were mostly below 0.1 for each scenario except scenarios in 2014 due to large standard deviation of DCL collected in 2014 (Fig. 5).

Sample size

The numbers of shrimp simulated in each scenario increased with sampling intensity, and simple random sampling strategy tended to generate larger sample sizes than stratified random sampling strategy at a given sampling intensity (Figs. 5 and 6). When 20% of sampling locations were sampled, the total numbers of shrimp in the simulation for five years ranged from 129 to 349 for different strategies with different intensity (Fig. 6). When 30% of the locations were sampled, the total numbers of shrimp increased to 215–612 (Fig. 6).

The means, medians, and ranges of samples simulated in each scenario were compared with the assumed populations (samples collected from the surveys) in each year (Fig. 7). When more than 20% of the locations were sampled, the simulated samples could include the central 95% of DCL of the assumed population for both sampling strategies. When less than 50% of the location were sampled, the stratified random sampling, as expected, was more likely include the minimum and maximum of DCLs of the assumed population than the simple random sampling.

Discussion

The results of equivalence testing showed that there were no large differences between samples simulated with simple random sampling and stratified random sampling strategies when the population distribution is approximately normal. Both sampling strategies can collect samples that were representative of the population (*i.e.*, including the central 95% of the distribution) and the means and medians did not significantly differ from the specified effect size when more than 20% sampling locations were sampled. However, if we conducted traditional null hypothesis significance testing, many of the simulated samples would suggest statistical

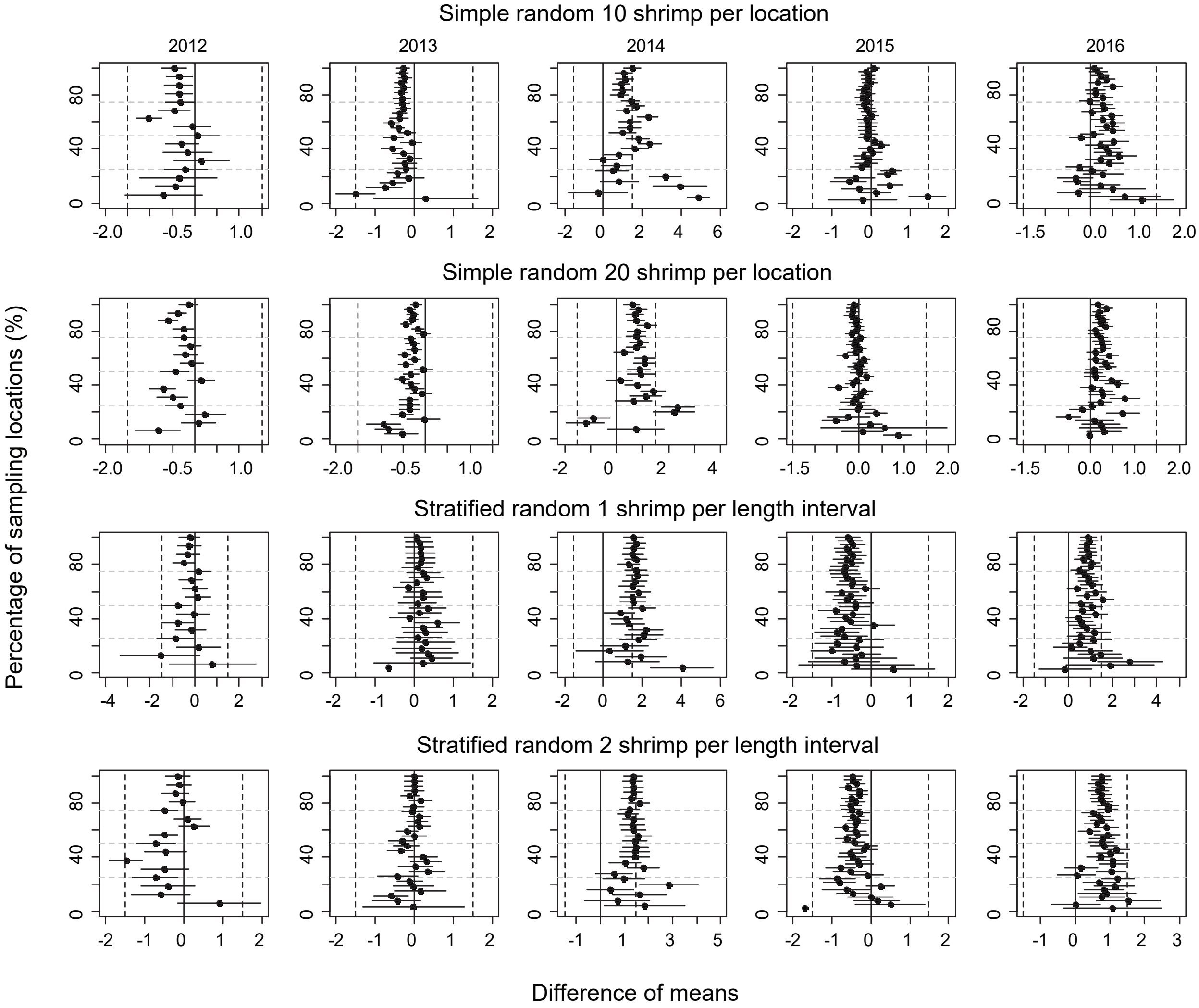

Fig. 3. Differences between means of samples in each scenario and the population (all shrimp collected in a given year) and 90% confidence intervals (dashed lines) with equivalence bounds (-1.5 and 1.5) for each scenario at percentage of sampling locations for each year. Vertical solid lines denote mean differences at zero. Gray dashed lines are y-axis grid lines, denoting 25, 50, and 75% of sampling locations.

significance as the confidence interval of error did not include zero, which might not be biologically significant. The results suggested the merits of equivalence testing over traditional null hypothesis significance testing with the ability to detect a biologically meaningful or ecologically important effect size (Parkhurst, 2001; Brosi and Biber, 2009).

The number of shrimp simulated for each scenario with different strategies, in general, linearly increased with the number of sampling locations. However, as the surveys were not specifically designed for northern shrimp, number of shrimp collected at a station could be only a few. Therefore, the ultimate sampling intensity (number of shrimp simulated for a scenario) was not exactly proportional to the number of locations sampled. An extreme example was the 20-shrimp scenario with three sampling stations with simple random sampling strategy, which had only four DCLs simulated in that scenario. The statistical power was hence low (Fig. 5). Our simulation reflects the discrepancy between samples collected in multispecies surveys and ideal sampling for fecundity data. Care should be taken to adjust sampling strategy in such circumstances.

Increasing sampling intensity by either raising the number of shrimp per location, length interval, or the number of sampling locations can reduce sampling error and

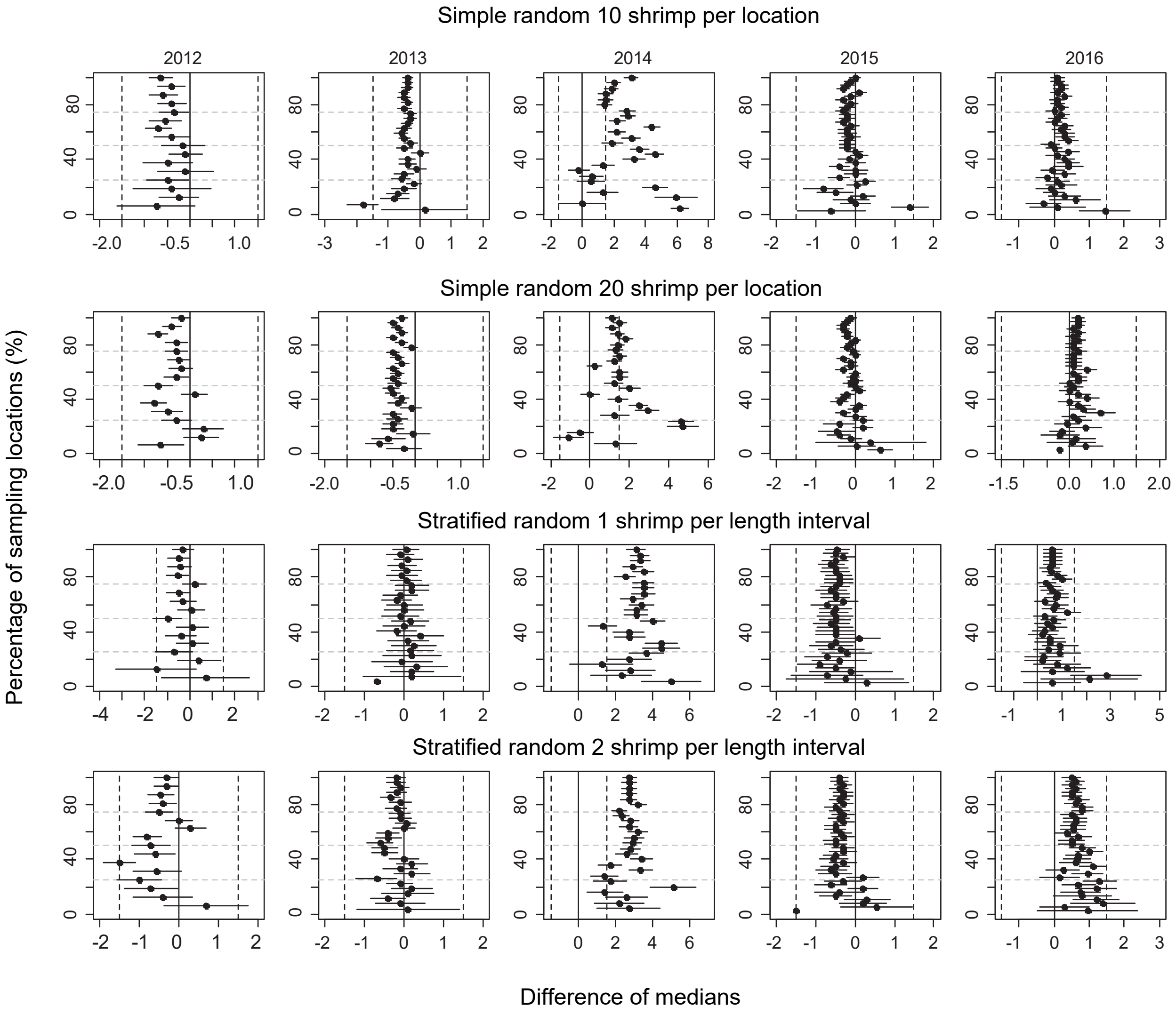

Fig. 4. Differences between medians of samples in each scenario and the population (all shrimp collected in a given year) and 90% confidence intervals (dashed lines) with equivalence bounds (-1.5 and 1.5) for each scenario at percentage of sampling locations for each year. Vertical solid lines denote mean differences at zero. Gray dashed lines are y-axis grid lines, denoting 25, 50, and 75% of sampling locations.

increase statistical power. However, the cost of increasing sampling intensity may not be effective as the magnitude of precision that can be improved is trivial when sampling intensity is above a certain level (Pennington *et al.*, 2002). Although both the sampling strategies we adopted in this study suggested that the equivalence interval can fall within the effect size interval when at least 20% of the locations were sampled (except for 2014), we determined stratified random sampling may be a more effective sampling strategy for collecting fecundity data as it requested for a low sample size compared to the simple random sampling.

With stratified random sampling at a fixed overall sampling size (number of shrimp simulated for all five years), based on the trade-off between the number of shrimp per length interval and the percentage of the locations, a desired statistical power can be achieved at a lower percentage of sampling locations for 2-shrimp per length interval scenarios. However, the stratified random sampling strategy with one shrimp per length interval is preferred in this case, as a higher percentage of sampling locations allows a broader spatial coverage of the study area. Therefore, the optimal sample size for collecting fecundity data was estimated at 215 shrimp for five years

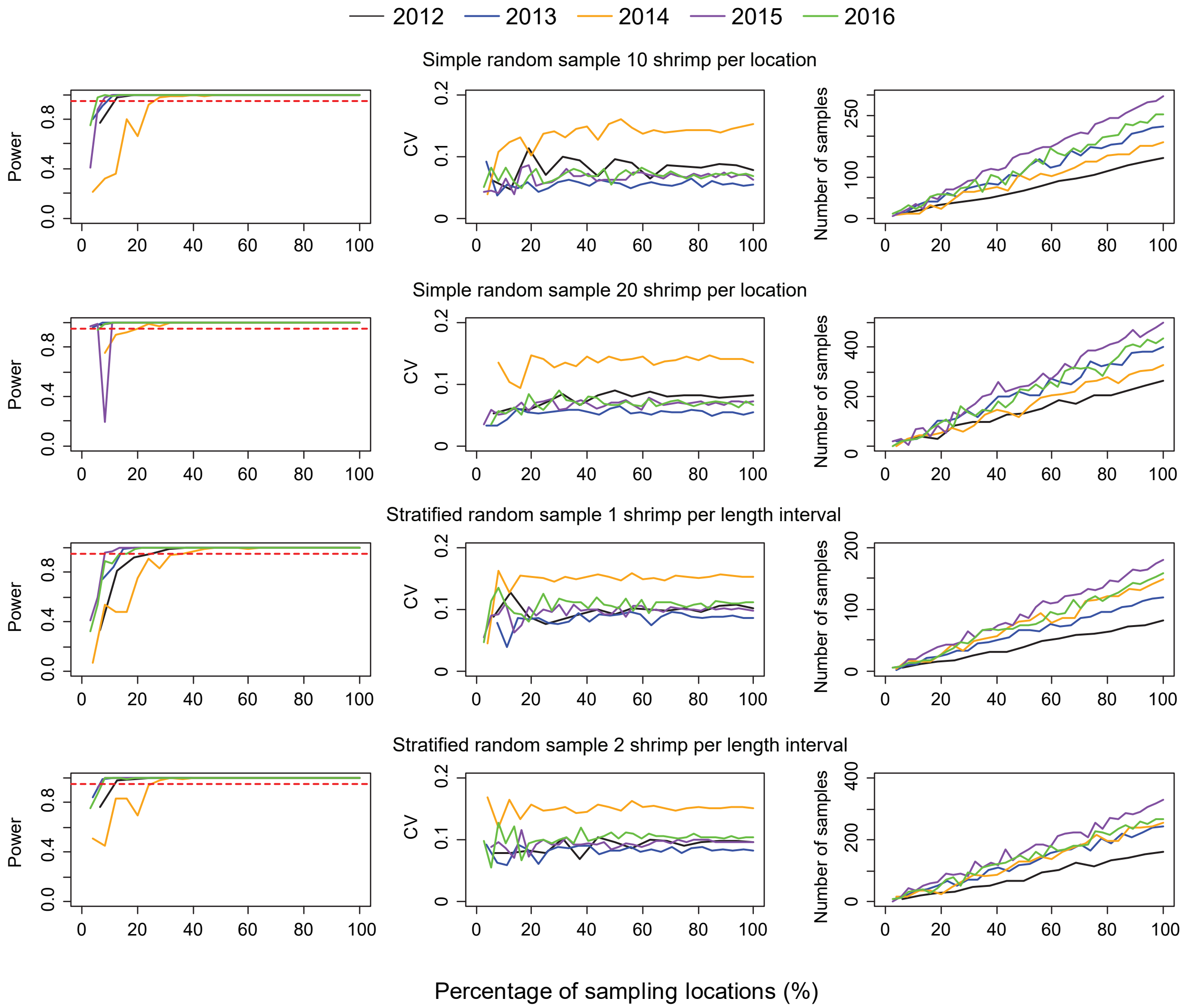

Fig. 5. Relationships between statistical power (Power), coefficient of variation (CV), number of samples, and percentage of sampling locations for each scenario. Left column: statistical power; middle column: coefficient of variation; right column: number of samples. Top 2 rows: 10 and 20 shrimp per sampling location for simple random sampling; bottom 2 rows: 1 and 2 shrimp per length interval for stratified random sampling.

(30% of the locations) with size-based stratified random sampling.

Both sampling strategies generated unrepresentative samples which were significantly different from the specified effect size when less than 50% of the locations were sampled for 2014 due to the skewed distribution of DCLs in 2014. Generally, it is not possible to know the length distribution of the population which is usually assumed to be approximately normally or log-normally distributed. It should be cautioned when many small spawners are observed in the population, which could be a sign of early sexual maturity resulting from fishing pressure, environmental changes and consequent food availability to females (O'Brien, 1999; Koeller *et al.*, 2007). Spawners at small sizes make less contribution per individual to reproductive potential of a population, as small spawners tend to produce fewer offspring per individual with lower survival rates (Shelton *et al.*, 2012; Barneche *et al.*, 2018).

Aanes and Volstad (2015) used simulation approach to evaluate subsampling strategies for collecting age data for Northeast Arctic cod (*Gadus morhua*), suggesting that length-stratified sampling is more effective than simple random sampling because length-stratified sampling can ensure a better coverage of the age composition when age data were collected from a small subsample of measured lengths of fish. Our findings agree with Aanes and Volstad (2015). For the purpose of collecting fecundity data, stratified random sampling strategy is preferred over simple random sampling when the size distribution of ovigerous females is actually skewed with many small spawners (deviated from the assumed normally distributed population). Because it is often not possible to have enough resources for a high sampling intensity, and simple random sampling is more likely to generate a biased sample in a low sampling intensity (Figs. 3, 4, and 7). Conversely, although stratified random sampling also generates biased samples, the variation of means and medians of samples are relatively stable when sampling intensity is low. Furthermore, labouratory process for collecting fecundity data can be very time-consuming and labour-intensive. The time needed for processing a shrimp to collect fecundity data is generally 3–4 hours. Given a sampling intensity of 20% of the sampling location, the 10-shrimp simple random sampling scenario generates a larger number of sample size than the 1-shrimp per length interval stratified random sampling scenario by 69 shrimp. Thus, the simple random sampling may take 207 additional hours (69 shrimp × 3 hours), which would cost additional $4140 (*i.e.*, 207 hours × $20 per hour per person) for laboratory process alone. Our analyses suggest that length-stratified random sampling is a more cost-effective strategy for collecting fecundity data.

The shrimp samples Haynes and Wigley (1969) used for collecting fecundity data ranged from 22 to 31-mm-DCL. Our data, except for 2014, the central 95% of ovigerous females collected from the survey ranged from a similar interval of 22–28-mm-DCL in this study. However, it appeared that if shrimp outside the central 95% length interval were excluded from the regression of length and fecundity, the regressed relationship may not be able to provide reliable estimates of fecundity for the population as the fecundity-DCL relationship developed with 47 female shrimp by Haynes and Wigley (1969) generates negative numbers for shrimp at DCLs<20-mm. It suggested that, when estimating size-based fecundity for a population, (1) a complete range of size data is necessary for developing a fecundity-body size relationship; (2) several years of samples may be needed for building a complete fecundity database; and (3) parabola equation should be used with caution as it may generate biologically meaningless estimates of fecundity (negative values). Estimating the magnitude of the bias in reproductive potential of a population is beyond the scope of this study. Consequently, before we take a further step into investigation of the misestimates of fecundity, there is a pressing need to develop a new fecundity-DCL relationship with proper sampling design for collecting fecundity data.

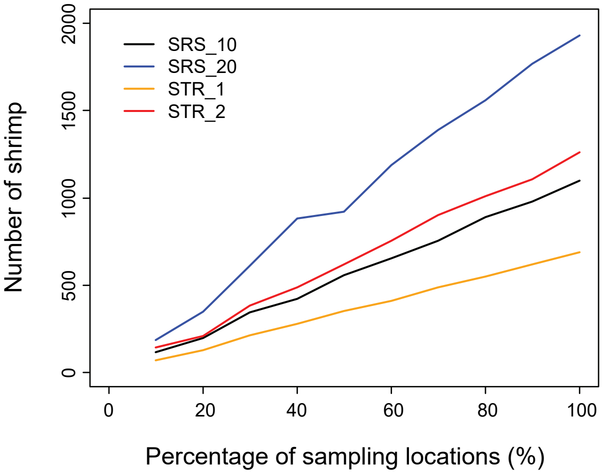

Fig. 6. Relationships between total number of samples and percentage of sampling locations. SRS_10 and SRS_20 are scenarios of 10 and 20 shrimp per sampling location for simple random sampling. STR_1 and STR_2 are scenarios of 1 and 2 shrimp per length interval for stratified random sampling.

This study proposes a simulation framework that can be used to develop a cost-effective sampling strategy for estimating fecundity data for many marine fish and crustacean species which share the characteristics of (1) a strong maternal effect on fecundity (*i.e.*, number of offspring increase with female body sizes; Haynes and Wiley, 1969); (2) number of individuals collected varied among sampling locations and number of sampling locations varied by year; and (3) extensive length frequency data have been collected for multiple years which can be used for sampling design. Collecting fecundity data can be very time-consuming and labour-intensive. Insufficient samples may result in biased estimates; however, excess samples can be a waste of resources. Therefore, an appropriate sampling design for optimizing effective sample size is needed for building a complete fecundity data base. We advocate the use of equivalence testing and power analysis before collecting samples in order to determine biologically meaningful effect size instead of statistical significance in traditional null hypothesis significance testing.

Acknowledgements

The authors thank Northeast Fisheries Science Center for providing data. This study was financially supported by NOAA Saltonstall-Kennedy grant (NA16NMF4270245).

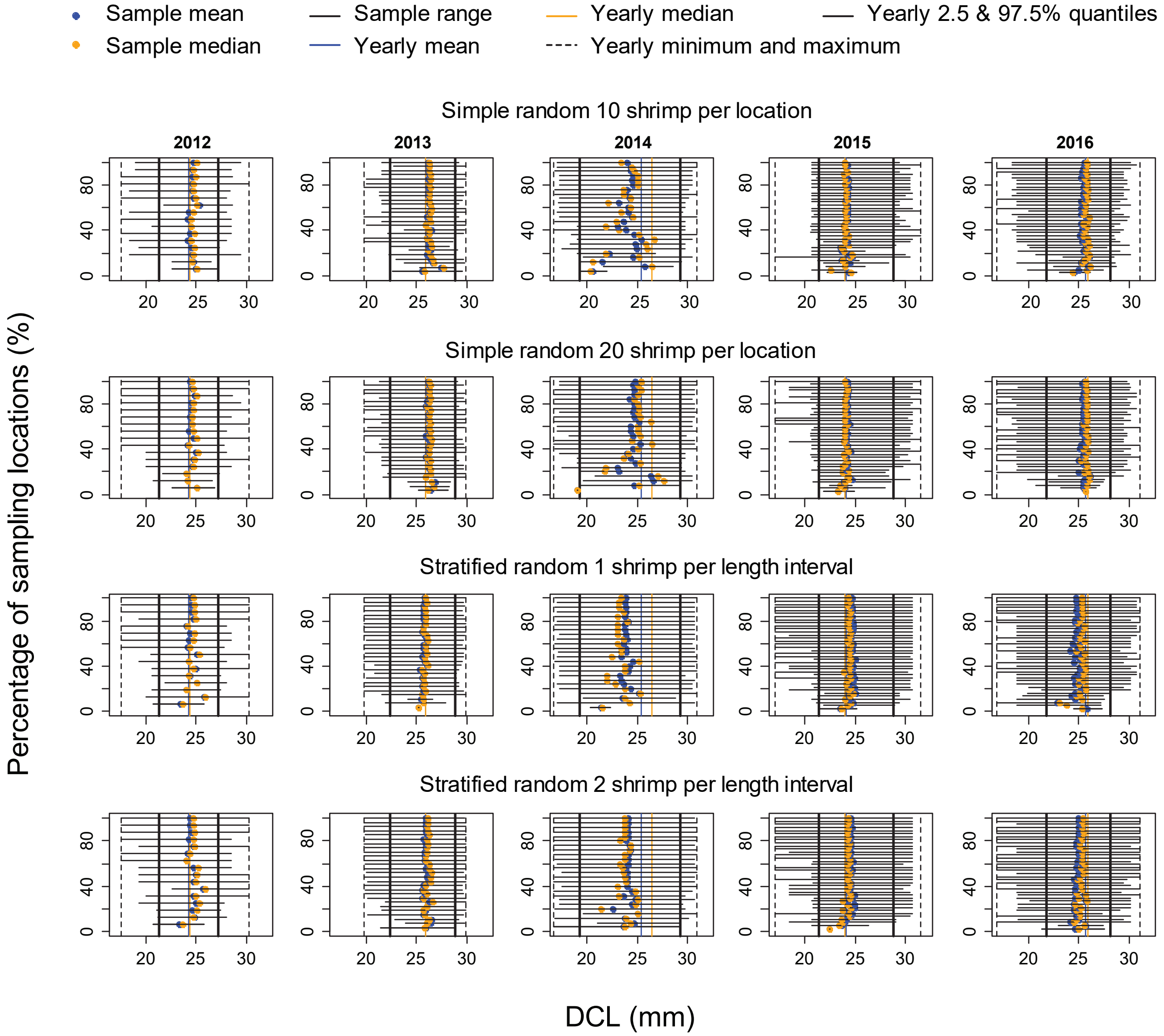

Fig. 7. A summary of the ranges, means, medians, and the central 95% intervals of dorsal carapace lengths (DCLs) for the assumed populations (all samples collected from the surveys in a year) and samples simulated in each scenario.

References

Aanes, S., and Vølstad, J. H. 2015. Efficient statistical estimators and sampling strategies for estimating the age composition of fish. *Canadian Journal of Fisheries and Aquatic Sciences*, **72**: 938–953. https://doi.org/10.1139/cjfas-2014-0408

ASMFC NSTC (Atlantic States Marine Fisheries Commission Northern Shrimp Technical Committee). 2018. Assessment report for Gulf of Maine northern shrimp.

Barneche, D. R., Robertson, D. R., White, C. R., and Marshall, D. J. 2018. Fish reproductive-energy output increases disproportionately with body size. *Science*, **360**: 642–645. https://doi.org/10.1126/science.aao6868

Beninger, P. G., Boldina, I. and Katsanevakis, S. 2012. Strengthening statistical usage in marine ecology. *Journal of Experimental Marine Biology and Ecology*, **426-427**: 97–108. https://doi.org/10.1016/j.jembe.2012.05.020

Brosi, B. J., and Biber, E. G.. 2009. Statistical inference, type II error, and decision making under the US Endangered Species Act. *Frontiers in Ecology and the Environment*, **7**: 487–494. https://doi.org/10.1890/080003

Collins, L. A., Johnson, A. G., Koenig, C. C. and Baker, M. S. 1998. Reproductive patterns, sex ratio, and fecundity in gag, *Mycteroperca microlepis* (Serranidae), a protogynous grouper from the northeastern Gulf of Mexico. *Fishery Bulletin*, **96**: 415–427.

Di Stefano, J. 2003. How much power is enough? Against the development of an arbitrary convention for statistical power calculations. *Functional Ecology*, **17**: 707–709. https://doi.org/10.1046/j.1365-2435.2003.00782.x

Hannah, R. W., Jones, S. A., and Long, M. R. 1995. Fecundity of the ocean shrimp (*Pandalus jordani*). *Canadian Journal of Fisheries and Aquatic Sciences*, **52**: 2098–2107.https://doi.org/10.1139/f95-803

Haynes, E. B., and Wigley, R. L. 1969. Biology of the northern shrimp, *Pandalus borealis*, in the Gulf of Maine. *Transactions of the American Fisheries Society*, **98**: 60–76. https://doi.org/10.1577/1548-8659(1969)98[60:BOTNSP]2.0.CO;2

Hixon, M. A., Johnson, D. W. and Sogard, S. M. 2014. BOFFFFs: on the importance of conserving old-growth age structure in fishery populations. *ICES Journal of Marine Science*, **71**: 2171–2185. https://doi.org/10.1093/icesjms/fst200

Koeller, P., Fuentes-Yaco, C., and Platt, T. 2007. Decreasing shrimp sizes off Newfoundland and Labrador—environment or fishing? *Fisheries Oceanography*, **16**: 105–115. https://doi.org/10.1111/j.1365-2419.2006.00403.x

Lakens, D. 2017. Equivalence Tests: A practical primer for t tests, correlations, and meta-analyses. *Social Psychological and Personality Science*, **8**: 355–362. https://doi.org/10.1177/1948550617697177

Marshall, C. T., Needle, C. L., Thorsen, A. Kjesbu, O. S., and Yaragina, N. A. 2006. Systematic bias in estimates of reproductive potential of an Atlantic cod (*Gadus morhua*) stock: implications for stock-recruit theory and management. *Canadian Journal of Fisheries and Aquatic Sciences*, **63**: 980–994. https://doi.org/10.1139/f05-270

Martinez-Abrain, A. 2008. Statistical significance and biological relevance: a call for a more cautious interpretation of results in ecology. *Acta Oecologica*, **34**: 9–11. https://doi.org/10.1016/j.actao.2008.02.004

Nakagawa, S., and Cuthill, I. C. 2007. Effect size, confidence interval and statistical significance: a practical guide for biologists. *Biological Reviews*, **82**: 591–605. https://doi.org/10.1111/j.1469-185X.2007.00027.x

O'Brien, L. 1999. Factors influencing the rate of sexual maturity and the effect on spawning stock for Georges Bank and Gulf of Maine Atlantic cod *Gadus morhua* stocks. *Journal of Northwest Atlantic Fishery Science*, **25**: 179–203. https://doi.org/10.2960/J.v25.a17

Parkhurst, D. F. 2001. Statistical significance tests: equivalence and reverse tests should reduce misinterpretation. *Bioscience*, **51**: 1051–1057. https://doi.org/10.1641/0006-3568(2001)051[1051:SSTEAR]2.0.CO;2

Parsons, D. G., and Tucker, G. E. 1986. Fecundity of northern shrimp, *Pandalus borealis*, (Crustacea, Decapoda) in areas of the Northwest Atlantic. *Fishery Bulletin*, **84**: 549–558.

Pennington, M., Burmeister, L-M., and Hjellvik, V. 2002. Assessing the precision of frequency distributions estimated from trawl-survey samples. *Fishery Bulletin*, **100**: 74–80.

Pennington, M., and Helle, K. 2011. Evaluation of the design and efficiency of the Norwegian self-sampling purse-seine reference fleet. *ICES Journal of Marine Science*, **68**: 1764–1768. https://doi.org/10.1093/icesjms/fsr018

Peterman, R. M. 1990. Statistical power analysis can improve fisheries research and management. *Canadian Journal of Fisheries and Aquatic Sciences*, **47**: 2–15. https://doi.org/10.1139/f90-001

R Core Team. 2018. R: A language and environment for statistical computing. R Foundation for Statistical Computing, Vienna, Austria. URL https://www.R-project.org/.

Richards, R. A., Fogarty, M. J., Mountain, D. G., and Taylor, M. H. 2012. Climate change and northern shrimp recruitment variability in the Gulf of Maine. *Marine Ecology Progress Series*, **464**:167–178. https://doi.org/10.3354/meps09869

Rogers, R., Rowe, S., Rideout, R. M., and Morgan, M. J. 2019. Fecundity of haddock (*Melanogrammus aeglefinus*) off southern Newfoundland. *Fisheries Research*, **220**: 105339. https://doi.org/10.1016/j.fishres.2019.105339

Shelton, A. O., Munch, S. B., Keith, D. and Mangel, M. 2012. Maternal age, fecundity, egg quality, and recruitment: linking stock structure to recruitment using an age-structured Ricker model. *Canadian Journal of Fisheries and Aquatic Sciences*, **69**: 1631–1641. https://doi.org/10.1139/f2012-082

Smith, T. D. 2002. The Woods Hole bottom-trawl resource survey: development of fisheries-independent multispecies monitoring. *ICES Marine Science Symposia*, **215**: 480–488.

J. Northw. Atl. Fish. Sci., Vol. 51: 45–104 Publication (Upload) date: 15 Oct 2020

A state-space stock assessment model for American plaice on the Grand Bank of Newfoundland

Andrea M.J. Perreault*[1], Laura J. Wheeland[2], M. Joanne Morgan[2], and Noel G. Cadigan[1]
[1]Centre for Fisheries Ecosystems Research, Fisheries and Marine Institute of Memorial University,
St. John's, NL, Canada, A1C 5R3
*Corresponding author: andrea.perreault@mi.mun.ca
noel.cadigan@mi.mun.ca

[2]Northwest Atlantic Fisheries Centre, Fisheries and Oceans Canada,
PO Box 5667, St John's, NL, Canada A1C 5X1
laura.wheeland@dfo-mpo.gc.ca
joanne.morgan@dfo-mpo.gc.ca

Perreault, A.M.J, Wheeland, L.J., Morgan, M.J., and Cadigan, N.G. A state-space stock assessment model for American plaice on the Grand Bank of Newfoundland . *J. Northw. Atl. Fish. Sci.*, **51**: 45–104. https://doi.org/10.2960/J.v51.m727

Abstract

The current stock assessment model for American plaice (*Hippoglossoides platessoides*) on the Grand Bank of Newfoundland (NAFO Divisions 3LNO) is a virtual population analysis (VPA). This model does not account for the considerable uncertainty about the landings data for this stock. Retrospective patterns have also been noted in the current assessment with overestimation of spawning stock biomass (SSB) and underestimation of fishing mortality (F). Via a thorough model selection process, we develop a state-space stock assessment model (SSM) for this stock that accounts for the uncertainties in the landings data and reduces the retrospective patterns. Our SSM fit the data well, with overall trends in SSB and average F (ages 9–14) similar to those estimated from the current VPA. The retrospective patterns for the SSM were reduced for both SSB and average F which should lead to the provision of better scientific advice for the management of this stock. An important result from our analysis suggests that the current assumption for natural mortality (M) in the stock assessment model may be too low. The lack of recovery of the stock of American plaice on the Grand Bank has often been attributed to overfishing, however fixing M within the model to be lower than is reasonable may be over-estimating the relative impact of F and subsequently over-stating the contribution of fishing mortality to the lack of recovery of the stock.

Keywords: American plaice, Grand Bank of Newfoundland, state-space models, retrospective patterns, landings data uncertainty

Introduction

American plaice (*Hippoglossoides platessoides*) on the Grand Bank of Newfoundland (NAFO Divisions 3LNO) supported an important commercial fishery historically, accounting for over ten percent of the Canadian groundfish fishery in the 1950s (DFO, 2011). The population size declined rapidly in the 1980s due mostly to overfishing and, although there has been no directed commercial fishing since 1994, there has since been little improvement in the state of the population (*see e.g.* Wheeland, 2018). The lack of recovery has been attributed to overfishing, which has occurred mainly through bycatch in the yellowtail flounder, skate, redfish, and Greenland halibut fisheries (Shelton and Morgan, 2005). It has also been suggested that an increase in the natural mortality rate due to changing ocean temperatures may also be contributing to the lack of recovery (COSEWIC, 2009).

The current stock assessment model for Grand Bank American plaice is an ADAPT virtual population analysis (*see e.g.,* Lassen and Medley, 2001) that was introduced in the late 1990s. This model is based on catch-at-age data that are derived in part from landings estimates and does not account for the considerable uncertainty about the landings data (Wheeland *et al.*, 2018). Sources of uncertainty include landings recorded as "unspecified flounder" by some countries in the earliest years of available data (*see e.g.* Pitt, 1972) and an increase in foreign catch outside the 200 mile economic exclusive zone in the mid-80s (*e.g.* South Korea reporting "non-specified flounder", Brodie, 1986). More recently, the lack of scientific observer data in the NAFO Regulatory Area has resulted in the need to estimate landings via various methods, including effort ratios and daily catch records (Dwyer *et al.*, 2016). As a result, the landings data may be under-estimated and a stock assessment model that incorporates uncertainty in these data may therefore provide a better assessment.

Another issue that has been noted in the current assessment for American plaice are retrospective patterns, which are consistent directional changes in estimates of stock size as years of data are removed from the assessment model (Mohn, 1999). Retrospective patterns are caused by changes in the accuracy of the data over time and/or spatial and time-varying population processes that are unaccounted for or mis-specified in the model (*see e.g.* Legault, 2009). Systematic retrospective patterns can lead to poor management advice as important population processes (*e.g.* biomass and fishing mortality) may be over- or under-estimated and can result in unsustainable or sub-optimal harvesting advice (Szuwalski *et al.*, 2017). To promote sustainable management advice for American plaice on the Grand Bank of Newfoundland, a stock assessment model that reduces or eliminates retrospective patterns is valuable. State-space stock assessment models are ideally suited for this purpose as they can include random errors in the underlying population dynamics model (*i.e.* for population abundance and fishing mortality rates) thereby accounting for underlying time-varying population processes that contribute to retrospective patterns. Additionally, state-space models allow for errors in the data (*see e.g.* Nielsen and Berg, 2014; Cadigan, 2015; Albertsen *et al.*, 2016), which is an improvement to the current VPA that treats the catch-at-age data as known with negligible error. In this paper, we present a state-space stock assessment model for American plaice on the Grand Bank of Newfoundland that reduces the retrospective problem and allows for errors in the landings data.

Materials and Methods

There are two components to a state-space stock assessment model: the process model and the observation model. The process model describes how the state of the unobserved fish stock abundance and fishing mortality rates at a given time depend on previous states. The observation model describes how the survey and commercial data depend on the unobserved states (*see e.g.* Aeberhard *et al.*, 2018).

American plaice Process Model

The model runs for the years $y = 1960, \ldots, 2017$ and for ages $a = 1, \ldots, 15^{+}$, where 15^{+} represents the oldest ages grouped together from ages 15 onwards, called the plus group (see Table 1 for model equations). For simplicity, we will refer to model ages $a = 1, \ldots, A^{+}$, and years $y = 1, \ldots, Y$. The process model describes how the abundance at age a in year y (*i.e.* $N_{y,a}$) and the fishing mortality, $F_{y,a}$ change over time. The $N_{y,a}$ for all ages and years are treated as random effects, with the cohort abundance model modelled as:

$$\log\left(N_{y,a}\right) = \log\left(N_{y-1,a-1}\right) - Z_{y-1,a-1} + \gamma_{y,a} \tag{1.1}$$

$$\log\left(N_{y,A^{+}}\right) = \log\left[N_{y-1,A^{+}-1} \exp^{-Z_{y-1,A^{+}-1}} + N_{y-1,A^{+}} \exp^{-Z_{y-1,A^{+}}}\right] + \gamma_{y,a},$$

where $Z_{y,a} = M_{y,a} + F_{y,a}$ is the total mortality rate given by the sum of the natural mortality rate, $M_{y,a}$ (*i.e.* all mortality unrelated to fishing) and $F_{y,a}$. Here, $M_{y,a}$ is assumed to be known and fixed at 0.50 for ages 1–3, 0.30 for age 4 and 0.20 for all ages 5 and above, except during 1989 to 1996, where it is fixed at 0.53 for all ages 5 and above, as recommended by Morgan and Brodie (2001), 0.83 for ages 1–3 and 0.63 for age 4. This formulation for $M_{y,a}$ for ages 5 and greater is identical to the formulation for the most recent stock assessment model for Grand Bank American plaice. Here we also include ages 1–4, which are not currently used in the stock assessment VPA, with values for M at these ages selected through peer consultation. $F_{y,a}$ is set to zero for ages 1–4, as reported catch at these ages is considered negligible. The $\gamma_{y,a}$ are the process errors, assumed to be independent and normally distributed with variance σ_{pe}^{2} to be estimated. The numbers at the first age $N_{y,1}$ are modelled as:

$$\log\left(N_{y,1}\right) = \mu_{R_y} + \delta_{R_y}, \tag{1.2}$$

where $\mu_{R_y} = \mu_{R_1}$ for $y < 1993$ and $\mu_{R_y} = \mu_{R_2}$ for $y \geq 1993$, and the two mean recruitment parameters $\mu_{R_1}, \mu_{R_2} \in (-\infty, \infty)$ account for the large differences in recruitment between the two time periods and are fixed effect parameters to be estimated. The deviations from the mean recruitment δ_{R_y} are assumed to follow a normal distribution with AR(1) correlation across years, with the AR parameters σ_{R}^{2} and ϕ_{R} to be estimated across the entire time series, as we expect recruitment to be more alike in years that are closer together.

We assume that the fishing mortality rates increase with age, *i.e.*,

$$F_{y,a} = F_{y,a-1} + \delta_{F_{y,a}}, \quad \text{for } a=7,..,15. \qquad (1.3)$$

For ages 5 and 6, $F_{y,a} = \mu_{F_{y,a}} + \delta_{F_{y,a}}$, where $\mu_{F_{y,a}}$ is the mean fishing mortality rate, a fixed effect parameter to be estimated. A separate $\mu_{F_{y,a}}$ is estimated for ages 5 and 6, for two blocks: 1960–1994 and 1995–2017 (*i.e.* four fixed effect $\mu_{F_{y,a}}$ parameters). The age blocking of the $\mu_{F_{y,a}}$'s was chosen to reflect overall fishery selectivity patterns, and the year blocks were chosen to account for the closure of the commercial fishery in 1994. The $\delta_{F_{y,a}}$ are positive deviations from the fishing mortality rate at the previous age and are treated as random effects. The $\delta_{F_{y,a}}$*'s* are assumed to follow a normal distribution, with the deviations at the first age, $\delta_{F_{y,5}}$, assumed to have AR(1) correlation across years with parameters $\sigma^2_{F_5}, \phi_{F_5}$ to be estimated. We treat the $\delta_{F_{y,a}}$*'s* separately for age 5 fish as visual inspection of the catch-at-age data indicated that age 5 fish were not actively targeted in the earliest years of the fishery. The $\delta_{F_{y,a}}$*'s* at ages 6–15$^+$ were treated as a correlated AR(1) process, separable across ages and years, with parameters $\sigma^2_{F6^+}, \phi_{F_{A6+}}, \phi_{F_{Y6+}}$ to be estimated. We fit an AR(1) process across ages and years for age 6–15$^+$ because fish that are closer in age and time are expected to have $\delta_{F_{y,a}}$ that are more similar than those that are further apart. The final formulation for the AR(1) parameters were determined via a model fitting process described in the exploratory process below.

Observation model

The observation model includes data from the commercial fishery and scientific research trawl surveys. There are two basic types of fishery information: total landed weight, and the size (length, weight) and age composition of the landings. Both these sources of information are used to derive annual fishery catch numbers-at-age. In the integrated assessment model philosophy, these data sources should enter into the assessment model fitting via separate observation models (*i.e.* one likelihood component for the age composition and one for the landings). We particularly want to focus our model estimation to include uncertainty in landings. Therefore, for pragmatic reasons, we used landings information (1960–2017) and the catch proportions-at-age (ages 5–15+ during 1960–2017) as independent data sources for model estimation. We only use commercial data from 1960 onwards as there was insufficient sampling before 1960. The current assessment model also does not use data prior to 1960. Age-based indices of stock abundance (*i.e.* numbers) are derived from the Canadian fall and spring research surveys in NAFO Divs. 3LNO (*see* Dwyer *et al.*, 2014 for details) and the Spanish research survey in the portions of NAFO Divs. 3NO outside of the Canadian Exclusive Economic Zone (EEZ; González-Troncoso *et al.*, 2017) were also used in model estimation. Indices were for ages 1–15+ for all surveys, for years 1990–2017 for the fall survey (2004 and 2014 omitted due to poor survey coverage), 1985–2016 for the spring survey (2006 and 2015 omitted due to poor survey coverage) and 1997–2016 for the Spanish survey.

Catch age composition data

We fit the age composition data using the continuation ratio logit (crl) transformation (*see e.g.* Cadigan, 2015; Berg and Kristensen, 2012; Agresti, 2003). A direct observation model for the matrix of observed catch proportions each year is complicated because of the constraints $P_{oa} \geq 0$ and $\sum P_{oa} = 1$. We use the crl which maps P_a for $a = 1, \ldots, A_{max}$ into $X_a \in (-\infty, \infty)$ for $a = 1, \ldots, A_{max} - 1$. The unconstrained crls are derived from the multiplicative logistic transformation,

$$X_a = \log\left[\frac{P_a}{P_{a+1} + \ldots + P_{A_{max}}}\right], a = 5, \ldots, A_{max} - 1. \qquad (1.4)$$

where A_{max} is the plus group. Recall that there is no catch data for ages 1–4. The inverse transformation of (1.4) is:

$$P_a = \begin{cases} \frac{\exp(X_a)}{\prod_{i=1}^{a}(1+\exp(X_i))}, & a = 5, \ldots, A_{max} - 1 \\ \frac{1}{\prod_{i=1}^{A_{max}-1}(1+\exp(X_i))}, & a = A_{max}. \end{cases} \qquad (1.5)$$

The crls for the observed catch proportions-at-age data (*i.e.* $X_{oy,a}$) are calculated from (1.4) and the observation model we use is based on assuming the model residuals $(X_{oy,a} - X_{y,a})$ have a normal distribution with AR(1) correlation separable across ages and years with parameters $\phi_{C_A}, \phi_{C_Y}, \sigma^2_{C_{y,a}}$ to be estimated, as we expect the crl errors to be similar for fish that are closer in age and time. Various age and year formulations were explored for $\sigma^2_{C_{y,a}}$ and are described in the exploratory process below.

Landings data

Dwyer *et al.* (2016) reported uncertainties about the reliability of the landings data for Grand Bank American plaice. To account for this, we treat reported landings as a lower bound for true landings (*i.e.* not all catches are reported). We assume that there is an upper bound for landings that varies with the reliability of data (see Table 2 for details). We used a censored likelihood approach in which the bounds are treated as the only information about landings (*see e.g.* Hammond and Trenkel, 2005; Bousquet *et al.*, 2010; Cadigan, 2015; Van Beveren *et al.*, 2017). We assume the true landings could be accurately estimated with a CV of 5%. Let B_{ly} and B_{uy} denote the lower and

Table 1. State-space model equations (see corresponding sections for details).

Process model		
Recruitment	$\log(\mathrm{N}_{y,1}) = \mu_{\mathrm{R}_y} + \delta_{\mathrm{R}_y}$	$\delta_{\mathrm{R}_y} \sim \mathrm{N}(\mu_{\mathrm{R}_y},\sigma_{\mathrm{R}})$ AR1(y) in δ_{R_y} μ_{R_1} for $y \leq 1993$ μ_{R_2} for $y > 1993$
Abundance	$\log(\mathrm{N}_{y,a}) = \log(\mathrm{N}_{y-1,a-1}) - \mathrm{Z}_{y-1,a-1} + \gamma_{y,a}$ $\log(\mathrm{N}_{y,A^+}) = \log\left[\mathrm{N}_{y-1,A^+-1}\exp^{-\mathrm{Z}_{y-1,A^+-1}} + \mathrm{N}_{y-1,A^+}\exp^{-\mathrm{Z}_{y-1,A^+}}\right] + \gamma_{y,a}$	$\gamma_{y,a} \sim \mathrm{N}(0,\sigma_{pe})$
Fishing mortality	$\mathrm{F}_{y,a} = \mu_{\mathrm{F}_{y,a}} + \delta_{\mathrm{F}_{y,a}}$ for $a = 5,6$ $\mathrm{F}_{y,a} = \mathrm{F}_{y,a-1} + \delta_{\mathrm{F}_{y,a}}$ for $a = 7-15$	$\delta_{\mathrm{F}_{y,a}} \sim \mathrm{N}(0,\sigma_{\mathrm{F}_5};\sigma_{\mathrm{F}_{6+}})$ AR1(y) in $\delta_{\mathrm{F}_{y,5}}$ AR1(y, a) in positive $\delta_{\mathrm{F}_{y,6+}}$ $\mu_{\mathrm{F}_{y,a}}$ for ages 5, 6, for 1960–1994/1995–2017
Observation model		
Landings	Censored likelihood: $\Pr(\mathrm{B}_{ly} \leq \mathrm{L}_y \leq \mathrm{B}_{uy}) = \Phi\left\{\frac{\log(\mathrm{B}_{uy}/\mathrm{L}_y)}{\sigma_{\mathrm{LC}}}\right\} - \Phi\left\{\frac{\log(\mathrm{B}_{ly}/\mathrm{L}_y)}{\sigma_{\mathrm{C}}\mathrm{L}}\right\}$	$\varepsilon_{\mathrm{L}} \sim \mathrm{LN}(0,0.05)$
Age composition	$\mathrm{X}_{\mathrm{O}_{a,y}} = \mathrm{X}_{a,y} + C_{y,a}$	$\varepsilon_{\mathrm{C}_{y,a}} \sim \mathrm{LN}(0,\sigma_{\mathrm{C}_{y,a}})$
Survey indices Catchability	$\mathrm{I}_{s,y,a} = \mathrm{q}_{s,a}\mathrm{N}_{y,a}\exp^{-\mathrm{f}_{s,y}\mathrm{Z}_{y,a}} + \varepsilon_{\mathrm{I}_{s,y,a}}$ $\mathrm{q}_{s,a} = \mathrm{q}_{s,a-1} + \delta_{\mathrm{q}_{s,a}},$	$\varepsilon_{\mathrm{I}_{s,y,a}} \sim \mathrm{N}(0, cv_s \cdot \mathrm{I}_{s,y,a}),$ $\delta_{\mathrm{q}_{s,a}}$ are positive separate q for Campelen and Engel trawls for ages 1–4 for fall and spring

upper bounds and $\sigma_L = 0.05$. The negative loglikelihood (nll) for the landings bounds data is:

$$\mathrm{nll}\left(L_1,\ldots,L_Y \middle| \{B_{ly},B_{uy};y = 1,\ldots Y\}\right) = \sum_{y=1}^{Y}\log\left[\Phi\left\{\frac{\log(B_{uy}/L_y)}{\sigma_L}\right\} - \Phi\left\{\frac{\log(B_{ly}/L_y)}{\sigma_L}\right\}\right], \qquad (1.6)$$

where $L_1,\ldots,L_Y$ are the model predicted landings. We fixed σ_{L} at a small value to ensure that the estimates of landings are between the bounds for most years.

The Baranov catch equation is used to model commercial catch as a function of N, F and Z,

$$C_{y,a} = \frac{F_{y,a}}{Z_{y,a}}\left(1 - \exp^{-Z_{y,a}}\right)N_{y,a}. \qquad (1.7)$$

Model predicted catch proportion at age ($P_a = C_a/\sum_a C_a$) were fit to observed proportions, as described in the previous section. Commercial average weights-at-age ($W_{y,a}$) were calculated by Rivard's method (Rivard, 1980) and are used to calculate model predicted landings each year, $L_y = \sum_a W_{y,a}C_{y,a}$.

Survey data

The model-predicted catch for survey s is:

$$I_{s,y,a} = q_{s,a}N_{y,a}\exp^{-f_{s,y}Z_{y,a}} \qquad (1.8)$$

where f represents the fraction of the year the survey takes place (0.460 for the Canadian spring and Spanish surveys and 0.875 for the Canadian fall survey). As in our treatment of the fishing mortality rates, we model the survey catchabilities, $q_{s,a}$, as increasing with age for each survey:

$$q_{s,a} = q_{s,a-1} + \delta_{q_{s,a}}, \quad \text{for a=2,..,15.}$$

Here, the $\delta_{q_{s,a}}$ are positive deviations from the $q_{s,a}$ in the previous year and are treated as fixed effects. We note that the $\delta_{q_{s,a}}$ are always positive to ensure that the q's increase with age and are treated as fixed effects since they are part of the observation equation and not the unobserved population process. For age 1 fish, the $q_{s,a}$ parameters are freely estimated, with no added deviation. In 1995 the trawl used in the Canadian surveys changed from the Engel to the Campelen (*see e.g.* Dwyer *et. al.,* 2016). Although Engel catch data were adjusted based on information from comparative fishing to match the Campelen catches, in our model ages 1–4 are given a separate q for each gear period due to issues in conversion of survey catches at these ages (Dwyer *et. al.,* 2016). The indices are assumed to follow a normal distribution, with mean $I_{s,y,a}$ and standard deviation $\sigma_{s,a} = \text{cv}_{s,a} \cdot I_{s,y,a}$, where CV_s represents a separate coefficient of variation (CV) parameter for each survey, to be estimated. Various age formulations for each survey CV were explored and are detailed in the exploratory process below. We treated each survey as from an AR(1) process across ages with independent parameter*s* ϕ_s to be estimated. A constant CV variance model for I is approximately the same as assuming $\log(I)$ has constant variance; however, an advantage of our approach is that we can use observed zero indices directly in the model whereas in other assessment packages these index zeros are typically excluded which is not appropriate when there are many zeros which occur non-randomly over time.

Estimation

The fixed-effects parameters to estimate (*i.e.* θ) are listed in Table 3. The unobserved states (*i.e.* $\delta_{F_{y,a}}, N_{y,a}$) are integrated out of the joint likelihood function and the estimation of θ is based on maximizing the marginal likelihood $L(\theta)$:

$$L(\theta) = \iiint_{\Psi} f_\theta(D|\Psi)\, g_\theta(\Psi)\, \partial\Psi \qquad (1.9)$$

where Ψ is the vector of all random effects, $f_\theta(D|\Psi)$ is the joint probability density function of the data (D; commercial landings, catch proportions at-age, commercial average weights-at-age, and Canadian fall, Canadian spring and Spanish survey indices) and $g_\theta(\Psi)$ is the joint probability density function for the random effects. The TMB (Kristensen *et al.*, 2016) package in R is used to integrate the marginal likelihood (1.9), which is performed via the Laplace approximation (*see* Skaug and Fournier, 2006 for details). The nlminb package in R is used to minimize the negative log likelihood function provided by TMB.

The final model formulation was determined via a thorough exploratory process. The overall goal of the exploratory process was to determine the best model formulation for the survey CVs, the crl $\sigma^2_{C_{y,a}}$ (sds) and the q age-aggregating (detailed below). The Bayesian information criterion (BIC) was used in model selection since BIC penalizes more heavily for extra parameters when the sample size is large. Previous work has shown that the correlation parameters can be difficult to estimate reliably (*see, e.g.*, Johnson *et al.,* 2016; Xu *et al.*, 2019), thus for our exploratory process, we conducted four exploratory runs with fixed AR(1) parameters: S1) ϕ_s freely estimated for each survey, all $\phi_F = 0.90$, $\phi_{C_A} = 0.9$, $\phi_{C_Y} = 0.75$; S2) ϕ_s freely estimated for each survey, all $\phi_F = 0.90$, $\phi_{C_A} = 0.9$, $\phi_{C_Y} = 0$; S3) all ϕ_s, ϕ_F, $\phi_C = 0.50$; S4) all ϕ_s, ϕ_F, $\phi_C = 0$. In all cases, the exploratory process began with the simplest model: with one sd parameter estimated for the crls, and one CV parameter per survey (see Table 3) and followed the six

Table 2. Upper catch bounds (UB) for estimated landings with associated justification for bounds; RC is reported catch. Discussion on catch uncertainties can be found in Wheeland *et al.* 2018, and references therein

Period	**UB**	**Comments**
1960–1976	2xRC	"Unspecified flounder" by some countries. See, for example, (Pitt, 1972).
1977–1982	1.2xRC	Landings by primarily Canada (>95%) after establishment of 200 mile exclusive economic zone (EEZ).
1983–1993	1.5xRC	Increased foreign catch outside 200 miles. Various estimates used for catch estimates. Issues with unspecified flounder records and discarding
1994–2010	1.2xRC	No directed fishing in 1994 (bycatch quota), 0 TAC 1995 onwards. Catches defined from various sources with those considered most reliable by Scientific Council used for totals
2011–2017	1.5xRC	Loss of availability of scientific observer data in the NAFO Regulatory area and surveillance estimates. Varying methods applied to obtain catch estimates including effort ratios (Dwyer *et al.*, 2016), daily catch records, and NAFO CESAG estimates (NAFO, 2017)

steps below. Within each step, the model was refit for each assumption (*e.g.* in step 1 the model was refit 10 times, for *q* age-aggregating 5,..,14):

1) ***q age-aggregating***: for each age 5,..,14 fix survey $\delta^+_{q_{s,a}} = 0$ for all subsequent ages (*e.g.* *q*5+ is one run with $\delta^+_{q_{s,a}}$ fixed at 0 for ages 6+). *q* age-aggregating selected from run with lowest BIC[1].

2) ***CV combinations:*** for each survey using *q* age-aggregating from 1) fit all combinations (pooled and unpooled; s*ee Supplementary Materials 1* for details) of CV ages while keeping one CV parameter for other two surveys. Survey CV formulations for each survey selected from run with lowest BIC.

3) ***re-check q:*** with survey CVs from 2), re-run 1) to check that *q* age-aggregation is the same as in 1)

4) ***crl sd ages:*** with survey CVs from 2) and *q* from 1), fit all combinations of crl sd ages. crl sd age formulation selected from run with lowest BIC.

5) ***crl sd years:*** with *q* from 1), survey CVs from 2), and crl sd ages from 4), fit two scenarios:

    a. pre/post moratorium split: fit a separate age sd parameter pre/post moratorium for year split start $\in$ (1990, 1999)

    b. moratorium gap: fit one separate sd parameter (no age splitting) for 10-year mortarium gap for year gap start $\in$ (1990, 1999).

    crl sd year formulation selected from run with lowest BIC from both a and b

6) ***re-check q:*** with survey CVs from 2), crl sd ages and years from 4–5, re-do 1) to check that *q* age-aggregation is the same as in 1)

The best fitting model was selected from step 6 for each of the four runs (*i.e.* one best fitting model for runs S1-S4 selected via lowest BIC from step 6) and model fit compared across all four via a detailed examination of model residuals and BIC. Evidence of patterns in residuals (*i.e.* blocks of ages and years having residuals of the same sign, and whether or not overall residual variability matches assumption) was used to evaluate potential model mis-specification. The survey and continuation ratio logit residuals, which are correlated in our observation models, were standardized using the Choleski factorization of their estimated covariance matrix. We did not use the one-step ahead residual method (*see e.g.* Thygesen *et al.*, 2017) because it does not allow for correlations in the observations. A final model was selected from the four S1–S4 best fitting runs (*i.e.* via BIC and residual fits) and in the final step, two extra runs were fit; one with all ϕ_F parameters freely estimated and all ϕ_C fixed and one with all AR(1) parameters freely estimated (O2). These two runs were compared to the run with the fixed AR(1) parameters (O1), and a final model selected from the three. In all subsequent text, SSM will refer to the final model.

The SSM fit was also assessed through retrospective model fitting for the years 2011–2017. Each retrospective model fit used one less year of data (*i.e.* model for year 2011 used data up to 2011) and predicted abundance, biomass, spawning stock biomass and average *F*'s were examined for systematic patterns and the severity of retrospective pattern was assessed using Mohn's rho (*see* Mohn, 1999). Ideally, no discernable directional patterns will be present in the retrospective plots.

Biomass-at-age was calculated by multiplying predicted numbers at age (*i.e.* $N_{y,a}$) and stock weights-at-age, which were estimated externally via a spatiotemporal biphasic Von Bertalanffy growth model (*see* Kumar *et al.,* 2020). Length and age data are collected for American plaice from research survey vessels using a length-stratified age sampling design and Perreault *et al.* (2019) showed that ignoring this sampling design can lead to biased growth model parameter estimates. Kumar *et al.*'s method (2020) accounted for the length-stratified age sampling design. The 3LNO stock weights were combined for each division by weighting the values for each division by the average abundance index at age during 1975–2017. Stock weights prior to 1975 were fixed at the mean values for 1975–77. Estimates of maturity-at-age were taken from Wheeland *et al.* (2018).

Simulation and sensitivity testing

A full simulation study is beyond the scope of this paper; however, we conducted a simple self-simulation test and jittered start on the SSM to examine the reliability of the model estimates (*see e.g.* Cadigan, 2015; Nielsen and Berg, 2014). The self-simulation test randomly generates survey indices and continuation ratio logit catch proportions from the model predictions and assumed distributions detailed above. Process errors and other random effects are treated as fixed when generating the data and the model is re-fitted to the simulated data. This process is repeated 1000 times and estimates of SSB, average fishing mortality rates (ages 9–14), recruitment,

---

[1] Note for *q* exploratory purposes (*i.e.* Step 1), the lowest AIC (Akaike information criterion) was used for model selection, since in all cases, the BIC selected the model with the fewest *q* parameters, and this was considered unrealistic for this stock

Table 3: Base model for exploratory process; a+ is *q* age-aggregation (*e.g.* q5+ is model with *q* deviations fixed at 0 for ages 6+). Age groupings for survey CVs and sd crls are for subsequent ages (*e.g.* a separate sd parameter pooled for ages (1–4) (5–6)(7–15)). *See Supplementary Materials 1* for details.

Type	Parameters
Base model	
Process error variance	σ^2_{pe}
Mean recruitment	μ_{R_1} for $y \leq 1993$ and μ_{R_2} for $y > 1993$
Variance and correlation of log-recruitment deviations	σ^2_R, ϕ_R
Mean F	$\mu_{F_{y,a}}$ for ages 5, 6, and two time blocks: 1960–1994/1995–2017
Variance at age 5, 6–15+	$\sigma^2_{F_5}$, $\sigma^2_{F6^+}$
Model exploration S1-S4	
Survey q's	
Canadian spring survey	$\delta_{s,a+}$, for s = Canadian spring, fall, Spanish surveys a+ = age aggregation explored for ages 5–14
Canadian fall survey	
Spanish survey	
Survey coefficients of variation	
Canadian spring survey	$cv_{s,a}$, for s = Canadian spring, fall, Spanish surveys a = various age groupings (1–15)
Canadian fall survey	
Spanish survey	
Catch age composition variance	$\sigma^2_{C_{y,a}}$, for a = various age groupings (5−14)
Survey residual correlations	ϕ_s for s=Canadian spring, fall, Spanish surveys
Year-correlation of F deviations at age 5, 6–15+	$\phi_{F_5}, \phi_{F_{A6^+}}, \phi_{F_{Y6^+}}$
Catch age correlation	ϕ_{C_A}, ϕ_{C_Y}

variance and autocorrelation parameters are stored. We calculated the relative difference of the estimates for each year (*i.e.* (simulation SSB_y – data-based SSB_y)/ data-based SSB_y) for comparison.

The jittered start test re-fits the model with random noise added to the starting parameter values, generated from $N(0, 0.25 \cdot \hat{\mu})$, where $\hat{\mu}$ is the model predicted parameter of interest. The model is re-optimized 100 times and the negative log-likelihood is stored for each iteration. Ideally, we expect an identical model fit from the jittered starting parameter values.

We also examined the model sensitivity to our assumptions about M and catch bounds. A profile likelihood was constructed for a range of $M_{a,y}$'s; that is, $M_{a,y} = M + \Delta M$, where M is the SSM M model formulation and $\Delta M \in (-0.1, 0.35)$. We also re-fit the model with upper catch bounds fixed at half the original model formulation upper bounds (M2) and with the upper catch bounds fixed (M3) at 1% of the reported bounds (*i.e.* "fixed landings"). Model fit for the catch bounds was assessed using BIC and an examination of the retrospective plots.

Results

For brevity, we provide a summary table of the exploratory process that describes the final model from each run (Table 4); additionally, only the full exploratory process results from the best fitting run (S2) are given in *Supplementary Materials 1* (SM1) and discussed. For exploratory step 1 (run S2), the model with an age-aggregation of 7+ ($\delta^+_{q_{s,a}} = 0$ for ages 8+) had the lowest AIC and this was selected as the age-aggregation for step 2 (see footnote 2 for details and SM1 Table 1). Overall, the BIC for the fall model fits ranged between approximately 9970 and 9890, 9940 and 9860 for the spring survey and 9970 and 9900 for the Spanish survey, indicating the grouping of the Spanish survey coefficient of variations (CVs) provided the least improvement in model fit (SM1 Tables 2–5). This is not surprising since the data for the Spanish survey do not cover the entire 3LNO region and are not as informative as the fall and spring surveys (see, *e.g.* Wheeland *et al.,* 2018 for more details). Rechecking the q age-aggregation in Step 3 confirmed that the age-aggregation of 7+ provided the lowest AIC and BIC with the new survey CV formulations (SM1 Table 6). The continuation ratio logit (crl) age exploratory runs in Step 4 had BICs that ranged from approximately 9600 to 9570, and the age aggregation of (5–6)(7–11)(12–14) was selected as the final crl sd age formulation (SM1 Table 7). For Steps 5a and 5b, the BICs ranged from approximately 9560 to 9480 (SM1 Table 8). Rechecking the q's in Step 6 confirmed that the age-aggregation of 7+ provided the lowest AIC and BIC with the new survey CV and crl sd formulations (SM1 Table 9). The AIC and BIC from Step 1 with a q age-aggregation of 7+ were 9690 and 9922 in comparison to the Step 6 run that were 9194 and 9481 respectively, indicating a substantial improvement in model fit.

In all four exploratory model scenarios, q7+ was the best formulation for the survey catchabilities (q; Table 4). Overall, the survey CV formulations were similar for all four model formulations. For example, for the fall survey, models S1–S3 provided identical formulations, with S4 (all AR(1) parameters fixed to zero) providing a better fit with an extra CV parameter for ages (2–4). Both the spring and Spanish CV formulations were similar for all four runs, providing the best fit with separate parameters at the oldest and youngest ages. In all formulations, the best fit for the crl sd parameters had a separate variance parameter from 1990–1999, with various formulations for the age groupings. For example, S1 provided the best fit with separate sd parameters for ages 5–7,14, and pooled for ages (8–13), whereas S4 pooled the sd parameters for ages (5–11) and (12–14). Overall, S2 had the lowest BIC, and had the best residual fits for both the surveys and the crls (*see Supplementary Materials 2*), and we selected this model as the best fitting model. For the final exploratory step (*i.e.*, one run with all ϕ_F parameters freely estimated and all ϕ_C fixed and one run with all AR(1) parameters freely estimated), the lowest BIC was for the model with all but the crl AR(1) parameters freely estimated (SSM; Table 5), and this was selected as the final state space model.

The SSM fit the data well with no patterns in the survey or continuation ratio logit residual plots (*see Supplementary Materials 3*). In 2017, recruitment, abundance and spawning stock biomass (SSB) were estimated near the lowest historical levels (Fig. 1). The model predicted landings were estimated within the upper and lower bounds, with the predicted landings closest to the upper bound in the early 80s, and again in 2010 (Fig. 2) and closest to the lower bound in the early 1990s. At ages 1–4, the catchability pattern (Fig. 3) for the fall and spring surveys was lower for the Engels than the Campelen trawl. The differences were most pronounced for ages three and four, with the catchability estimates for the Campelen trawl almost twice as large as for the Engels trawl. For ages 1–5, the process errors (Fig. 4) were close to zero until the mid-nineties. Overall, there were no noticeable trends in the process errors at the older ages. Mohn's rho for the full retrospective run (Fig. 5) was 0.30 for abundance and -0.19 for recruitment. In comparison to the most recent stock assessment model for Grand Bank American plaice (which we refer to as the VPA), the SSM had a lower Mohn's rho for SSB at 0.43 compared to 0.69 for the VPA (Fig. 6). Mohn's rho for aveF for the SSM was almost half the VPA Mohn's rho, at -0.27 for the SSM and -0.45 for the VPA.

The overall trends in SSB and aveF were similar for the SSM and the VPA (Fig. 7). Noticeable differences included the SSM predictions of historical SSB (*i.e.* years 1960–1972) that were larger (but with high uncertainty) than the historical SSB predictions from the VPA. The VPA model also predicted a higher average fishing mortality rate in the early 1990s, at approximately 1.1, with the SSM prediction at approximately 0.80 for the same period.

The self-simulation study lower 2.5% and upper 97.5% intervals for both SSB and aveF covered zero until the mid-1990s,(Fig. 8), indicating that the simulated samples produced estimates that were similar to the SSM estimates in those years. In the earliest years (1960–1972), the median of relative differences for aveF was mostly positive, with the converse for SSB. After 1990, there was a consistent positive bias in aveF and a negative bias in SSB, except in the final years, where aveF was underestimated and SSB overestimated. The boxplots of parameter estimates (Fig. 9) showed that the largest range were for estimated $\mu_{F_{5\_Pre1995}}$. TMB has an option (*see* Thorson and Kristensen, 2016) to reduce bias in nonlinear random effects models, and we implemented this method in a self-simulation run as a potential fix to the bias in our self-simulation study (see M4; Table 5). The bias across the entire time series for both SSB and aveF was much larger with the bias-correction turned on (*see Supplementary Materials 4*) than without. The jittered-start test did not converge for 5% of the simulations, with 100% of the converged models producing negative log-likelihoods that were identical to the original formulation.

Table 4: Best fitting models from exploratory process. For all models, parentheses represent pooled ages and **,.,** represent separate ages (*e.g.* 1,.,3(4–12) is a separate sd parameter for ages 1,2,3, and pooled for ages 4–12). (1990–1999) represents a separate crl sd parameter for the year block. S1 is run with ϕ_s freely estimated for each survey, all ϕ_F= 0.90, ϕ_{C_A}= 0.9, ϕ_{C_Y}= 0.75; S2 is run with ϕ_s freely estimated for each survey, all ϕ_F= 0.90, ϕ_{C_A}= 0.9, ϕ_{C_Y}= 0; S3 is run with all ϕ_s, ϕ_F, ϕ_C = 0.50; S4 all ϕ_s, ϕ_F, ϕ_C = 0. AIC is the Akaike information criterion and BIC is the Bayesian information criterion.

	S1	**S2**	**S3**	**S4**
nll	4548	4540	4878	5545
AIC	9216	9194	9861	11196
BIC	9519	9481	10123	11463
	Optimal model formulation			
q	7+	7+	7+	7+
Fall cv	1(2–11)(12–15)	1(2–11)(12–15)	1(2–11)(12–15)	1,(2–4)(5–12)(13–15)
Spring cv	1,.,2(3–7)(8–13)(14–15)	1,.,2(3–13)(14–15)	1,.,2(3–13)(14–15)	(1–2)(3–10)(11–14)15
Spanish cv	1(2–7)(8–15)	1,(2–7)(8–15)	(1–5)(6–15)	(1–5)(6–15)
Crl sd	5,.,7(8–13)(1990–1999)	(5–6)(7–11)(12–14) (1990–1999)	5(6–14) (1990–1999)	(5–11)(12–14) (1990–1999)

The minimum negative log-likelihood from the M profile likelihood plot was 4472, with an associated Δ M of 0.30 (Fig. 10). For this model fit, the average fishing mortality rate in 2017 was estimated at 0.01 with SSB in 2017 at 100.83 hundred thousand tons. Results from the sensitivity tests (Table 5) showed that the SSM had a lower BIC than the runs that halved the catch bounds (M2) and "fixed" the landings (M3). This is expected because more narrow catch bounds restrict the flexibility of the model. Mohn's rho for both M1 and M2 for aveF were slightly larger than the Mohn's rho from the SSM at -0.29 (Fig. 11). Similarly, Mohn's rho for M1 and M2 for SSB were slightly larger than for the SSM at 0.39.

Discussion

Overall, our state-space model (SSM) that accounted for uncertainties in the landings data and allowed for process errors fit the data well, with no obvious patterns in the survey and continuation ratio logit residual plots (*see Supplementary Materials 3*). The retrospective patterns were reduced for spawning stock biomass (SSB) and greatly reduced for average fishing mortality for ages 9–14 (aveF) compared to the most recent stock assessment model (VPA).

The M profile plot provided the best fit when M was increased by 0.30, suggesting that the values we used for M's may be too low. Previous research found evidence that M's during 1989 to 1996 (Morgan and Brodie, 2001) had increased to 0.53 and the current VPA model and our SSM include this increase. However, since the closure of the commercial fishery, estimates of total mortality rates have remained high for some periods (*e.g.* Fig. 7 for years 2000–2006), and this may suggest that M is higher than 0.20 in recent years. This is supported by preliminary work that suggests that M has increased since the mid-1990s (COSEWIC, 2009; Morgan *et al.*, 2011). The lack of recovery of the stock has largely been attributed to overfishing, however the mis-specification of M not only in the SSM but in historical assessment models could be over-estimating the relative impact of F. Thus, although a thorough study of M is beyond the scope of this paper, research that improves our understanding of M for this species should be of high priority as we may be fixing M within the model to be lower than is reasonable and subsequently over-stating the contribution of fishing mortality to the lack of recovery of the stock.

Mohn's rho from the SSM retrospective analyses for both aveF and SSB were closer to zero than Mohn's rho from the VPA retrospective analysis, which is a key improvement compared to the current assessment model. Including process error in the population dynamics model helped account for underlying time-varying population processes (*e.g.* M) that were not accounted for in the VPA, thereby reducing retrospective patterns. There is still evidence of slight retrospective patterns, and this may be caused by underlying spatial or time-varying processes that are mis-specified in the observation model since process errors can only account for misspecifications in the process equations.

Table 5. Model estimates of variance parameters and some population parameters with percent (%) coefficient of variation. (O1 is the final model from exploratory runs (S2) with all ϕ_F= 0.9, ϕ_{C_A}= 0.9, ϕ_{C_Y}= 0, O2 is the final model from exploratory runs with all AR(1)parameters freely estimated. M2 is the final model with upper catch bounds set to half the SSM upper bounds, M3 is final model with fixed landings and M4 is the final model fit with the bias correction option in TMB turned on). AIC is the Akaike information criterion and BIC is the Bayesian information criterion.

	SSM		**O1**		**O2**		**M2**		**M3**		**M4**	
nll	4524		4540		4521		4557		4781		4524	
AIC	9168		9194		9164		9234		9682		9168	
BIC	9470		9481		9471		9537		9984		9470	
	Est	**CV**	**Est**	**CV**	**Est**	**CV**	**Est**	**CV**	**Est**	**CV**	**Est**	**CV**
σ_{F5}	2.25	49	1.52	13	2.29	48	2.01	45	2.13	46	2.25	49
σ_{F6^+}	2.21	20	1.42	8	2.22	19	2.14	19	2.19	19	2.21	20
σ_{pe}	0.22	6	0.22	6	0.22	6	0.23	6	0.23	6	0.22	6
σ_{R}	0.71	15	0.70	14	0.71	15	0.71	14	0.71	14	0.71	15
σ_{C5-6}	0.60	10	0.56	10	0.53	11	0.61	10	0.61	9	0.60	10
σ_{C7-11}	0.33	9	0.29	11	0.28	11	0.33	9	0.33	9	0.33	9
σ_{C12-14}	0.23	13	0.22	13	0.20	13	0.23	13	0.23	13	0.23	13
σ_{C90-99}	0.95	9	0.98	9	0.76	12	0.96	9	0.96	9	0.95	9
$\mathrm{cv}_{\mathrm{Fall\ 1}}$	0.66	20	0.67	19	0.67	20	0.66	20	0.66	20	0.66	20
$\mathrm{cv}_{\mathrm{Fall\ 2\text{-}11}}$	0.31	8	0.31	8	0.31	8	0.31	8	0.31	8	0.31	8
$\mathrm{cv}_{\mathrm{Fall\ 12\text{-}15}}$	0.45	10	0.45	10	0.45	10	0.45	10	0.45	10	0.45	10
$\mathrm{cv}_{\mathrm{Span.\ 1}}$	1.55	33	1.56	33	1.56	33	1.54	32	1.54	32	1.55	33
$\mathrm{cv}_{\mathrm{Span.\ 2\text{-}7}}$	0.81	12	0.81	12	0.81	12	0.81	12	0.81	12	0.81	12
$\mathrm{cv}_{\mathrm{Span.\ 8\text{-}15}}$	0.46	11	0.46	11	0.46	11	0.46	11	0.47	11	0.46	11
$\mathrm{cv}_{\mathrm{Spr.\ 1}}$	1.35	28	1.35	27	1.34	27	1.35	27	1.34	27	1.35	28
$\mathrm{cv}_{\mathrm{Spr.\ 2}}$	0.70	18	0.70	17	0.70	17	0.70	18	0.70	17	0.70	18
$\mathrm{cv}_{\mathrm{Spr.\ 3\text{-}13}}$	0.37	11	0.37	11	0.37	11	0.37	11	0.37	11	0.37	11
$\mathrm{cv}_{\mathrm{Spr.\ 14\text{-}15}}$	0.48	13	0.49	13	0.48	13	0.47	13	0.47	13	0.48	13
$\varphi_{F_{A6^+}}$	0.95	2	-	-	0.95	2	0.95	2	0.95	2	0.95	2
φ_{F5}	0.97	4	-	-	0.97	4	0.95	5	0.96	4	0.97	4
$\varphi_{F_{Y6^+}}$	0.98	1	-	-	0.98	1	0.97	1	0.98	1	0.98	1
φ_{R}	0.32	46	0.32	47	0.33	46	0.31	48	0.31	48	0.32	46
φ_{Fall}	0.60	8	0.61	8	0.61	8	0.60	8	0.60	8	0.60	8
$\varphi_{\mathrm{Span.}}$	0.70	6	0.69	6	0.70	6	0.70	6	0.70	6	0.70	6
$\varphi_{\mathrm{Spr.}}$	0.87	3	0.87	3	0.87	3	0.87	3	0.87	3	0.87	3
φ_{C_A}	-	-	-	-	0.83	4	-	-	-	-	-	-
F_{2017}	0.11	20	0.11	19	0.11	19	0.09	20	0.08	18	0.09	28
SSB_{2017}	10.13	16	9.80	16	9.89	16	9.83	17	9.58	17	11.51	18
F_{VPA}	0.06	-	-	-	-	-	-	-	-	-	-	-
SSB_{VPA}	18.24	-	-	-	-	-	-	-	-	-	-	-

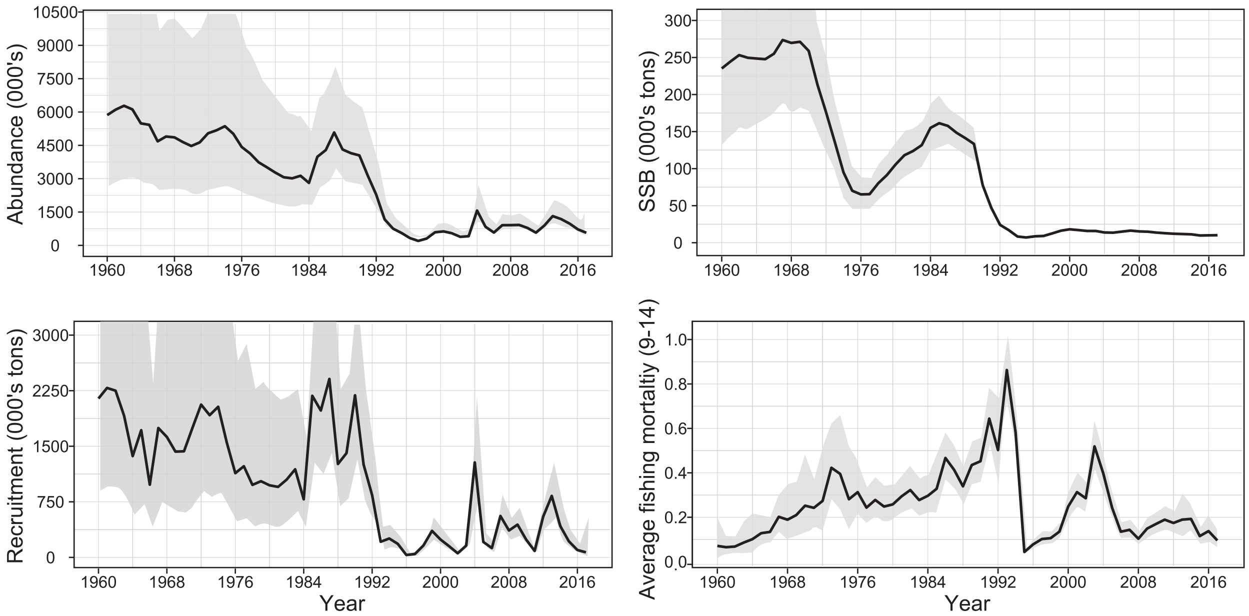

Fig. 1. SSM estimated population abundance, spawning stock biomass (SSB), average fishing mortality rate (ages 9–14) and recruitment

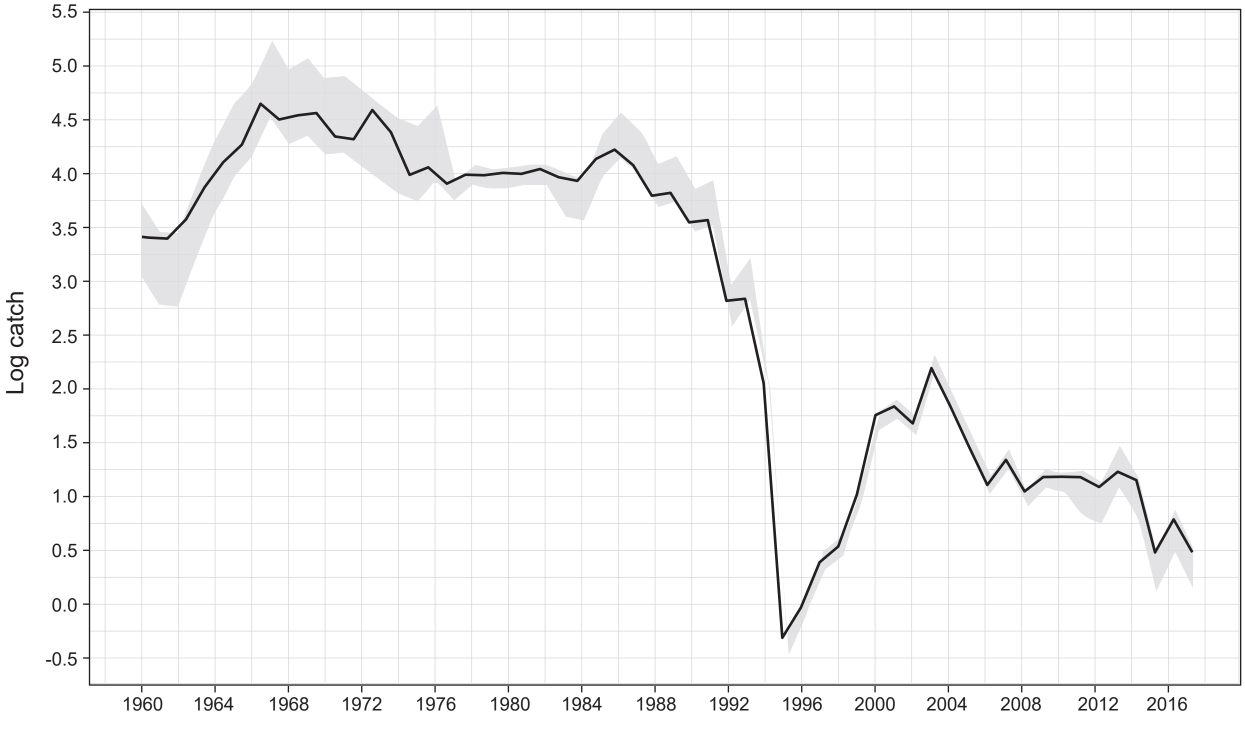

Fig. 2. SSM estimated log catch numbers for ages 5–15+ (solid line), the shaded grey represents the region between the log lower catch bounds and the log upper catch bounds.

The estimate for survey catchability q is defined as the value required to scale swept-area abundance to the population abundance (*see e.g.* Dickson, 1993; Fraser *et al.*, 2007). An estimate of q less than one implies that fewer fish are caught than occupied the area of the trawl, and a value greater than one implies that more fish are caught than occupied the area. Bryan *et al.* (2014) found evidence of herding behavior in over 90% of observed flatfish in the presence of survey trawls and this herding underestimates the width used in area swept calculations and can result in q estimates that are greater than one. Therefore, larger q estimates are not unrealistic for American plaice; however, the q estimates from the SSM are very large, with the maximum at 6.7. The maximum q estimate from the SSM is however much smaller than the maximum q estimated from the VPA at 13.6[2] (Table 26, Wheeland *et al.,* 2018). Additional research is required to better understand why the stock assessment model estimates are so high.

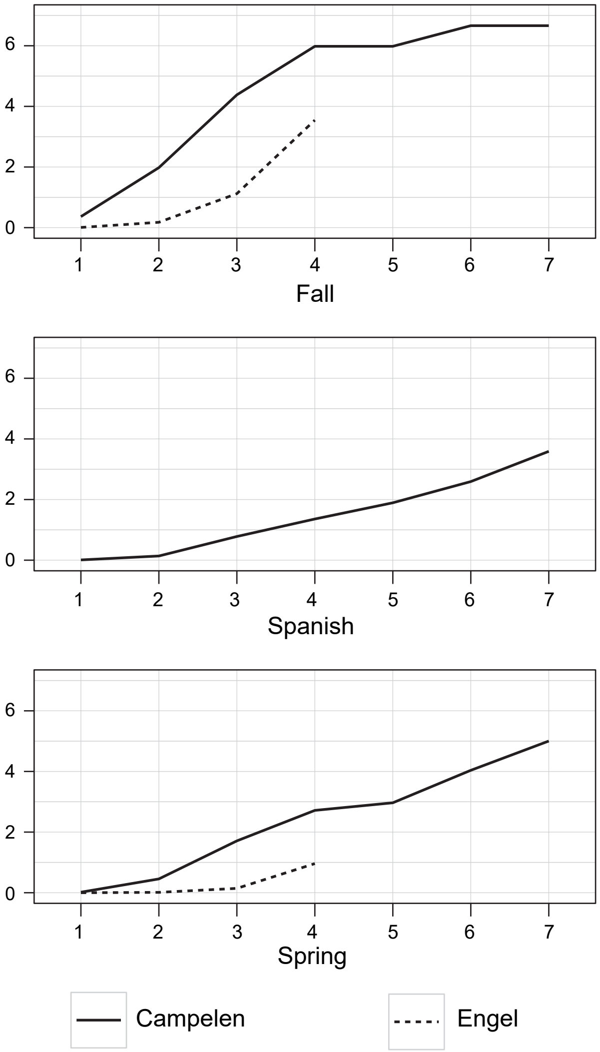

Fig. 3. Survey catchability patterns for the fall, spring and Spanish surveys with a separate catchability for two gear types (Engel and Campelen) for the spring and fall surveys for ages 1–4. Catchability for ages 7+ is fixed at the value for age 7.

A difference to note between the SSM and the VPA is that the SSM assumes that the survey indices have a normal distribution with a constant coefficient of variation (CV) whereas the VPA assumes that the log of the survey indices have a lognormal distribution. The lognormal distribution does not allow for zeros in the survey data; however, this assumption may not be appropriate when there are many zeros in the data or when zeros are "true" zeros (*i.e.* no fish available to be caught). The assumption of normality with a constant CV avoids the problem of dropping zeros altogether. However, the normal distribution assumption supports negative indices which are infeasible. A solution to this problem is to use a truncated normal distribution in place of the normal distribution (*e.g.* Albertsen *et al.*, 2016). However, a normal distribution with constant CV is virtually identical to a truncated normal distribution when the CV is small. Consider two random variables (*e.g.* X and Y) that both have mean μ and a constant coefficient of variation, $\tau = \sigma/\mu$. If $X \sim N(\mu, \sigma = \tau\mu)$ and $Y \sim TN(\mu, \sigma = \tau\mu; Y > 0)$ has a truncated normal distribution then their density functions differ by a multiplicative constant that only depends on τ and does not depend on μ. The constant is $\int_0^\infty \varphi(\frac{z-1}{\tau})\,dz$ where $\varphi(\cdot)$ is the density function for $Z \sim N(0,1)$. The constant is close to 1 for $\tau < 0.5$. Hence, for our model, using the truncated normal distribution instead of the normal distribution will only affect estimation through differences in the weighting of survey indices with different τ's, especially when $\tau \gg 0.5$. For our SSM we only have large τ's for the Spanish survey and ages 1–2 for the Canadian surveys, thus in our case there should be little difference in model fit for the truncated normal vs the normal. However, although the approaches are theoretically similar, future research is needed to compare the performance of the three methods.

Fitting the age composition and landings data separately is in line with the integrated model philosophy, but our treatment of stock and catch weights is not. Ideally, each source of data should enter independently into the likelihood equation; however, the stock and catch weights at age data for American plaice are collected in complex length-stratified sampling designs and how to model these likelihoods is difficult and beyond the scope of this paper. In the future, state-space stock assessment models will ideally fit to the raw data (*e.g.*, maturity at age, weights

---

[2] Note that the survey index from the NAFO assessment is in millions and the catch is in thousands; to get the qs on the same scale as the SSM we multiplied the NAFO q estimate by 1000

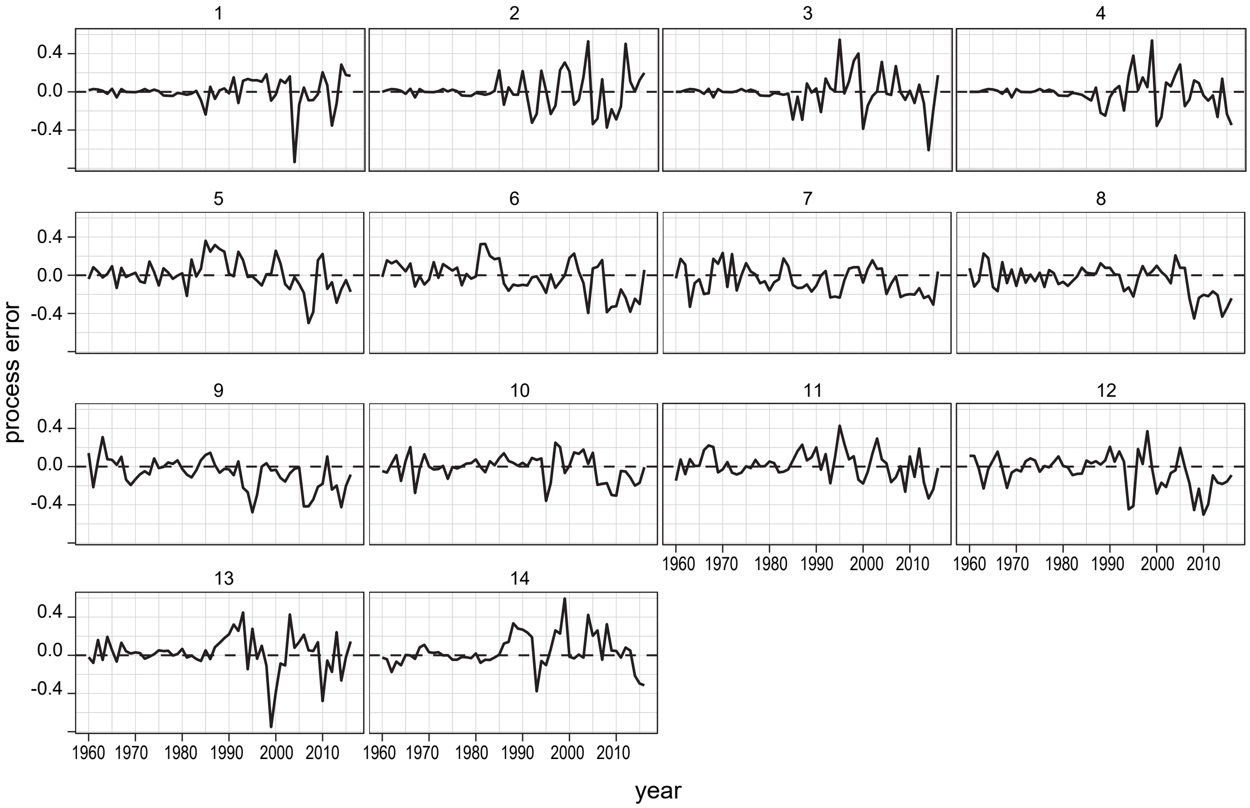

Fig. 4. SSM estimated process errors for ages 1–14 for years 1960–2016.

at age) and this will require complex stock assessment models that can account for the spatial nature of the stock assessment data.

The self-simulation study lower 2.5% and upper 97.5% did not cover zero for years 2006–2010 and again in 2013–2015. This bias was also present in models O1 (fixing all crl and F AR(1) parameters) and O2 (freely estimating all AR(1) parameters; *see Supplementary Materials 4*). In a self-test simulation the model is specified exactly so stock size estimation bias cannot be the result of model misspecification, but rather it must be related to estimation bias and possibly related to nonlinear modelling of random effects. Our self-simulation run that implemented the TMB bias correction option had larger bias than the SSM self-simulation run without (*Supplementary Materials 4*), which provides evidence that the bias is related to estimation bias. Also, preliminary research that fit the SSM with an increase in M (both across the entire time series, and another run increasing M only in the later years) did not produce the self-simulation bias in SSB and aveF in these later years (*see Supplementary Materials 4*). Hence, it seems that the bias is related to the particular settings of the model, and perhaps the magnitude of variance parameter estimates, and this requires additional research to better understand this type of bias.

Although M profile plots are useful in providing a general picture of the role of the M assumption, it is also useful to examine which data sources are more informative about M, and Lee *et al.* (2011) suggested that informative length or age composition data is needed to reliably estimate M. Data-specific M profiles are commonly produced by more traditional stock assessment models without random effects and process error (*e.g.* SS3; Methot and Wetzel, 2013) but in a state-space stock assessment model it is not straight-forward how to do this because the integrated log-likelihood cannot be split into a sum of log-likelihoods due to various data sources and other model assumptions. Further development of diagnostics designed to detect M misspecification (*e.g.* Cadigan and Farrell, 2002) also seems useful.

While overall trends in stock trajectory are similar, our new SSM is an improvement to the current stock assessment model that is used to inform the management of American plaice on the Grand Bank of Newfoundland

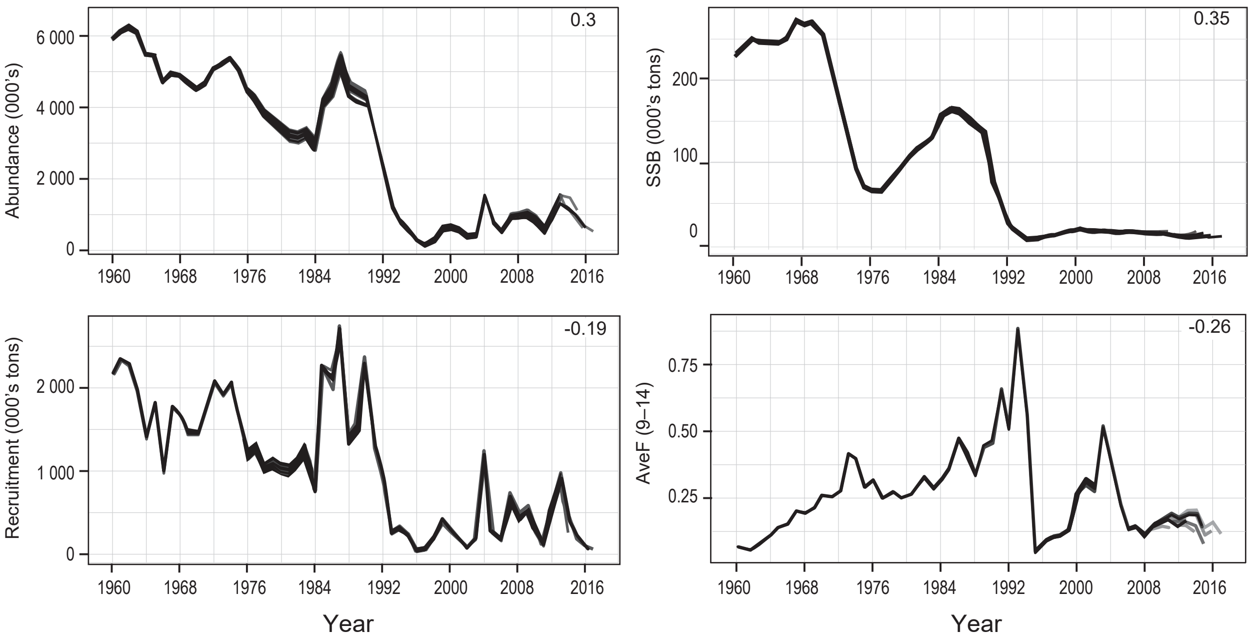

Fig. 5. SSM retrospective estimates from 2011–2017 for total abundance, spawning stock biomass (SSB), average fishing mortality rates (ages 9–14) and recruitment for years 1960–2017. Mohn's rho is given in the top right corner.

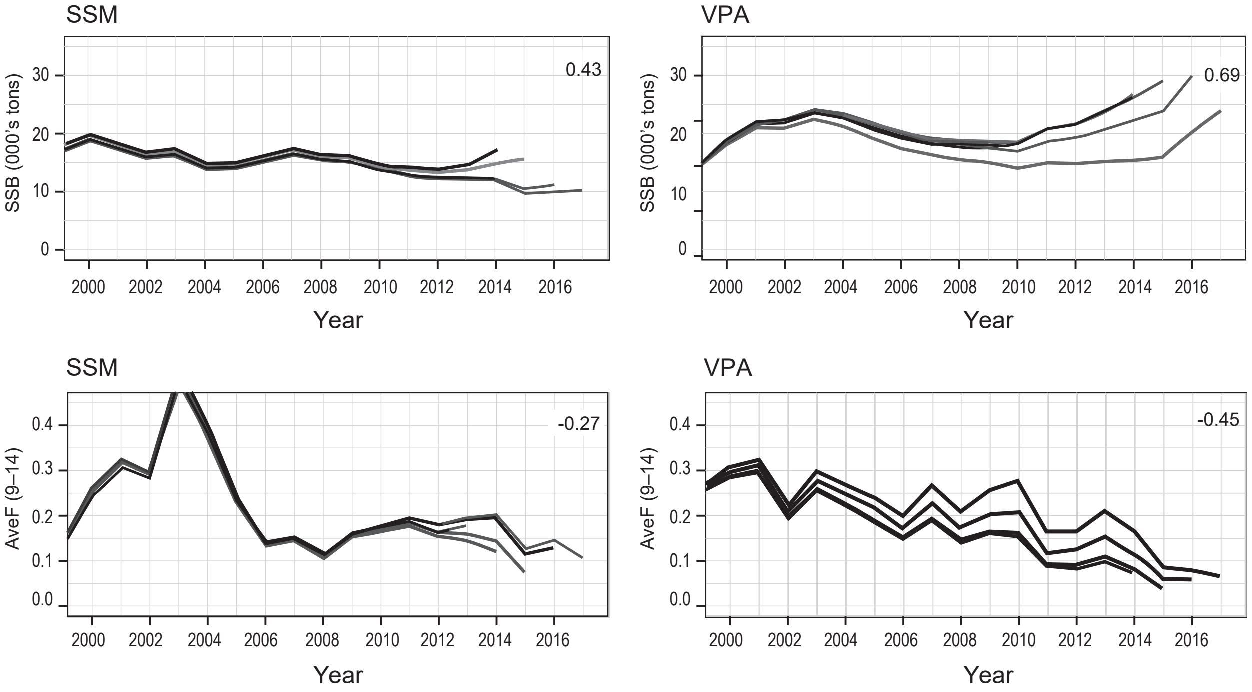

Fig. 6. Retrospective estimates for spawning stock biomass (SSB) and average fishing mortality rates (ages 9–14) for the SSM and VPA for years 1960–2017. Mohn's rho is given in the top right corner

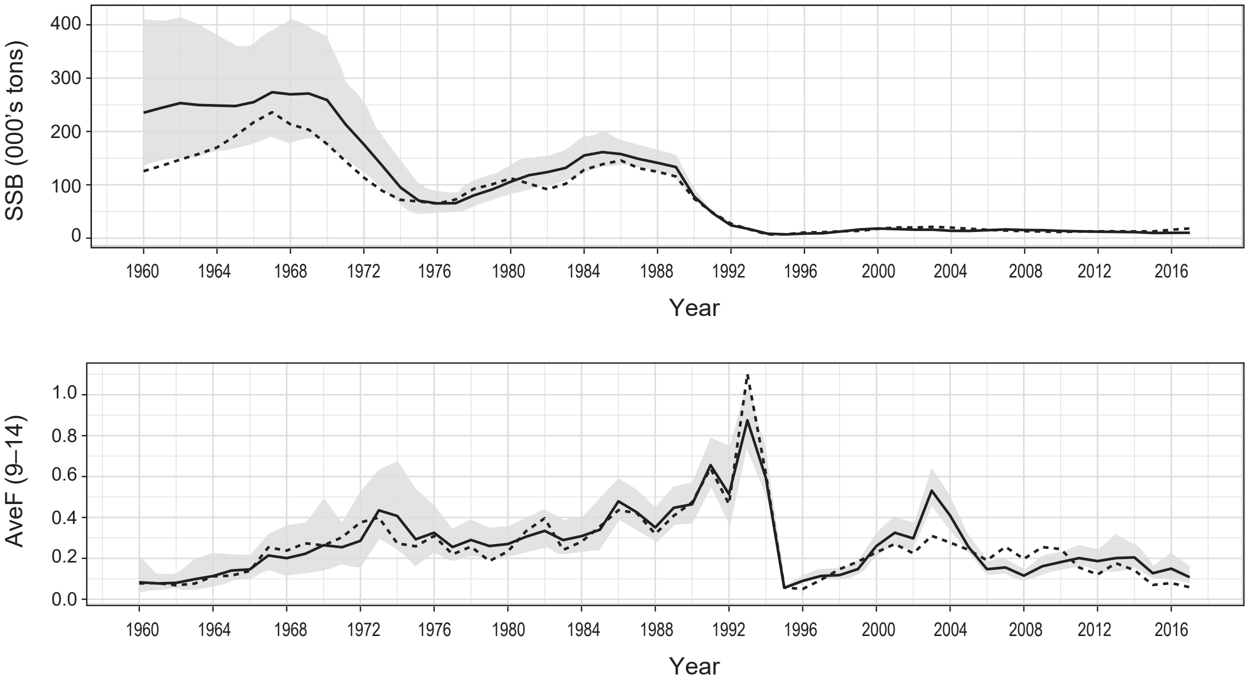

Fig. 7. SSM (solid line) and VPA (dashed line) estimated spawning stock biomass for years 1960–2017 and average fishing mortality rates (ages 9–14) for years 1960–2017. The shaded grey region represents the SSM model predicted uncertainty.

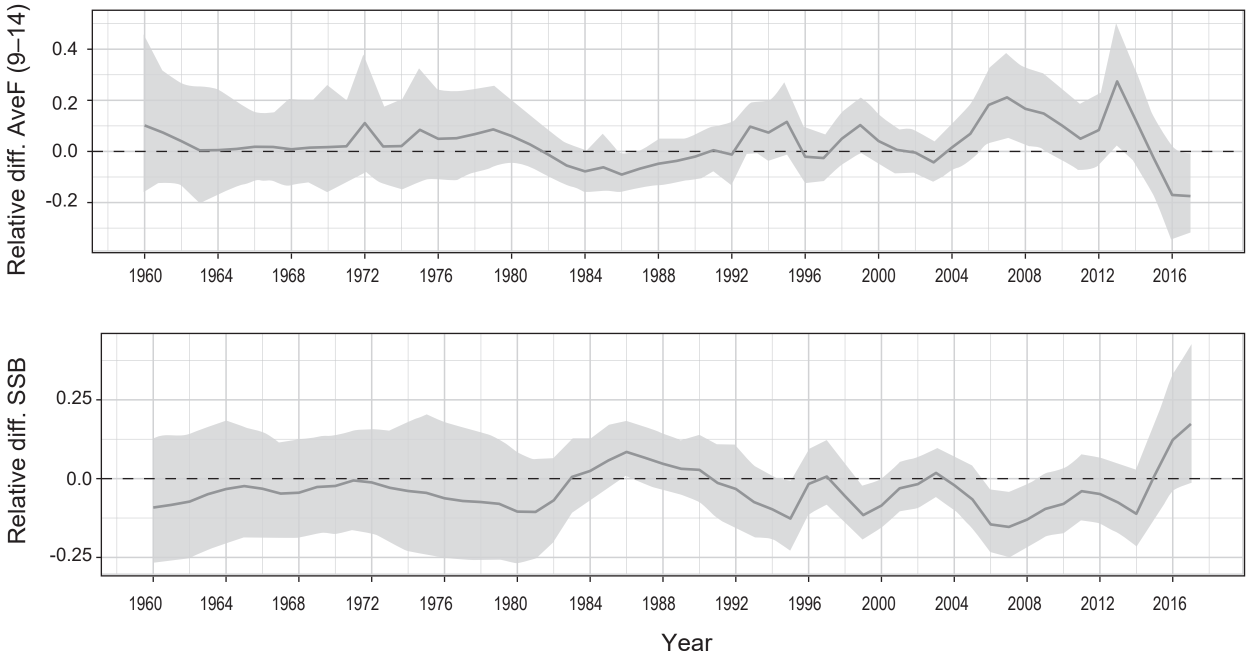

Fig. 8. Relative difference from the SSM self-simulated sample for spawning stock biomass and average fishing mortality rates (ages 9–14). The solid grey line in the median of the estimates and shaded grey regions represent the lower 2.75% and upper 97.5% bounds.

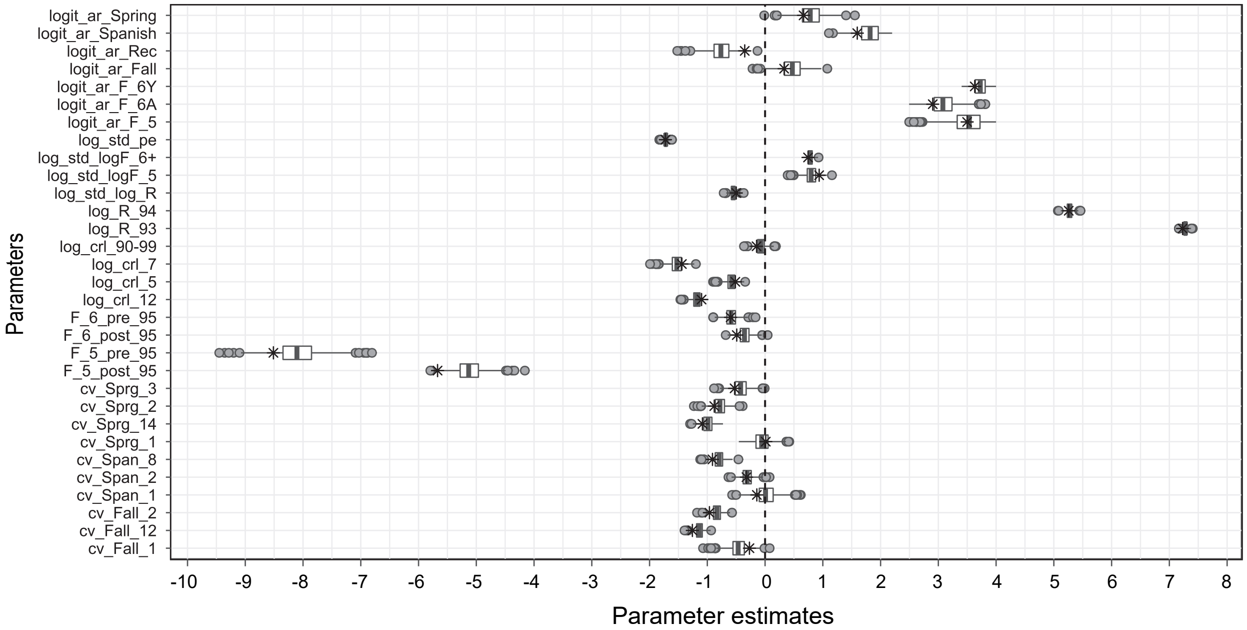

Fig. 9. Boxplots of self-simulated parameter estimates. The asterix represents the SSM (true) parameter estimate.

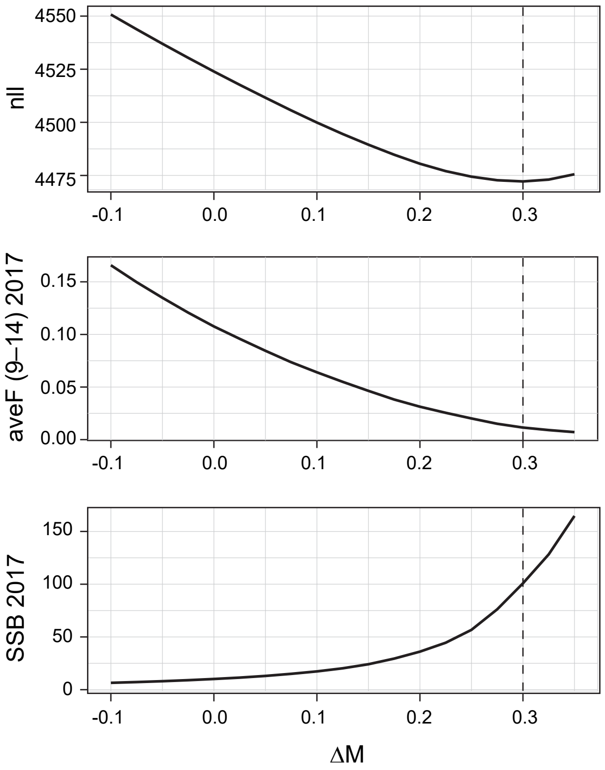

Fig. 10. Profile plot (top panel) for various ΔM formulations with corresponding average fishing mortality rate (ages 9–14) (aveF; middle panel) and spawning stock biomass (SSB; bottom panel).

as it allows for errors in the landings data and reduces the retrospective patterns. Additionally, the thoroughness of our model selection process has the potential to increase the confidence in the selected final model and thereby in the assessment output that is being provided to fisheries managers. Our results also suggest that the current values used for natural mortality rates may be too low as our diagnostic model fitting found the best model fit when M was increased by 0.30. This is an important note not only for American plaice, but for all stocks that are managed under the assumption of a fixed M. We suggest that M profile plots (and/or alternative diagnostics) should be routinely provided to facilitate a better understanding of model behavior for various assumptions about M. This can provide motivation for research into more realistic values of M for future stock assessment models. Overall, this model is a valuable first step in improving our understanding of the stock of American plaice on the Grand Bank of Newfoundland as the flexibility of state-space models are an ideal foundation to build more realistic models.

Acknowledgements

Research funding was provided by the Ocean Frontier Institute, through an award from the Canada First Research Excellence Fund. Research funding to NC was also provided by the Ocean Choice International

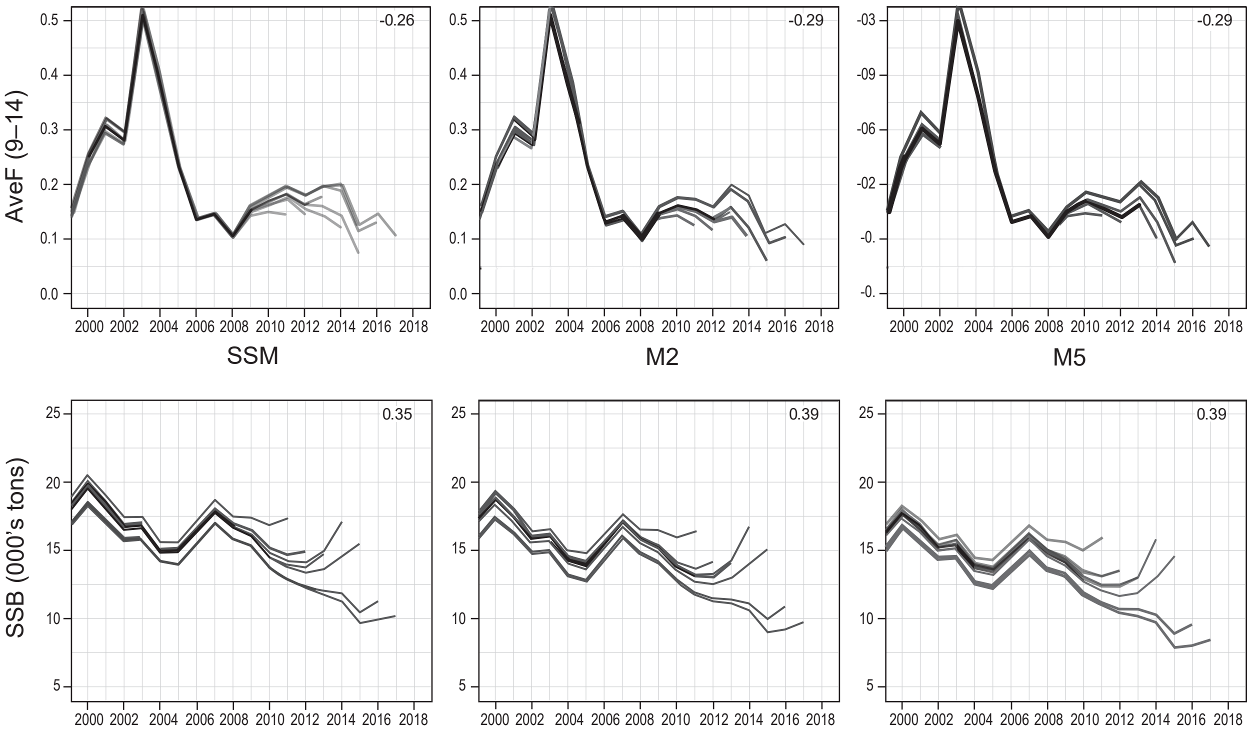

Fig. 11. Retrospective plots for sensitivity runs. SSM is the final model formulation, M2 is with upper catch bounds set to half the SSM upper bounds, M3 is model with "fixed" landings. Mohn's rho is given in the top right corner.

Industry Research Chair program at the Marine Institute of Memorial University of Newfoundland. Funding to AP was also provided by a Natural Sciences and Engineering Research Council of Canada Master's Graduate Scholarship. Many thanks are also extended to Dr. Anders Nielsen, Danish Technical University, for advice on more computationally efficient ways to implement our model in TMB and to the associate editor and two reviewers for their comments and suggestions that greatly improved the final version of this paper.

References

Aeberhard, W. H., Mills-Flemming, J. and Nielsen, A. 2018. A review of state-space models for fisheries science. *Annual Review of Statistics and its Application*, **5**: 215–23. https://doi.org/10.1146/annurev-statistics-031017-100427

Agresti, A. 2003. Categorical data analysis. Vol. 482. John Wiley and Sons. https://doi.org/10.1002/0471249688

Albertsen, C. M., Nielsen, A. and Thygesen, U.H. 2016. Choosing the observational likelihood in state-space stock assessment models. *Canadian Journal of Fisheries and Aquatic Sciences*, **74(5)**: 779–789. https://doi.org/10.1139/cjfas-2015-0532

Berg, C. W. and Kristensen, K. 2012. Spatial age-length key modelling using continuation ratio logits. *Fisheries Research*, **129**: 119–126. https://doi.org/10.1016/j.fishres.2012.06.016

Bousquet, N., Cadigan, N., Duchesne, T. and Rivest, L. P. 2010. Detecting and correcting underreported catches in fish stock assessment: trial of a new method. *Canadian Journal of Fisheries and Aquatic Sciences*, **67(8)**: 1247–1261. https://doi.org/10.1139/F10-051

Brodie, W. B. MS 1986. An assessment of the American plaice stock on the Grand Bank (NAFO Divisions 3LNO). *NAFO SCR Doc.* 86/41, Serial No., N1157.

Bryan, D. R., Bosley, K. L. Hicks, A. C., Haltuch, M. A., and Wakefield, W. W. 2014. Quantitative video analysis of flatfish herding behavior and impact on effective area swept of a survey trawl. *Fisheries Research*, **154**: 120–126. https://doi.org/10.1016/j.fishres.2014.02.007

Cadigan, N. G., and Farrell, P. J. 2002. Generalized local influence with applications to fish stock cohort analysis. *Journal of the Royal Statistical Society: Series C (Applied Statistics)*, **51(4)**: 469–483. https://doi.org/10.1111/1467-9876.00281

Cadigan, N. G. 2015. A state-space stock assessment model for northern cod, including under-reported catches and variable natural mortality rates. *Canadian Journal of Fisheries and Aquatic Sciences*, **73(2)**: 296–308. https://doi.org/10.1139/cjfas-2015-0047

COSEWIC. 2009. COSEWIC assessment and status report on the American Plaice *Hippoglossoides platessoides*, Maritime population, Newfoundland and Labrador population and Arctic population, in Canada. Committee on the Status of Endangered Wildlife in Canada. Ottawa. x + 74 pp.

DFO. MS 2011. Recovery potential assessment of American plaice (*Hippoglossoides platessoides*) in Newfoundland and Labrador. DFO Can. Sci. Advis. Sec., *Sci. Advis. Rep.* 2011/030.

Dickson, W. 1993. Estimation of the capture efficiency of trawl gear. I: development of a theoretical model. *Fisheries Research*, **16(3)**: 239–253. https://doi.org/10.1016/0165-7836(93)90096-P

Dwyer K., Rideout, R., Ings, D., Power, D., Morgan, J.,Brodie, B. and Healy, P. B. MS 2016. Assessment of American plaice in Div. 3LNO. *NAFO SCR Doc.* No. 16/30, Serial No. N6573.

Dwyer K., Morgan, J., Brodie, B., Maddock Parsons, D., Rideout, R., Healy, P. B. and Ings, D. MS 2014. Survey indices and STATLANT 21A bycatch information for American plaice in NAFO Div. 3LNO. *NAFO SCR Doc.* 14/31, Serial No. N6327.

Fraser, H. M., Greenstreet, S. P. and Piet, G. J. 2007. Taking account of catchability in groundfish survey trawls: implications for estimating demersal fish biomass. *ICES Journal of Marine Science*, **64:(9)**. 1800–1819. https://doi.org/10.1093/icesjms/fsm145

González-Troncoso, D., Gago, A., Nogueira, A., and Román, E. MS 2017. Results for Greenland halibut, American plaice and Atlantic cod of the Spanish survey in NAFO Div. 3NO for the period 1997–2016. *NAFO SCR Doc.* 17-018, Serial No. N6670.

Hammond, T. R., and Trenkel, V. M. 2005. Censored catch data in fisheries stock assessment. *ICES Journal of Marine Science*, **62(6)**, 1118–1130. https://doi.org/10.1016/j.icesjms.2005.04.015

Johnson, K. F., Councill, E., Thorson, J. T., Brooks, E., Methot, R. D., and Punt, A. E. 2016. Can autocorrelated recruitment be estimated using integrated assessment models and how does it affect population forecasts? *Fisheries Research*, **183**: 222–232. https://doi.org/10.1016/j.fishres.2016.06.004

Kristensen, K., Nielsen, A., Berg, C.W., Skaug, H., and Bell, B. M. 2016. TMB: Automatic differentiation and Laplace approximation. *Journal of Statistical Software*, **70**: 1–26. https://doi.org/10.18637/jss.v070.i05

Kumar, R., Cadigan, N. G., Zheng, N., Varkey, D. A., and Morgan, M. J. 2020. A state-space spatial survey-based stock assessment (SSURBA) model to inform spatial variation in relative stock trends. *Canadian Journal of Fisheries and Aquatic Sciences*, **77(10)**: 1638–1658. https://doi.org/10.1139/cjfas-2019-0427.

Lassen, H., and Medley, P. 2001. Virtual population analysis: a practical manual for stock assessment (No. 400). Food & Agriculture Org.

Lee, H. H., Maunder, M. N., Piner, K. R., and Methot, R. D. 2011. Estimating natural mortality within a fisheries stock assessment model: an evaluation using simulation analysis based on twelve stock assessments. *Fisheries Research*, **109(1)**, 89–94. https://doi.org/10.1016/j.fishres.2011.01.021

Legault C. M., Chair. MS 2009. Report of the Retrospective Working Group, January 14–16, 2008, Woods Hole, Massachusetts. *Northeast Fish Sci Cent Ref Doc.* 09–01 30.

Methot Jr., R. D., and Wetzel, C. R. 2013. Stock synthesis: a biological and statistical framework for fish stock assessment and fishery management. *Fisheries Research*, **142**: 86–99. https://doi.org/10.1016/j.fishres.2012.10.012

Mohn, R. 1999. The retrospective problem in sequential population analysis: An investigation using cod fishery and simulated data. *ICES Journal of Marine Science*, **56(4)**: 473–488. https://doi.org/10.1006/jmsc.1999.0481

Morgan, M. J., and Brodie, W. B. MS 2001. An exploration of virtual population analyses for Divisions 3LNO American plaice. *NAFO SCR Doc.*, 01/4, Serial No. N4368.

Morgan, M. J., Bailey, J., Healey, B. P., Maddock Parsons, D., and Rideout, R. MS 2011. Recovery potential assessment of American Plaice (*Hippoglossoides platessoides*) in Newfoundland and Labrador. DFO Can. Sci. Advis. Sec. *Res. Doc.* 2011/047.

Nielsen, A., and Berg, C. W. 2014. Estimation of time-varying selectivity in stock assessments using state-space models. *Fisheries Research*, **158**: 96–101. https://doi.org/10.1016/j.fishres.2014.01.014

Perreault, A. M., Zheng, N., and Cadigan, N. G. 2019. Estimation of growth parameters based on length-stratified age samples. *Canadian Journal of Fisheries and Aquatic Sciences*, **77(3)**: 439–450. https://doi.org/10.1139/cjfas-2019-0129

Pitt, T. K. MS 1972. Nominal catches of American plaice in Divisions 3L and 3N for the years 1960–1970. *ICNAF Res. Doc,* 72/90.

Rivard, D. MS 1980. Back-calculating production from cohort analysis, with discussion on surplus production for two redfish stocks. *CAFSAC Res. Doc.*, 80/23.

Shelton, P. A., and Morgan, M. J. 2005. Is by-catch mortality preventing the rebuilding of cod (*Gadus morhua*) and American plaice (*Hippoglossoides platessoides*) stocks on the Grand Bank. *Journal of Northwest Atlantic Fisheries Science*. **36**: 1–17. https://doi.org/10.2960/J.v36.m544

Skaug, H. J. and Fournier, D. A. 2006. Automatic approximation of the marginal likelihood in non-Gaussian hierarchical models. *Computational Statistics & Data Analysis*, **51(2)**: 699–709. https://doi.org/10.1016/j.csda.2006.03.005

Szuwalski, C. S., Ianelli, J. N., and Punt, A. E. 2017. Reducing retrospective patterns in stock assessment and impacts on management performance. *ICES Journal of Marine Science*, **75(2)**: 596–609. https://doi.org/10.1093/icesjms/fsx159

Thygesen, U. H., Albertsen, C. M., Berg, C. W., Kristensen, K., and Nielsen, A. 2017. Validation of ecological state space models using the Laplace approximation. *Environmental and Ecological Statistics*, **24(2)**, 317–339. https://doi.org/10.1007/s10651-017-0372-4

Van Beveren, E., Duplisea, D., Castonguay, M., Doniol-Valcroze, T., Plourde, S. and Cadigan, N. 2017. How catch underreporting can bias stock assessment of and advice for northwest Atlantic mackerel and a possible resolution using censored catch. *Fisheries Research*, **194**, 146–154. https://doi.org/10.1016/j.fishres.2017.05.015

Wheeland, L., Dwyer, K., Morgan, M. J., Rideout, R. and Rogers, R. MS 2018. Assessment of American plaice in Div. 3LNO. *NAFO SCS Doc.* 18/039, Serial No. N6829.

Xu, H., Thorson, J. T., Methot, R. D. and Taylor, I. G. 2019. A new semi-parametric method for autocorrelated age-and time-varying selectivity in age-structured assessment models. *Canadian Journal of Fisheries and Aquatic Sciences*, **76(2)**: 268–285. https://doi.org/10.1139/cjfas-2017-0446

Supplementary materials - pp. 65–104 can be found online at:
https://journal.nafo.int
https://journal.nafo.int/dnn/Volumes/Articles/ID/654/A-state-space-stock-assessment-model-for-American-plaice-on-the-Grand-Bank-of-Newfoundland

J. Northw. Atl. Fish. Sci., Vol. 51: 105–116 Publication (Upload) date: 13 Nov 2020

Reproductive biology of *Isurus oxyrinchus* captured by the south Brazilian surface longline commercial fleet in the Southwest Atlantic Ocean, with data on CPUE and size distribution by sex

Gabriel Canani[1] and Maria Cristina Oddone[2*]
[1]Programa de Pós-graduação em Oceanografia Biológica, Instituto de Oceanografia,
Universidade Federal de Rio Grande, Avenida Itália, Km 8, Campus Carreiros,
Rio Grande, RS, Brasil, CEP 96203-900

[2]Instituto de Ciências Biológicas, Setor de Morfologia,
Universidade Federal de Rio Grande, Avenida Itália, Km 8, Campus Carreiros,
Rio Grande, RS, Brasil, CEP 96203-900
*mcoddone@gmail.com

Canani, G. and Oddone, M.C. 2020. Reproductive biology of *Isurus oxyrinchus* captured by the south Brazilian surface longline commercial fleet in the Southwest Atlantic Ocean, with data on CPUE and size distribution by sex. *J. Northw. Atl. Fish. Sci.*, 51**:** 105–116. https://doi.org/10.2960/J.v51.m724

Abstract

Knowledge of reproductive parameters is necessary to efficiently evaluate and manage fishing stocks. Shortfin Mako constitutes the second most captured shark by the longline hook fleet situated in Rio Grande, RS, Brazil. However, little is known about the reproductive traits or abundance of this species in the Southwest Atlantic. Here we report on size and maturity, from 37 males and 46 females sampled in scientific cruises between September 1996 and August 1999, and commercial fishing cruises between December 2014 and September 2016, in South Brazilian Waters and Northern Uruguayan Waters. First results for male maturity are presented. Males between 119.0 and 270.0 cm TL (Total length) including all maturity stages were captured; eighteen adults, nine juveniles and ten immature individuals. The observed size at maturity was between 137 and 182.0 cm TL. Maturity ogive analyses indicate an L50 of 180.1 cm TL and L90 was 199.0 cm TL. Juveniles presented testicle weight between 84.4 and 92.2 g, while adult weights were between 158.4 and 352.8 g. Only immature females were captured (*n* = 46), with sizes between 104.0 and 230.0 cm TL, and oviduct width between 4.1 and 7.15 mm. The CPUE varied between 0.57 and 2.38 individuals per thousand hooks. Overall sex ratio slightly favored females, 1.24:1 (F|M).

Key words: South Brazil, reproductive biology, population structure, pelagic shark

Introduction

Reproductive parameters such as size or age at maturity are important for evaluating recruitment of sharks, and therefore evaluating fisheries and population status (Holden, 1974; Cortés *et al.*, 2012). Acquiring information on sexual maturity can inform biological and ecological traits of the species. These traits may be even sex biased, given that sexual dimorphism and site segregation are common in sharks (Francis and Duffy 2005; Semba *et al.*, 2011, Tsai *et al.*, 2014). Tsai *et al.* (2014) indicated from a fishery management perspective that ignoring the differences in population growth rates between sexes, as well as in social structure *i.e.*, unsexed stock management can underestimate population decline risks.

The family Lamnidae ("mackerel" sharks, order Lamniformes), includes the genera *Carcharodon* Smith, 1838, *Lamna* Cuvier, 1816, and *Isurus* Rafinesque 1810 (Compagno, 2005). In regard to the Shortfin Mako *Isurus oxyrinchus* Rafinesque, 1810, Shortfin Mako is endothermic, being able to maintain higher temperatures than the surrounding water with counter-current vascular heat exchange (Carey and Teal, 1969). This physiological trait facilitates a high movement and migratory capacity. The species is oceanic, semipelagic and littoral and distribution is circumglobal in temperate and tropical seas. In the Western Atlantic, Shortfin Mako occurs from Newfoundland (Canada) (Casey and Kohler, 1992) to northern Argentina (Compagno, 1984; 1990).

In the South and Central Atlantic waters, Shortfin Mako is the second most captured shark in longline fisheries (Barreto *et al.*, 2016a). Having such a wide range exposes the Shortfin Mako to a large number of fishing fleets, the longline hook fishery being the primary threat (Cortés *et al.*, 2010, Barreto *et al.*, 2016a). Barreto *et al.*, (2016a) reviewed historical catches by the longline fishery fleets in the South Atlantic Ocean, identifying three main phases. The first (1979–1997), a period with low effort employing multifilament lines targeting tunas was characterized by increasing shark catches as the fishery developed. The second phase (1998–2007) was a period of expansion and monofilament line was introduced targeting sharks as well as tunas, resulting in a decline of 55% in Shortfin Mako catches. Finally, during a third phase, shark catches stabilized at a lower level. Mourato *et al.*, (2011) found high percentages of captures of the Shortfin Mako, regardless of the targeted species in longline fisheries off the southeastern coast of Brazil. Shortfin Mako represent 2.6% of total catches in fisheries targeting blue sharks, *Prionace glauca* (Linnaeus 1758), 3.0% in fisheries for swordfish *Xiphias gladius* Linnaeus, 1758 and 4.4% in multi species fisheries (Mourato *et al.*, 2011). The overall declining trend of the Shortfin Mako captures could suggest a depletion of the stock, and thus an endangered status to the species (Barreto *et al.*, 2016a), currently categorized by the IUCN as “Endangered” both globally and regionally, in the Atlantic (Rigby *et al.*, 2018).

With respect to reproduction strategies, oophagy was documented in all members of the Lamniformes, including the Shortfin Mako (Gilmore, 1993; Mollet *et al.*, 2000; Joung and Hsu, 2005). Following initial yolk-sac nutrition, oophagy, a type of matrotrophic viviparity occurs where intrauterine embryos ingest unfertilized eggs continuously produced by the mother (Hamlett and Koob, 1999). As the embryos consume and store the yolk present in the ova, they develop an expanded abdomen called “cardiac” or “yolk” stomach, characteristic and exclusive of the Lamniformes (Gilmore 1993, 2005; Mollet *et al.*, 2000; Wyffels, 2009). Approximately two months before birth, the embryos consume the yolk and develop livers proportionally identical to the adults in relation to their weight (Gilmore, 1993, 2005; Mollet *et al.,* 2000; Joung and Hsu, 2005). Among oophagic species, the adelphophagy, embryophagy or “intrauterine cannibalism” has been recorded in *I. oxyrinchus* and *Carcharias taurus* Rafinesque, 1810 (Mollet *et al.*, 2000; Gilmore, 2005; Joung and Hsu, 2005).

Shortfin Mako size at sexual maturity ranges between 156 and 210 cm for males and between 256 and 285 cm for females, with great variation among regions and studies (Mollet *et al.*, 2000; Joung and Hsu 2005; Semba *et al.,* 2011, see Table 3 for details). Regardless of the growing amount of information on biology and reproductive parameters of the Shortfin Mako in the last 30 years, there is still a considerable lack of information about this species, as for most of Lamniformes (Gilmore 1993, 2005; Mollet *et al.*, 2000). Moreover, size at maturity estimates for male Shortfin Mako were not available for the South West Atlantic.

Stevens (2008) stated that, in spite of being commonly captured, the biology of this species is still not well understood. The economical and ecological importance of the species, the apparent declining populations trend, lack of reproductive studies in the Southwest Atlantic, discrepancies among studies and differences among populations of the Shortfin Mako highlight the need to acquire fishing and reproductive biology information for this species. The aim of this study was to study the reproductive biology of *Isurus oxyrinchus* captured by the south Brazilian surface longline commercial fleet in the Southwest Atlantic Ocean, and to provide data on CPUE and size distribution by sex. Here, we present population structure data, average size per season sampled and reproductive parameters.

Material and methods

Study Area

The fishing cruises were carried out in the area situated in the Southwest Atlantic Ocean, between latitude 29° and 36° S, and longitude 47° and 53° W (Fig. 1), in depths between 140 and 2200 m. This area corresponds to the southernmost Brazilian states; Santa Catarina and Rio Grande do Sul, respectively and including the northernmost Uruguayan waters. The main currents acting on the surface waters are the Brazil Current, which flows southward, characterized by warm and oligotrophic waters, and the Malvinas (Falklands) Current, flowing northward, composed by Antarctic Circumpolar Waters which are mixed with coastal waters coming from the La Plata River, these mixed waters are characterized by cold and nutrient-rich waters. These two currents with opposite flows meet each other, forming the South Atlantic Subtropical Convergence (Garcia, 1997).

Sample collection

Samples were collected during six trips aboard a 22 m length steel longliner, fishing in the south Brazilian inner and outer shelves from December 2014 to September 2016 (Table 1). An additional specimen was sampled during a single fish landing event in the port of the city of Rio Grande. Hooks were fixed using a steel line, appropriate for capturing large sharks and swordfishes. The usual set consisted of 800 hooks, varying between 600 and 1050 hooks. Also, data from scientific longline cruises obtained in the same area between 1996 and 1999 by the project ARGOS (conducted by the former Laboratório de Elasmobrânquios e Aves Marinhas, Instituto de Oceanografia, Universidade Federal do Rio Grande) were also included (Fig.1). Catch per unit effort (CPUE) was calculated only for fisheries cruises, using 800 hooks per set for effort calculation. The total effort per cruise was not available for the scientific cruises.

Biological and biometric sampling

The external measurements were taken at sea, as the fish were brought on board. For each specimen, total length (TL), fork length (FL) and interdorsal space (IS) were recorded to the nearest cm below. For males, the postcloacal length of the clasper (CL) was measured from the clasper distal end to the posterior margin of the cloaca opening, according to Maia *et al.* (2007). Clasper calcification was recorded manually, with the claspers being classified as 'rigid' or 'flexible' for maturity assessment. Due to access difficulties in biological sampling for reproduction assessment intrinsic of this species (also reported by Maia *et al.*, 2007, and Barreto *et al.*, 2016b), the testicles of seven specimens were weighed. Testicle weight (g) (including the epigonal

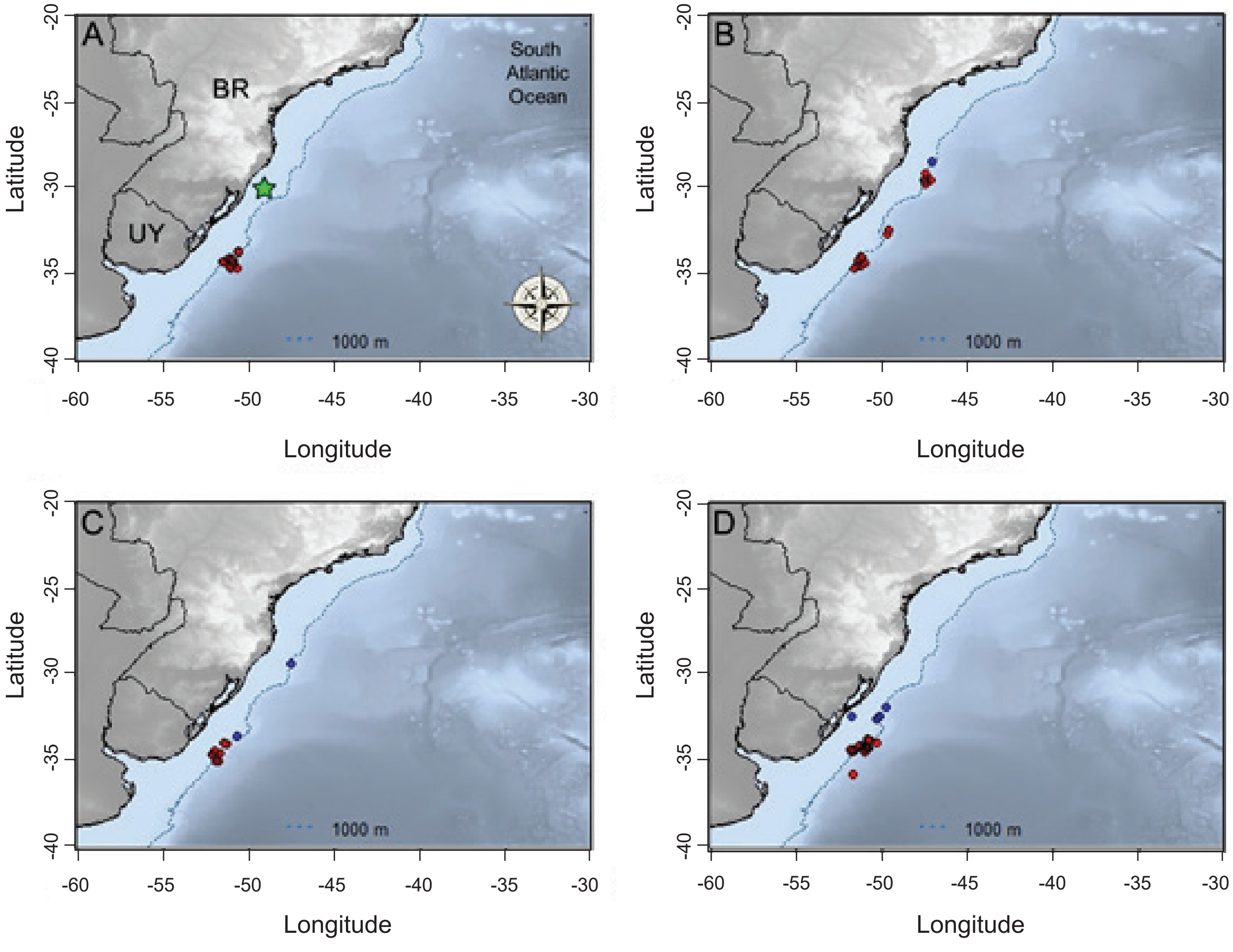

Fig. 1. The study area, the Southwestern Atlantic Ocean, off southern Brazil (BR) and northern Uruguay (UY), where the samples of the Shortfin Mako *Isurus oxyrinchus* were collected. Red dots represent the longline fisheries captures (2014–2016), blue dots represent scientific cruises (longline fishing gear), carried out between 1996 and 1998. Star symbol represents the nursery proposed by Vooren *et al.* (2005). Depth isobath: 1000 m. **A**: summer, **B**: autumn, **C**: winter, **D**: spring.

organ) was recorded using an electric scale (0.1 g precision) considering both testicles together. Also, uterus width was recorded for 12 females, being measured in the middle region of the oviduct.

Analysis and statistics

To assess sexual maturity, criteria proposed by Semba *et al.* (2011) for the shortfin mako shark were applied. To determine maturity in males, the calcification and mobility of the clasper were examined, and maturity was as follows: stage 1-immature (not calcified claspers); stage 2-juvenile (semi-rigid and calcified claspers with low mobility (clasper rotation forward along the caudal-cephalic body axis) and no spurs) and stage 3-adult (calcified, high mobility, spurs).

The normality of TL and CL measurements was tested using the Shapiro-Wilk test. Morphometrics were analyzed by plotting all measurements using linear regression (Pratt and Casey, 1983), to observe the relationship between total length and clasper length. The sex ratio was established as the ratio of total females to total males. A statistical X^2 test was applied to test differences between sexes. The logistic model $Y = [1 + \exp\{-(a + bX\}]\ -1$ (sensu Mollet *et al.*, 2000) was fitted to the relationship between the percentage of mature males (Y) and TL classes of 10 cm (X), and *a* and *b* are parameters estimated by a generalized linear model (GLM) with a binomial distribution. Statistical analyses and figures were performed using the program R, ver. 3.2.2 (R Development Core Team, 2019).

Ethical considerations

For the collection of specimens of *I. oxyrinchus* on board the fishing vessels, permission of the Instituto Chico Mendes de Conservação da Biodiversidade (ICMBio) and Sistema de Autorização e Informação em Biodiversidade (SISBIO) was requested, license number 45279-1. This research is part of the research project "The biology and conservation of shark populations in the extreme south of Brazil" registered at the Universidade Federal do Rio Grande under process number 814440/2014, with awareness of the Ethics Committee in Animal Use (Comissão de Ética Em Uso Animal – CEUA of the same university. No experimental work was undertaken with the specimens collected.

Table 1. Data on the overall commercial fishing cruises (between December 2014 and September 2016 by the sea-surface longline fleet based in south Brazil) and scientific fishing cruises (ARGOS, between September 1996 and August 1999) conducted off southern Brazil, Southwestern Atlantic Ocean, where samples of the Shortfin Mako *Isurus oxyrinchus* were obtained. Fishing sets were standardized in 800 hooks.

Cruise	Season	Area	Days at sea	Fishing sets	Mean depth (m)	Mean Temperature
November/December 2014	Summer	33–34ºS 50–51ºW	19	11	2030(1200–3500)	23.9ºC(21.2–23.9)
March 2015	Autumn	29–32ºS 49–47ºW	11	5	1800 (1525–2000)	25.1ºC(24.8–26.2)
June 2015	Winter	33–35ºS 51–52ºW	13	9	205 (150–438)	20.6ºC(16.8–21.1)
November 2015	Spring	34–35ºS 50–51ºW	17	9	1300 (144–2000)	20.4ºC(19.2–22)
March 2016	Autumn	29–34°S 47–51°W	15	9	1170 (487–1523)	24.9°C(24.2–25.3)
September 2016	Spring	33–34°S 50°W	13	10	1288 (1000–1500)	-
September 1996*	Spring	32ºS 50ºW	7	6	530 (200–960)	-
November 1996.2*	Spring	31–34ºS 49–51ºW	8	7	800 (400–1100)	21ºC
April 1998.2*	Autumn	28ºS 47ºW	9	6	570(376–760)	26ºC
August 1999.1*	Winter	29–33ºS 47–50ºW	10	6	1090(667–1500)	-

Results

Reproductive biology

The sample analyzed (Table 2) was composed of immature males (stage 1, $n = 10$), with (CL) ranging from 6.0 to 12.3 cm juveniles (stage 2, $n = 9$), with (CL) from 9.5 to 22 cm and adults (stage 3, $n = 18$) showing a CL range between 18.5 and 35.4 cm. The development of the clasper correlated with TL, exhibited three distinct phases. The first, with slow clasper growth and samples between 119.0 and 162.0 cm TL, followed by a rapid growth between 137.0 and 182.0 cm TL, and when maturity is reached, showing a slow growth once again (Fig. 2). The observed size (TL) at first maturity in the sample corresponded to the range 168.0–182.0 cm TL (TL of the smallest mature individual and largest immature individual, respectively). Regarding the maturity ogive analysis, TL at 50% maturity was found to lay at 180.1 cm, and 90% maturity at 199.0 cm (Fig. 3). Testicles weight ranged from 84.4 to 92.2 g in males stage 2 ($n = 3$) and from 158.4 to 352.8 g in adults ($n = 4$).

A total of 46 immature females were captured ranging from 104.0 to 230.0 cm TL. There was only one stage-2 (204.0 cm TL), and no stage-3 females in record. Eleven specimens had their oviduct width measured, presenting values between 4.1 and 7.15 mm.

Population structure

A total of 83 individuals were captured and measured over the six fishing cruises and four scientific cruises (Table 2), with number of individuals varying between 1 and 26 per cruise. The TL range for the total sample varied from 104.0 to 270.0 cm (Fig. 4), with a mean of 165.7 cm. Altogether, 37 males were captured, TL ranging between 119.0 and 270.0 cm, with a mean of 177 cm, while the 46 females captured had TL values between 104.0 and 230.0 cm, with a mean of 156.6. The smallest individual was 104.0 TL female, captured in July 2015, at 20.8ºC and 150 m depth, while the larger individual was a 270.0 cm male, captured in March 2015 at 24.9ºC surface temperature and 2000 m depth.

In relation to the CPUE, the highest value was recorded in the Spring sets, which presented 2.83 individuals per 1000 hooks, followed by Winter (1.67), Autumn (0.74) and Summer (0.57). The mean TL was smaller in the Winter sets (134), increasing in Spring (163), Summer (191) and Autumn (214).The largest individuals were captured in the March 2015 Cruise (Autumn), with the samples varying between 177.0 and 270.0 cm, and composed almost exclusively by males larger than 240.0 cm, with the exception of a 177.0 cm TL female, whilst the smaller individuals were recorded in the June 2015 cruise (Winter), with captures composed mostly by females smaller than 160.0 cm. The CPUE by season and maturity stage is presented in Figs. 5, 6 and 7. The overall sex ratio, 1.24:1, favoured females, was statistically significant ($\chi^2 = 0.38$, $p = 0.53$), and was highly variable among seasons. The higher F:M ratio was registered in the winter sets (6:1), decreasing in Spring (1.12:1), and favouring males in Autumn (0.8:1) and Summer (0.25:1).

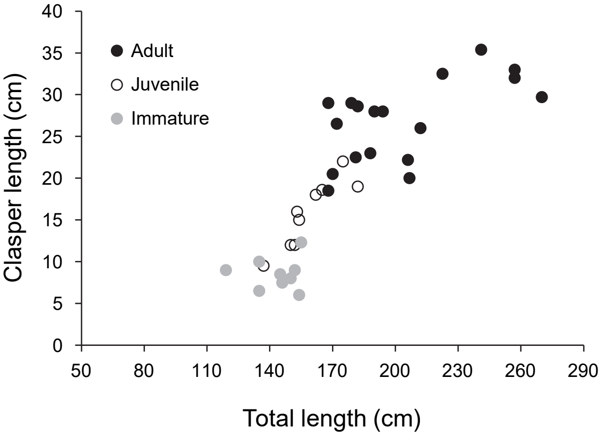

Fig. 2. Relationship between total length (cm) and clasper length (cm) for the maturity stages considered; immature (grey circle symbols), juvenile (empty circle symbols) and adult individuals (black circle symbols) of the Shortfin Mako *Isurus oxyrinchus* captured by pelagic longline vessels off southern Brazil and northern Uruguay, Southwestern Atlantic Ocean.

Discussion

Constituting the first estimate for the SW Atlantic Male TL at 50% maturity was estimated at 180 cm. For other areas of the Atlantic, Stevens (1983) and Maia *et al.* (2007) had provided estimations for the NW and NE Atlantic, respectively. Our estimate falls within the range of values observed elsewhere (from 150 to 180 cm TL) (Table 3). Our ogive analysis, although based on a relatively small sample of immature juveniles (19 in all), showed the expected sigmoidal curve and size at maturity for males, congruent with other studies. Compared to other clasper length-TL studies, immature males in the range of 50–100 cm are missing from the present study (see for instance, Conde-Moreno and Galván-Magaña, 2007; Semba *et al.*, 2011). As only immature females were captured, maturity estimates are not available in

Table 2. Data on the captures of the Shortfin Mako *Isurus oxyrinchus* by longline commercial fisheries cruises (between December 2014 and September 2016 by the sea-surface longline fleet off southern Brazil and northern Uruguay) and scientific fishing cruises* (between September 1996 and August 1999) in the Southwestern Atlantic Ocean. Fishing sets were standardized in 800 hooks.

Cruise	Season	Set	Depth	Sex ratio(Males|Females)	Mean TL ♂	Mean TL ♀
December 2014	Summer	4	1500	(1|0)	154	-
December 2014	Summer	5	2000	(1|0)	206	-
December 2014	Summer	6	1200	(1|1)	165	224
December 2014	Summer	7	1200	(1|0)	206.7	-
March 2015	Autumn	1	2000	(1|0)	270	-
March 2015	Autumn	2	1900	(1|1)	241	177
March 2015	Autumn	3	1525	(1|0)	257	-
June 2015	Winter	8	438	(0|1)	-	107
June 2015	Winter	9	250	(2|9)	147(119–175)	130(107–185.5)
November 2015	Spring	1	2000–800	(4|1)	198.6(190–212)	230
November 2015	Spring	3	1800	(0|2)	-	181(164–198)
November 2015	Spring	4	967	(2|1)	160.5(153–168)	174
November 2015	Spring	5	145	(0|2)	-	194.5(180–209)
November 2015	Spring	6	2000	(1|2)	154	176.5(142–211)
November 2015	Spring	8	1422	(1|2)	222.5	122
March 2016	Autumn	5	1429	(0|1)	-	186
March 2016	Autumn	6	1143–990	(1|1)	188	182
March 2016	Autumn	8	1900	(1|0)	257	
September 2016	Spring	3	1500	(2|5)	175	127.8
September 2016	Spring	4	1500	(2|3)	148.5	139
September 2016	Spring	5	1500	(0|1)	-	186
September 2016	Spring	6	1500	(1|1)	170	152
September 2016	Spring	8	1500	(1|0)	146	-
September 2016	Spring	9	1000	(5|2)	160.2	132.5
September 2016	Spring	10	1000	(2|1)	165.5	143
September 96*	Spring	1	510	(0|1)	-	164
September 96*	Spring	2	865	(0|1)	-	204
November 96*	Spring	1	1000	(3|3)	152.6(135–168)	167(155–191)
November 96*	Spring	6	900	(2|0)	143.5(137–150)	-
November 96*	Spring	7	1100	(0|2)	184.5(152–217)	-
April 98*	Autumn	3	376	(0|1)	-	169
August 99*	Winter	2	667	(0|1)	-	160
August 99*	Winter	6	1300	(0|1)	-	126.5

this study. Given the effort concentrated in the same area, close to the Brazil-Uruguay Economic Exclusive Zone southernmost border, our data suggests size segregated groups, varying seasonally, with larger individuals concentrating northwards, in warmer waters and immature and juveniles migrating southwards as they grow.

Sampling oceanic and pelagic sharks is an expensive and difficult task, requiring many resources and structure, rarely allowing scientific cruises to be undertaken, thus leaving the assessment of their biological traits to fishery-dependent means (Baum *et al.*, 2003, Barreto *et al.*, 2016a). In the specific case of the Shortfin Mako, access

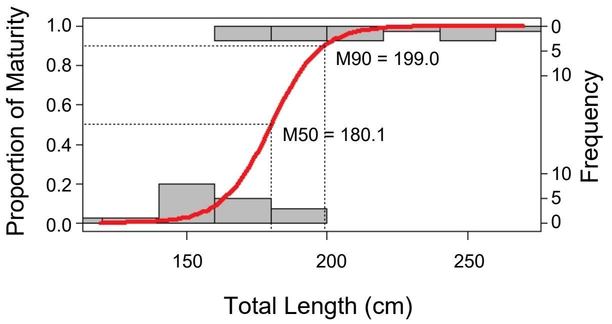

Fig. 3. Maturity ogive for male Shortfin Mako *Isurus oxyrinchus* captured by pelagic longline vessels off southern Brazil and northern Uruguay, Southwestern Atlantic Ocean. The curve represents the proportion of mature males calculated in relation to total length classes of 10 cm (left Y axis). The histogram represents the frequency of individual's size classes in the sample (right Y axis). Site at 50% maturity (M50) and at 90% maturity (M90) are indicated.

to fish for biological sampling is even more problematic. Its valuable meat may discourage commercial skippers from allowing sampling (Barreto *et al.,* 2016b). Fishery-dependent sampling tends to concentrate efforts in areas of aggregation of other target species, varying in depths and areas. However, these snapshots can yield important information.

In winter months, the fleet sets its fishing gear in southernmost waters less than 500 m depth, catching mostly immature females and eventually juvenile males, while in the summer, autumn and spring months, the fishing operations were conducted in waters deeper than 800 m, catching mostly adult and juvenile males, and occasionally immature females. These trends in distribution may provide information on spatial distribution and abundance of genders and maturity classes. Our data indicates mainly juvenile and immature aggregations with occasional presence of adult males in Southern Brazil pelagic waters. Vooren *et al.* (2005) reported neonates and young-of-the-year captures by gillnet fishery between January and March, in shallow coastal waters (28 to 63 m depth) between 29 and 31°S, classifying the area as a nursery in the summer. Costa *et al.* (2002), analyzing pregnant females captured between September and February by longline tuna fishing vessels, northwards, between 20–28°S, concluded that the birth period in Southeastern Brazil occurs in Spring (October to December). Migratory capacity among young-of-the-year and neonates is reported by Maia *et al.,* (2007), and may explain our pattern observed in capture sizes observed, with the individuals going southwards, to feeding areas.

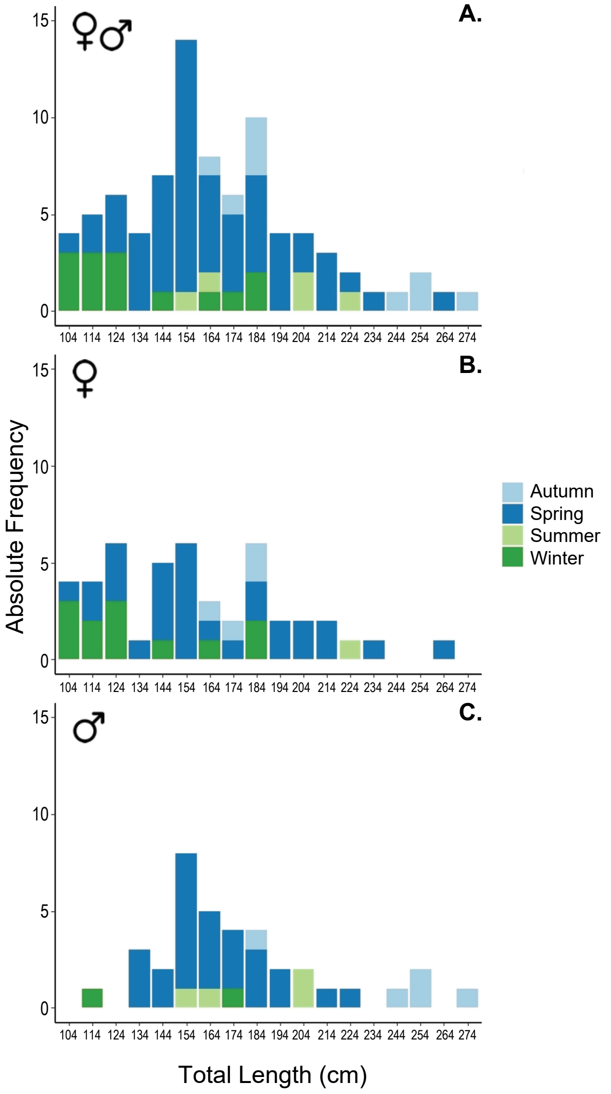

Fig. 4. Absolute frequency of individuals by total length class of 10 cm, for total (**A**), female (**B**) and male (**C**) Shortfin Mako *Isurus oxyrinchus* captured by pelagic longline vessels off southern Brazil and northern Uruguay, Southwestern Atlantic Ocean, between December 2014 and September 2016.

The high migratory capacity and behavior of this species widely exposes its populations to a variety of fishing fleets and techniques, with young and neonates being captured by gillnet fisheries in shallower water closer to the continent and larger individuals being captured by more oceanic techniques such as longlines (Vooren *et al.*, 2005; Costa *et al,* 2002; personal observations). This exposure makes the Shortfin Mako the second most captured shark in the South Atlantic, with immature individuals being the most exposed to fisheries (Barreto *et al.,* 2016a). Tsai *et al.* (2014) showed by modeling sex-

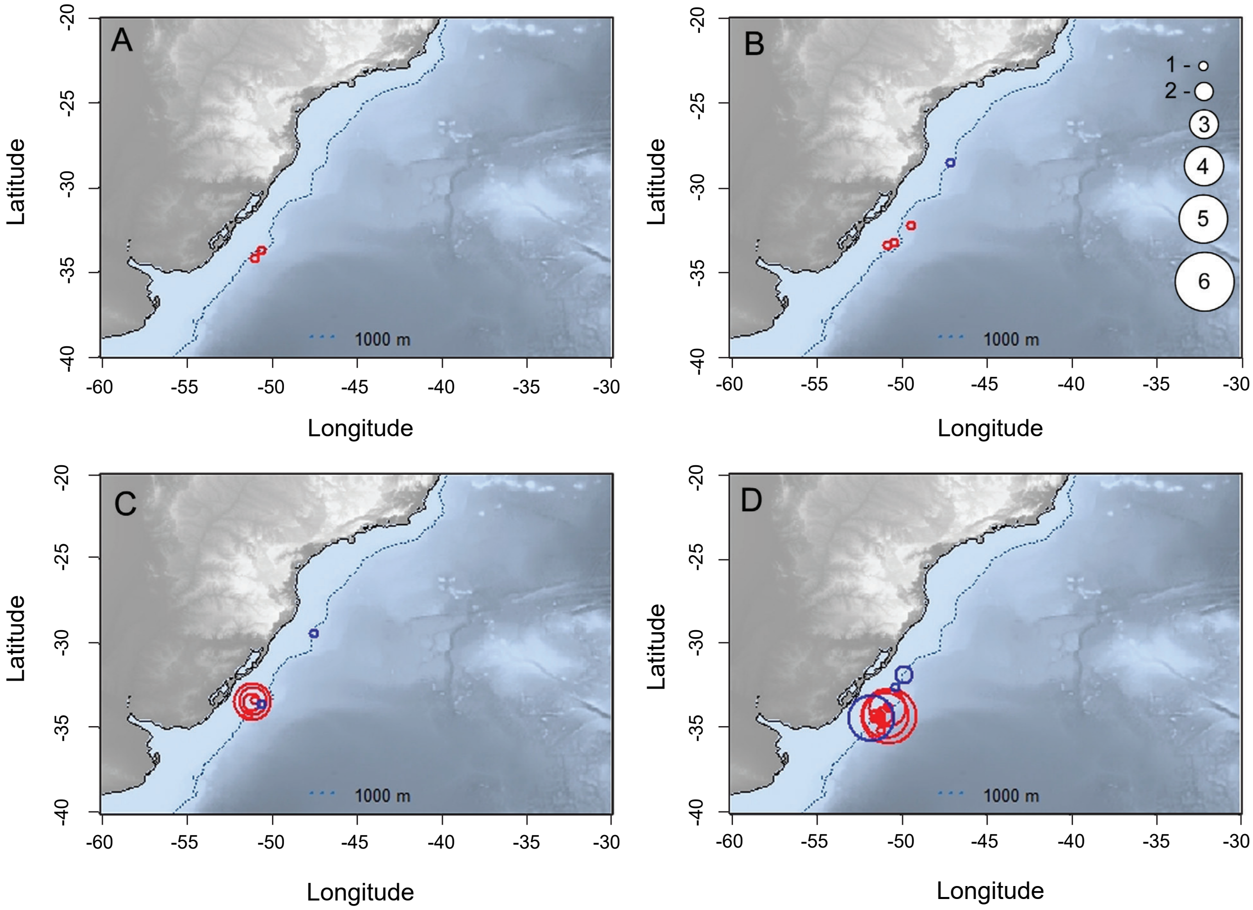

Fig. 5. Fishing sets and capture per unit effort for fisheries sampling of immature Shortfin Mako *Isurus oxyrinchus* captured by pelagic longline vessels off southern Brazil and northern Uruguay, Southwestern Atlantic Ocean, between December 2014 and September 2016 in South Brazil. The CPUE is represented by the size of circles symbols in individuals captured per set (blue=Scientific cruises; red=commercial fishing cruises). **A**: summer; **B**: autumn; **C**: winter; **D**: spring.

specific reproductive stocks that single-sex models could be biased, leading to wrong risk analyses and population estimates. Not only the capture of females (from all size classes) is detrimental to the population, captures of the male stock may lead to population depletion, depriving it from viable reproductive pairs (Tsai *et al.*, 2014).

Genetic studies have suggested that the North and South Atlantic Shortfin Mako populations are not segregated, having some gene flow between them (Schrey and Heist, 2003). Nevertheless, female reproductive traits reviewed by Mollet *et al.* (2000) differ between hemispheres, which could be explained by habitat variation, with different food availability, for example. This situation signifies a discrete management approach, rather than to extrapolate trends and patterns from one hemisphere to the other.

Conservation decisions and laws have changed in Brazil in the last few years, as stated by Barreto *et al.* (2016a), with the prohibition on capturing Sphyrnids (any kind of landing, even as bycatch), among other threatened sharks. The changes in fishing laws have led to modifications of the fishing areas which had become shallower, and closer to nursery areas. These are important areas for fishery management, providing a greater contribution for recruitment than other areas (Beck *et al.,* 2001). Monitoring captures in these areas is necessary. Immature individuals are not able to reproduce, and their capture may lead to future reduction of the reproductive stock and therefore reducing the population resilience, especially in slow growth and low fecundity species, as the Shortfin Mako. However, proper management should not focus on a given maturity stage. All stages should be subject of concern when conservation decisions are made. More detailed studies are necessary, quantifying not only number of individuals or biomass captured, but also length, age and maturity class distributions, allowing for a responsible and sustainable management of fisheries, conserving the stocks and the economic viability of fisheries.

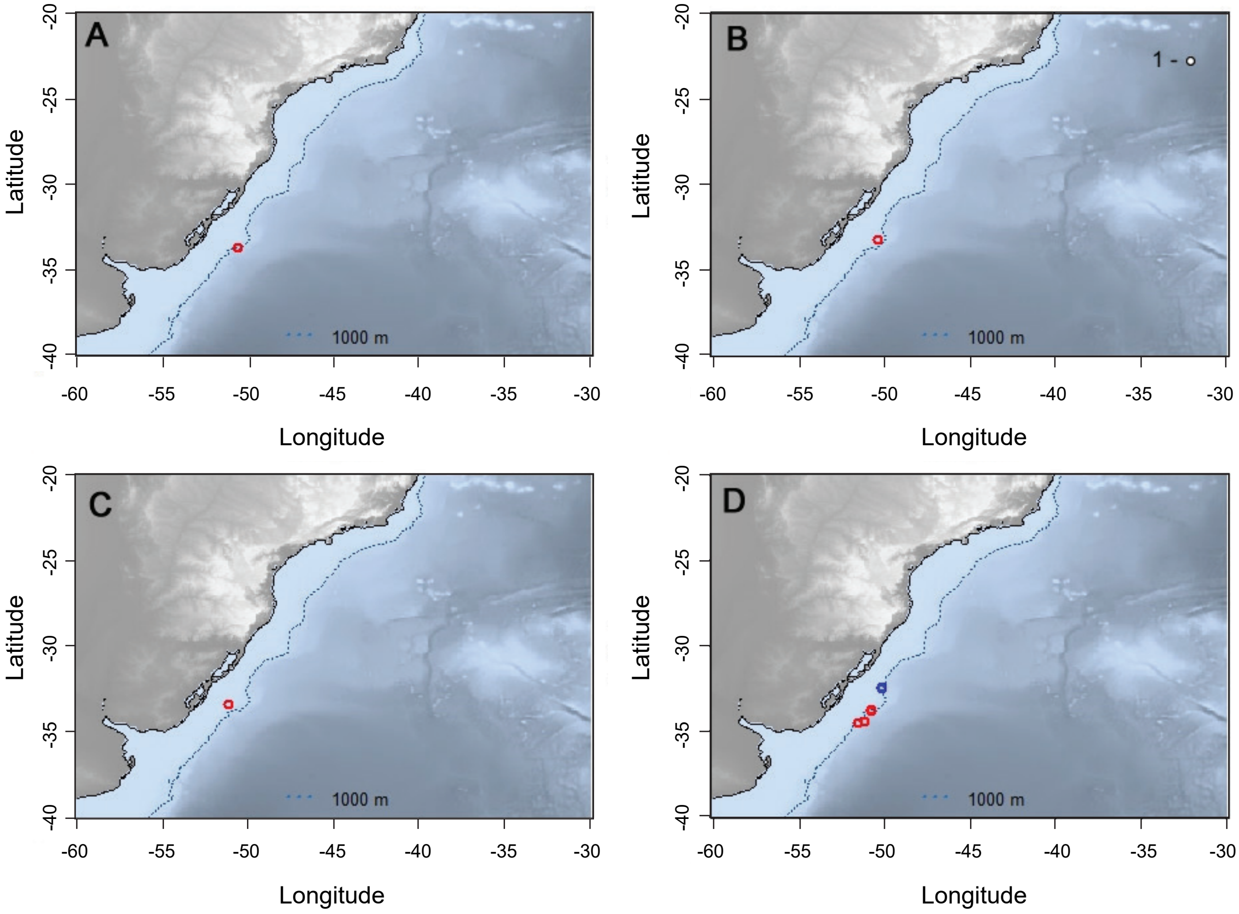

Fig. 6. Fishing sets and capture per unit effort for fisheries sampling of juvenile Shortfin Mako *Isurus oxyrinchus* captured by pelagic longline vessels off southern Brazil and northern Uruguay, Southwestern Atlantic Ocean, between December 2014 and September 2016 in South Brazil. The CPUE is represented by the size of circles symbols in individuals captured per set (blue=Scientific cruises; red=commercial fishing cruises). **A**: summer; **B**: autumn; **C**: winter; **D**: spring

Table 3. Total length at 50% maturity (L50) for the Shortfin Mako *Isurus oxyrinchus*, in centimetres, reported by another studies and their location. Some studies provided 50% maturity estimates in terms of fork length (FL).

Study	Male L50	Female L50	Location
Conde-Moreno and Galván-Magaña (2007)	158–207	-	Baja California – NE Pacific
Stevens (1985)	195	280	Florida – NW Atlantic
Mollet *et al.* (2000)	180	280	World Wide Review
Semba *et al.* (2011)	156–173	256–274	NW and Central Pacific
Maia *et al.* (2007)	180 FL	210–290 FL	Portugal – NE Atlantic
Francis and Duffy (2005)	180–185 FL	275–285 FL	New Zealand – SW Pacific
Joung-Hsu (2005)	210	178	Taiwan – NE Pacific
This Study	180	-	Brazil – SW Atlantic

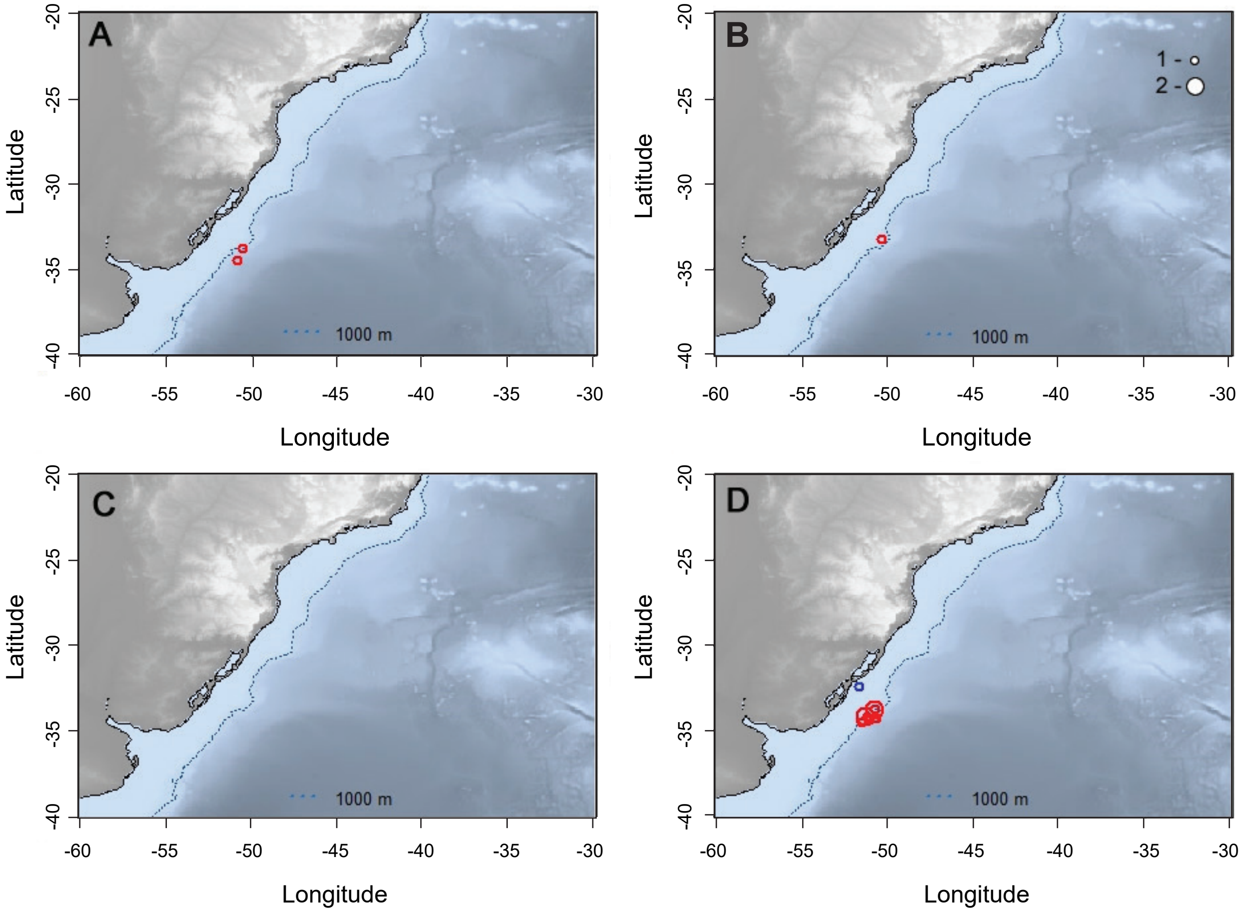

Fig. 7. Fishing sets and capture per unit effort for fisheries sampling of adult Shortfin Mako *Isurus oxyrinchus* captured by pelagic longline vessels off southern Brazil and northern Uruguay, Southwestern Atlantic Ocean, between December 2014 and September 2016 in South Brazil. The CPUE is represented by the size of circles symbols in individuals captured per set (blue=Scientific cruises; red=commercial fishing cruises). **A**: summer; **B**: autumn; **C**: winter; **D**: spring

Acknowledgements

We are very grateful to those who were involved in the realization of this research, particularly to the skippers for their receptivity and solicitude in receiving us on their boats. We also wish to thank the Instituto de Oceanografia/FURG, for sharing the Project ARGOS data, and to Projeto Albatroz, specially to Augusto Costa, for the logistical support. This project was funded by the Coordenação de Aperfeiçoamento de Pessoal de Nível Superior (CAPES) with a master's degree scholarship.

References

Barreto, R. R., Ferretti, F., Flemming, J. M., Amorim, A. F., Andrade, H., Worm, B. and Lessa, R. 2016a. Trends in the exploitation of South Atlantic shark populations. *Conservation Biology*, **30**: 792–804. https://doi.org/10.1111/cobi.12663

Barreto, R. R., Farias, W. K. T., Andrade, H., Santana, F. M. and Lessa, R. 2016b. Age, growth and spatial distribution of the life stages of the shortfin mako, *Isurus oxyrinchus* (Rafinesque, 1810) caught in the Western and Central Atlantic. PLoS ONE 11(4): e0153062. https://doi.org/10.1371/journal.pone.0153062

Baum, J. K., Myers, R. A., Kehler, D. G., Worm, B., Harley, S. J. and Doherty, P. A. 2003. Collapse and conservation of shark populations in Northwest Atlantic. *Science*, **299**: 389–392. https://doi.org/10.1126/science.1079777

Beck, M.W., Heck, K. L., Able, K. W. Childers, D. L., Eggleston, D. B., Gillanders, B. M., Halpern, B., Hays, C. G., Hoshino, K., Minello, T. J., Orth, R. J., Serdan, P. F. and Weinstein, M. P. 2001. The Identification, conservation, and management of estuarine and marine nurseries for fish and invertebrates. *BioScience*, **51**: 633–641. https://doi.org/10.1641/0006-3568(2001)051[0633:TICAMO]2.0.CO;2

Cailliet, G. M., Martin L. K., Harvey, J. T., Kusher, D. and Welden, B. A. 1983. Preliminary studies on the age and growth of the blue shark, *Prionace glauca*, common thresher, *Alopias vulpinus*, and shortfin mako, *Isurus oxyrinchus*, from California waters. US Department of Communication, *NOAA Technical Reports, NMFS* **8**: 179–188.

Carey, F. G., and Teal, J. M. 1969. Mako and porbeagle: warm-bodied sharks. *Comparative Biochemistry and Physiology*, **28**(1), 199–204. https://doi.org/10.1016/0010-406X(69)91335-8

Casey, J. G. and Kohler, N. E. 1992. Tagging studies on the shortfin mako shark (*Isurus oxyrinchus*) in the western North Atlantic. *Australian Journal of Marine and Freshwater Research*, **43**: 45–60. https://doi.org/10.1071/MF9920045

Compagno, L. J. V. 1984. FAO species catalogue: sharks of the World: an annotated and illustrated catalogue of shark species known to date. *FAO Fisheries Synopsis*, **4**(1–2): 665p.

Compagno, L. J. V. 1990. Alternative life history styles of cartilaginous fishes in time and space. *Environmental Biology of Fishes*, **28**: 33–75. https://doi.org/10.1007/978-94-009-2065-1_3

Compagno, L. J. V. 2005. Checklist of living Chondrichthyes. *In:* W. Hamlett (Ed.), Reproductive Biology and Phylogeny of Chondrichthyes: Sharks, Batoids and Chimaeras, pp. 503–548. Science Publishers, Inc., Enfield, New Hampshire, USA.

Conde-Moreno, M., and Galván-Magaña, F. 2006. Reproductive biology of the mako shark *Isurus oxyrinchus* on the south-western coast of Baja California, Mexico. *Cybium,* **30**(4): 75–83.

Cortés, E., Arocha, F., Beerkircher, L., Carvalho F., Domingo, A., Heupel, M., Holtzhausen, H., Santos, M.N., Ribera, M., Simpfendorfer, C. 2010. Ecological Risk Assessment of Pelagic Sharks Caught In Atlantic Pelagic Longline Fisheries. *Aquatic Living Resources*, **23**: 25–34. https://doi.org/10.1051/alr/2009044

Costa, F. E. S., Braga, F. M. S., Arfelli, C. A., and Amorim, A. F. 2002. Aspects of the reproductive biology of the Shortfin mako, *Isurus oxyrinchus* (elasmobranchii Lamnidae), in the southeastern region of Brazil. *Brazilian Journal of Biology*, **62**(2): 239–248. https://doi.org/10.1590/S1519-69842002000200007

Francis, M. P., and Duffy, C. 2005. Length at maturity in three pelagic sharks (*Lamna nasus*, *Isurus oxyrinchus*, and *Prionace glauca*) from New Zealand. *Fishery Bulletin*, **103**(3): 489–500.

Garcia, C. E. 1997. Physical oceanography. *In:* U. Seeliger, C. Odebrecht, and J. P. Castello (Eds.), Subtropical convergence environments. pp 94–96. The coast and sea in the southwestern Atlantic. Springer, Berlin Heidelberg New York.

Gilmore, R. G. 1993. Reproductive biology of Lamnoid sharks. *In:* L. S. Demski and J. P. Wourms, (Eds.), The reproduction and development of sharks, skates, rays and ratfishes. *Environmental Biology of Fishes*, **38**(1–3): 95–114. https://doi.org/10.1007/BF00842907

Gilmore, R. G. 2005. Oophagy, intrauterine canibalism and reproduction strategy in Lamnoid Sharks. *In* W. Hamlett, (Ed.), Reproductive Biology and Phylogeny of Chondrichthyes: sharks, batoids and chimaeras. pp 435–462. Science Publishers, Inc., Enfield, New Hampshire, USA.

Hamlett, W. C. and Koob, T. J. 1999. Female reproductive system. *In:* W. Hamlett, (Ed.), Sharks, Skates, and Rays. The Biology of Elasmobranch Fishes. pp. 398–443. Baltimore, MD. The John Hopkins University Press.

Holden, M. J. 1974. Problems in the rational exploitation of elasmobranch populations and some suggested solutions. *In:* F. R. Harden-Jones (Ed.) Sea fisheries research. pp. 117–137. John Wiley and Sons, New York.

Joung, S., and Hsu, H. 2005. Reproduction and embryonic development of the shortfin mako, *Isurus oxyrinchus* Rafinesque, 1810, in the Northwestern Pacific Zoology Studies, **44**(4): 487–496.

Maia, A., Queiroz, N., Cabral, H. N., Santos, A. M., and Correia, J. P. 2007. Reproductive biology and population dynamics of the shortfin mako, *Isurus oxyrinchus* Rafinesque, 1810, off the southwest Portuguese coast, eastern North Atlantic. *Journal of Applied Ichthyology*, **23**: 246-251 https://doi.org/10.1111/j.1439-0426.2007.00849.x

Mollet, H. F., Cliff, G., Pratt Jr. H. L., and Stevens, J. D. 2000. Reproductive biology of the female shortfin mako, *Isurus oxyrinchus* Rafinesque, 1810, with comments on the embryonic development of lamnoids. *Fishery Bulletin*, **98**: 299–318.

Mollet, H. F., Testi, A.D., Compagno, L. J. V. and Francis, M. P. 2002. Re-identification of a lamnid shark embryo. *Fishery Bulletin*, **100**: 865–875.

Mourato, B. L., Arfelli, C. A., Amorim, A. F., Hazin, H. G., Carvalho, F. C., and Hazin, F. H. V. 2011. Spatio-temporal distribution and target species in a longline fishery off the Southeastern Coast of Brazil. Brazilian Journal of Oceanography, **59**(2):185–194. https://doi.org/10.1590/S1679-87592011000200007

Pratt H. L. Jr., and Casey J. G. 1983. Age and growth of the shortfin mako, *Isurus oxyrinchus*, using four methods. *Canadian Journal of Fisheries and Aquatic Science*, **40**: 1944–957. https://doi.org/10.1139/f83-224

R Core Team (2019). R: A language and environment for statistical computing. R Foundation for Statistical Computing, Vienna, Austria. URL: https://www.R-project.org/.

Rigby, C. L., Barreto, R., Carlson, J., Fernando, D., Fordham, S., Francis, M. P., Jabado, R. W., Liu, K. M., Marshall, A., Pacoureau, N., Romanov, E., Sherley, R. B. and Winker, H. 2019. *Isurus oxyrinchus*. The IUCN Red List of Threatened Species 2019: e.T39341A2903170. https://doi.org/10.2305/IUCN.UK.2019-1.RLTS.T39341A2903170.en. Downloaded on 20 October 2020.

Schrey, A.W. and Heist, E. J. 2003. Microsatellite analysis of population structure in the shortfin mako (*Isurus oxyrinchus*) *Canadian Journal of Fisheries Science*, **60**: 67–675 https://doi.org/10.1139/f03-064

Semba, Y., Ichiro, A., and Kotaro, Y. 2011. Size at maturity and reproductive traits of shortfin mako, *Isurus oxyrinchus*, in the Western and Central North Pacific. *Marine and*

Freshwater Research, **62**: 20–29 https://doi.org/10.1071/MF10123

Stevens, J. D. 1983. Observations on reproduction in the shortfin mako *Isurus oxyrinchus*. *Copeia*: 126–130. https://doi.org/10.2307/1444706

Stevens, J. D. 2008. The Biology and Ecology of the shortfin mako shark, *Isurus oxyrinchus*. *In:* M. D. Camhi, E. K. Pikitch and E. A. Babcock (Eds.), Sharks of the Open Ocean: Biology, Fisheries and Conservation. pp 260–267. Blackwell, Oxford. https://doi.org/10.2307/1444706

Tsai, W., Liu, K., Punt, A. E. and Sun, C. 2014. Assessing the potential biases of ignoring sexual dimorphism and mating mechanism in using a single-sex demographic model: the shortfin mako shark as a case study. *ICES Journal of Marine Science*, **72**(3): 793–803. https://doi.org/10.1093/icesjms/fsu210

Vooren, C. M., Klippel, S., and Galina, A. B. 2005. Elasmobrânquios das águas costeiras da Plataforma Sul. *In:* C. M. Vooren and S. Klippel (Eds.), Ações para a conservação de tubarões e raias no sul do Brasil. pp. 113–120. Porto Alegre: Igaré.

Wyffels, J. T. 2009. Embryonic development of chondrichthyan fishes: a review. *In:* Y. Kunz, B. G. Kapoor, and C. A. Lauer (Eds.), Development of Non-Teleost Fishes. pp. 1–103. Science Publishers Inc., Enfield. https://doi.org/10.1201/b10184-2

Scientific Publications of the Northwest Atlantic Fisheries Organization

In efforts to reduce paper usage and ensure publications are accessible to all,
most publications are available FREE electronically at *www.nafo.int* or *https://journal.nafo.int*

The NAFO publications listed below are available through the NAFO Secretariat.
Prices include postage and handling.

Please note: Pricing for volumes shipped overseas is higher due to increased postage costs.

Early Stages of Fishes in the Western North Atlantic Ocean (Davis Strait, Southern Greenland and Flemish Cap to Cape Hatteras)

This comprehensive scientific publication is the only up-to-date textbook providing detailed descriptions and accurate drawings of the early life-history stages of the fishes from the Northwest Atlantic Ocean north of 35°N and west of 40°W. The region covers the world's most famous fishing grounds and includes the Davis Strait, southern Greenland, Flemish Cap, Georges Bank, northern Sargasso Sea and Middle Atlantic Bight to Cape Hatteras.

	Price North America (CAD $)	Price Overseas (CAD $)
Hardcover 2-Volume Edition by Michael. P. Fahay	120.00	135.00

Identification Guides

	Price North America (CAD $)	Price Overseas (CAD $)
Coral, Sponge, and Other Vulnerable Marine Ecosystem Indicator Identification Guide, NAFO Area (A pictorial Identification Guide for some species of Coral, Sponge, and other indicator species produced in full-colour on water-resistant paper and bound in a water-proof binder, with tab separators. Additions can be easily added)	30.00	35.00
Sponge Identification Guide NAFO Area (A pictorial Identification Guide for some species of Sponge found on the Grand Banks of Newfoundland and Flemish Cap produced in full-colour on waterproof/tearproof stock)	30.00	35.00
Coral Identification Guide NAFO Area (A pictorial Identification Guide for some species of Coral found on the Grand Banks of Newfoundland and Flemish Cap produced in full-colour on waterproof/tearproof stock)	25.00	30.00
Identification Guide of Wolffish, Hake and Rockling in the Northwest Atlantic (1-page Identification Guide produced in full-colour on laminated stock)	10.00	15.00

Journal of Northwest Atlantic Fishery Science - *Available FREE online at http://journal.nafo.int*

This publication provides an international forum for the primary publication of original research papers on fisheries science in the Northwest Atlantic, with emphasis on environmental, biological, ecological and fishery aspects of the living marine resources and ecosystems.

Please note: Scientific publications during ICNAF times (1949–1979) are available at the Secretariat in print format and also available online at www.nafo.int

	Price North America (CAD $)	Price Overseas (CAD $)
Vol. 51, 2020 (Regular Issue)	40.00	45.00
Vol. 50, 2019 (Regular Issue)	40.00	45.00
Vol. 49, 2017 (Regular Issue)	40.00	45.00
Vol. 48, 2016 (Regular Issue)	40.00	45.00
Vol. 47, 2015 (Regular Issue)	40.00	45.00
Vol. 46, 2014 (Regular Issue)	40.00	45.00
Vol. 45, 2013 (Regular Issue)	40.00	45.00
Vol. 44, 2012 (Regular Issue)	40.00	45.00
Vol. 43, 2010-2011 (Regular Issue)	40.00	45.00
Vol. 42, 2009-2010 (The Role of Marine Mammals in the Ecosystem in the 21st Century)	40.00	45.00
Vol. 41, 2008-2009 (Reproductive and Recruitment Processes of Exploited Marine Fish Stocks)	40.00	45.00
Vol. 40, 2008 (Regular issue)	40.00	45.00
Vol. 39, 2007-2008 (Environmental and Ecosystem Histories in the Northwest Atlantic – What Influences Living Marine Resources?)	40.00	45.00

Vol. 38, 2007 (Regular issue)	40.00	45.00
Vol. 37, 2005-2007 (Flemish Cap Symposium)	40.00	45.00
Vol. 36, 2005-2006 (Regular issue)	36.00	41.00
Vol. 35, 2005 (Symposium on Elasmobranch Fisheries: Managing for Sustainable Use and Biodiversity Conservation)	46.00	51.00
Vol. 34, 2004 (Mini-symposium on Hydrographic Variability in NAFO Waters for the Decade 1991–2000 in Relation to Past Decades)	31.00	36.00
Vol. 33, 2003 (Reproductive Potential of Fish Populations of the North Atlantic)	31.00	36.00
Vol. 32, 2003 (Regular issue)	31.00	36.00
Vol. 31, 2003 (Joint NAFO/ICES/CSIRO Symposium entitled "Deep-Sea Fisheries")	41.00	46.00
Vol. 30, 2002 (Regular issue)	31.00	36.00
Vol. 29, 2001 (Regular issue)	31.00	36.00
Vol. 28, 2000 (Special Issue on A Review of the Cod Fisheries at Greenland, 1910-1995)	31.00	36.00
Vol. 27, 2000 (NAFO/ICES/PICES Symposium on Pandalid Shrimp Fisheries – Science and Management at the Millennium)	41.00	46.00
Vol. 26, 2000 (Regular issue)	31.00	36.00
Vol. 25, 1999 (Variations in Maturation, Growth, Condition and Spawning Stock Biomass Production in Groundfish)	Out of Print	
Vol. 24, 1998 (Regular issue)	26.00	31.00
Vol. 23, 1998 (What Future for Capture Fisheries)	36.00	41.00
Vol. 22, 1997 (NAFO/ICES Symposium on The Role of Marine Mammals in the Ecosystem)	31.00	36.00
Vol. 21, 1997 (Regular issue)	26.00	31.00
Vol. 20, 1996 (Special Issue on North Atlantic Fishery Management Systems: A Comparison of Management Methods and Resource Trends)	26.00	31.00
Vol. 19, 1996 (Gear Selectivity/Technical Interactions in Mixed Species Fisheries Symposium)	26.00	31.00
Vol. 18, 1996 (Regular issue)	23.00	28.00
Vol. 17, 1994 (Special Issue on Report of the Canada–USSR Capelin Symposium)	21.00	26.00
Vol. 16, 1994 (Regular issue)	21.00	26.00
Vol. 15, 1993 (Special Issue on Decapod Crustacean Larvae from Ungava Bay)	21.00	26.00
Vol. 14, 1992 (Special Session on Changes in Biomass, Production and Species Composition)	21.00	26.00
Vol. 13, 1992 (Regular issue)	16.00	21.00
Vol. 12, 1992 (Regular issue)	16.00	21.00
Vol. 11, 1991 (Regular issue)	16.00	21.00
Vol. 10, 1990 (Special issue on The Delimitation of Fishing Areas in the Northwest Atlantic)	16.00	21.00
Vol. 9, No. 2, 1989 (Regular issue)	16.00	21.00
Vol. 9, No. 1, 1989 (Regular issue)	16.00	21.00
Vol. 8, 1988 (Regular issue)	16.00	21.00
Vol. 7, No. 2, 1987 (Regular issue)	16.00	21.00
Vol. 7, No. 1, 1986 (Regular issue)	16.00	21.00
Vol. 6, No. 2, 1985 (Regular issue)	16.00	21.00
Vol. 6, No. 1, 1985 (Regular issue)	16.00	21.00
Vol. 5, No. 2, 1984 (Regular issue)	16.00	21.00
Vol. 5, No. 1, 1984 (Regular issue)	16.00	21.00
Vol. 4, 1983 (Guide to the Early Stages of Marine Fishes in the Western North Atlantic Ocean, Cape Hatteras to the Southern Scotian Shelf)	26.00	31.00
Vol. 3, No. 2, 1982 (Regular issue)	14.00	19.00
Vol. 3, No. 1, 1982 (Regular issue)	14.00	19.00
Vol. 2, 1981 (Regular issue)	14.00	19.00
Vol. 1, 1980 (Regular issue)	14.00	19.00

NAFO Scientific Council Reports - *Available FREE online at www.nafo.int*

This publication contains reports of Scientific Council Meetings held through each year since NAFO replaced ICNAF. (The comparable publication during ICNAF was entitled the *Redbook*).

2019 (issued May 2020)	Online only	
2018 (issued Apr 2019)	Online only	
2017 (issued May 2018)	Online only	
2016 (issued Apr 2017)	Online only	
2015 (issued Apr 2016)	Online only	
2014 (issued Jan 2015)	Online only	
2013 (issued Jan 2014)	Online only	
2012 (issued Jan 2013)	36.00	41.00

2011 (issued May 2012)	36.00	41.00
2010 (issued April 2011)	36.00	41.00
2009 (issued May 2010)	36.00	41.00
2008 (issued May 2009)	36.00	41.00
2007 (issued May 2008)	36.00	41.00
2006 (issued May 2007)	36.00	41.00
2005 (issued May 2006)	36.00	41.00
2004 (issued January 2005)	36.00	41.00
2002/2003 Supplement (issued January 2004)	21.00	26.00
2002/2003 (issued August 2003)	31.00	36.00
2002 (issued January 2003)	31.00	36.00
2001 (issued January 2002)	31.00	36.00
2000 (issued January 2001)	29.00	34.00
1999 (issued January 2000)	29.00	34.00
1998 (issued January 1999)	26.00	31.00
1997 (issued January 1998)	23.00	28.00
1996 (issued January 1997)	23.00	28.00
1995 (issued January 1996)	23.00	28.00
1994 (issued January 1995)	21.00	26.00
1993 (issued January 1994)	21.00	26.00
1992 (issued December 1992)	18.00	23.00
1991 (issued December 1991)	16.00	21.00
1990 (issued December 1990)	14.00	19.00
1989 (issued December 1989)	14.00	19.00
1988 (issued December 1988)	12.00	17.00
1987 (issued December 1987)	12.00	17.00
1986 (issued December 1986)	12.00	17.00
1985 (issued December 1985)	12.00	17.00
1984 (issued December 1984)	12.00	17.00
1983 (issued December 1983)	12.00	17.00
1982 (issued December 1982)	12.00	17.00
1981 (issued December 1981)	12.00	17.00
1979–80 (issued December 1980)	12.00	17.00

NAFO Scientific Council Studies: This publication includes papers of topical interest and importance to the current and future activities of Scientific Council.

No. 48, 2017 (Annual Temperature Curves in Twelve Regions of the Gulf of Maine 1985–2013)	Online only	
No. 47, 2015 (Coral, Sponge, and Other Vulnerable Marine Ecosystem Indicator Identification Guide, NAFO Area)	Online only	
No. 46, 2014 (Protocols of the EU bottom trawl survey of Flemish Cap)	Online only	
No. 45, 2013 (NAFO Secretariat. NAFO Research Vessel Stock-by-Stock Surveys Summary 2000–2010)	Online only	
No. 44, 2012 (Report of the Workshop on Implementation of Stock Reproductive Potential into Assessment and Management Advice for Harvested Marine Species)	Online only	
No. 43, 2010 (Sponge Identification Guide - NAFO Area)	Online only	
No. 42, 2009 (Coral Identification Guide - NAFO Area)	Online only	
No. 41, 2008 (Report of the Greenland Halibut (*Reinhardtius hippoglossoides*) Age Determination Workshop)	Online only	
No. 40, 2007 (Identification of Wolffish, Hake and Rockling in the Northwest Atlantic)	Online only	
No. 39, 2005 (Workshop on Mapping and Geostatistical Methods for Fisheries Stock Assessment)	31.00	36.00
No. 38, 2005 (Yellowtail Flounder Ageing Manual)	36.00	41.00
No. 37, 2003 (Working Group on Reproductive Potential)	41.00	46.00
No. 36, 2003 (Workshop on Assessment Methods)	41.00	46.00
No. 35, 2002 (Workshop: The Canada-United States Yellowtail Flounder Age Reading)	31.00	36.00
No. 34, 2001 (Regular issue)	31.00	36.00
No. 33, 2000 (Regular issue)	31.00	36.00
No. 32, 1999 (Regular issue)	31.00	36.00
No. 31, 1998 (Regular issue)	31.00	36.00
No. 30, 1997 (Miscellaneous Selected Papers)	26.00	31.00
No. 29, 1997 (Selected Studies Related to Assessment of Cod in NAFO Divisions 2J+3KL)	26.00	31.00
No. 28, 1996 (Assessment of Groundfish Stocks Based on Bottom Trawl Survey Results	26.00	31.00

No. 27, 1996 (Miscellaneous Selected Papers)	26.00	31.00
No. 26, 1996 (Selected Papers on Harp and Hooded Seals)	26.00	31.00
No. 25, 1996 (Flemish Cap Selected Environmental and Other Papers)	26.00	31.00
No. 24, 1996 (Symposium on Impact of Anomalous Oceanographic Conditions at the Beginning of the 1990s in the Northwest Atlantic on the Distribution and Behaviour of Marine Life)	26.00	31.00
No. 23, 1995 (Miscellaneous Selected Papers)	26.00	31.00
No. 22, 1995 (Miscellaneous Selected Papers)	26.00	31.00
No. 21, 1994 (Collection of Papers Related to Northern Cod and Seals in NAFO Divisions 2J and 3KL)	26.00	31.00
No. 20, 1994 (Miscellaneous Selected Papers)	26.00	31.00
No. 19, 1993 (Miscellaneous Selected Papers)	21.00	26.00
No. 18, 1993 (Symposium on Changes in Abundance and Biology of Cod Stocks and Their Possible Causes)	21.00	26.00
No. 17, 1993 (Workbook: Introduction to Sequential Population Analysis)	18.00	23.00
No. 16, 1991 (Special Session on Management Under Uncertainties, 5–7 September 1990)	21.00	26.00
No. 15, 1991 (Miscellaneous Selected Papers)	18.00	23.00
No. 14, 1990 (Miscellaneous Selected Papers)	18.00	23.00
No. 13, 1989 (Miscellaneous Selected Papers)	18.00	23.00
No. 12, 1988 (Miscellaneous Selected Papers)	18.00	23.00
No. 11, 1987 (Miscellaneous Selected Papers)	18.00	23.00
No. 10, 1986 (Miscellaneous Selected Papers)	18.00	23.00
No. 9, 1985 (Special Session on Squids, September 1984)	21.00	26.00
No. 8, 1985 (Miscellaneous Selected Papers)	16.00	21.00
No. 7, 1984 (Miscellaneous Selected Papers)	14.00	19.00
No. 6, 1983 (Miscellaneous Selected Papers)	14.00	19.00
No. 5, 1982 (Symposium on Environmental Conditions in the Northwest Atlantic During 1970–79, September 1981)	14.00	19.00
No. 4, 1982 (Special Session on Remote Sensing September 1981)	14.00	19.00
No. 3, 1982 (Miscellaneous Selected Papers)	12.00	17.00
No. 2, 1982 (Manual on Groundfish Surveys in the Northwest Atlantic)	11.00	16.00
No. 1, 1981 (Miscellaneous Selected Papers)	12.00	17.00

Statistical Bulletin - *Available FREE online at www.nafo.int*

Complete statistical data have been published in the Statistical Bulletin since 1951. The printed version of the statistics were discontinued after Vol. 49 - 1999. The electronic database of the **STATLANT 21** data are updated regularly as new information becomes available.

Information for Preparing Manuscripts for NAFO Scientific Publications

Journal of Northwest Atlantic Fishery Science

The Journal is for the primary publication of original practical and theoretical research that is unpublished and is not being submitted for publication elsewhere. While it is intended to be regional in scope, papers of general applicability and methodology may be considered. Space is also provided for notes, letters to the editor and notices. Each paper is assigned to an Associate Editor of the Journal's Editorial Board, and is normally reviewed by two referees regarding suitability as a primary publication.

NAFO Scientific Council Studies

The Studies publishes papers which are of topical interest and importance to the current and future activities of the Scientific Council, but which do not meet the high standards or general applicability required by the Journal. Such papers have usually been presented as research documents at Scientific Council meetings and nominated for publication by the Standing Committee on Publications. Studies papers are not peer reviewed.

Content of Paper

The paper should be in English. The sequence should be: Title, Abstract, Text, References, Tables and Figures.

Title

The paper should start with the title, followed by the name(s), address(es) and emails of the author(s) including professional affiliation, and any related footnotes.

Abstract

An informative concise abstract should be provided along with key words listed alphabetically.

Text

In general, the text should be organized into Introduction, Materials and Methods, Results, Discussion, and Acknowledgements. Authors should be guided by the organization of papers that have been published in the NAFO Journal or Studies.

Introduction should be limited to the purpose and rationale of the study.

Materials and Methods should describe in sufficient detail the materials and methods used, so as to enable other scientists to evaluate or replicate the work.

Results should answer the questions evolving from the purpose of the study in a comprehensive manner and in an orderly and coherent sequence, with supporting tables and figures.

Discussion should explain the main contributions from the study, with appropriate interpretation of the results focusing on the problem or hypothesis. Comparisons with other studies should be included here.

Acknowledgements should be limited to the names of individuals who provided significant scientific and technical support, including reviewers, during the preparation of the paper, and the names of agencies which provided financial support.

References

The references cited in the text should be listed alphabetically. References should be mainly restricted to significant published literature. Unpublished documents and data, papers in preparation, and papers awaiting acceptance to other journals, may be cited with full contact addresses as unpublished or personal communications.

Examples:

King, M. 1995. Fisheries biology, assessment and management. Fishing News Books, UK, 341 p.

Crowder, L.B., and Murawski, S.A. 1998. Fisheries by-catch: implications for management. *Fisheries*, **23**: 8–16. doi:10.1577/1548-8446(1998)023<0008:FBIFM>2.0.CO;2

Ávila de Melo, A. M., Power, D. , and Alpoim, R. MS 2005. An assessment of the status of the redfish in NAFO Division 3LN, *NAFO SCR Doc.*, No. 52, Serial No. N5138, 19 p.

Text citations of the above would be (King, 1995; Crowder and Murawski, 1998; Ávila de Melo *et al.*, MS 2005). The surnames of two authors may be used in a citation, but *et al.* should be used for more than two authors. The citation of mimeographed reports and meeting documents should contain the abbreviation "MS". Abbreviations of periodicals can be found ftp://ftp.fao.org/fi/asfa/Monitoring_List/MASTER.txt . The Digital Object Identifier (doi) should be included if available. http://www.crossref.org/freeTextQuery/ can be used to checked this.

Tables and Figures

All Tables and Figures must be cited in the text. Tables and Figures must be numbered consecutively and correspond with the order of presentation in the text. Figure captions should be included as a separate page. Each table and figure should have a complete concise descriptive caption. Figures should always be submitted in black and white. Colour plots and photographs are acceptable only if colour is essential to the content.

All figures should be submitted as separate files in the following formats: .wmf, .emf, .ps, .eps files for vector figures. Raster images such as photos, pictures, maps can be in .jpeg, .png, .tiff formats and should be 300 ppi (high resolution).

If using excel, open the files in R and save the graphs by right clicking and saving as .wmf, .emf or postscript files. If using SlideWrite copy the files as Metafiles (WMF). Do not save them as bitmap files. They are not editable.

Paper Submission

Papers should be submitted online to:
http://journal.nafo.int/dnn/Contact OR https://jnafs.scholasticahq.com/
If this isn't possible, email the General Editor at:
journal@nafo.int

Contents